Roentgen stereophotogrammetric analysis to study dynamics and migration of stent grafts
Koning, O.H.J.

Citation
Koning, O. H. J. (2009, June 25). *Roentgen stereophotogrammetric analysis to study dynamics and migration of stent grafts*. Retrieved from https://hdl.handle.net/1887/13870

Roentgen stereophotogrammetric analysis to study
dynamics and migration of stent-grafts

Olivier H.J. Koning

Roentgen Stereophotogrammetric Analysis
to study
Dynamics and Migration of Stent-Grafts

PROEFSCHRIFT

ter verkrijging van
de graad van Doctor aan de Universiteit Leiden,
op gezag van Rector Magnificus prof. mr. P.F. van der Heijden,
volgens besluit van het College voor Promoties
te verdedigen op donderdag 25 juni 2009
klokke 15.00 uur

door
Olivier Henk Jan Koning
geboren te Amsterdam
in 1970

Voor Wally

Aan Wally, Charlotte en Juriaan

Contents

C H A P T E R

1

General Introduction

Abdominal Aortic Aneurysm

A n aneurysm of the aorta is defined as a permanent dilatation of the artery, exceeding 1.5 times the normal diameter.[1] In clinical practice, the definition of an abdominal aortic aneurysm (AAA) is set at 3-3.5cm.[2,3] The prevalence of AAA in The Netherlands is 2.1% in the population over 55 years of age, and occurs approximately 6 times more frequent in men.[4] A large Veterans Administration study (USA) in 1997 demonstrated a prevalence of 4.6% in 73.000 patients aged 50 to 79 years.[5] In specific subgroups, the percentage can be much higher, demonstrated by the study of Akkersdijk showing a prevalence of 11.4% in men over 60 years of age.[6] With a growing proportion of elderly people in the population, the incidence of aortic aneurysms is expected to increase in the future and could therefore constitute a major health risk.[7-9]

The main risk of this usually asymptomatic disease is rupture and subsequent death. Mortality rates have been reported to be as high as 75 - 90% in patients suffering from a ruptured aneurysm.[10,11] Therefore, the aim of treatment of the aneurysm is to reduce or preferably eliminate this risk of death due to rupture. Since the nature of the disease is one of gradual growth, much research has been undertaken to study the effect of lifestyle and medical therapy on the growth rate of AAA's. Cessation of smoking seems to be most effective to diminish the risk of AAA rupture.[12] The effects of statins, doxycyclin and other drugs to influence AAA growth rate, i.e. by altering the activity of inflammation and lytic enzymes look promising but this is still experimental.[13-17]

Treatment

The current consensus is to keep patients with a known AAA under surveillance until the AAA diameter reaches 5.5 cm.[18] An AAA size smaller than 5.5 cm constitutes only a low risk of rupture: 0.6-1% per year in AAA's of 4.0 - 5.4 cm.[19,20] If the AAA size is 5.5 – 5.9 cm, the annual risk of rupture increases to 9.4% in one year.[21] As aneurysm size increases further, the rupture rate rises dramatically up to 25% in 6 months for aneurysms larger than 8cm.[21]

Until 1991, the only option for treatment of an AAA was open surgical repair. This procedure has excellent long term results but is followed by considerable morbidity and mortality in the post operative phase. In 1991, the first clinical experience of endovascular aneurysm repair (EVAR)

was reported in literature.[22,23] The major advantage of this technique is that the procedure is less invasive than open aneurysm repair. The initial outcome after surgery compares favorably to open repair with a lower complication and mortality rate.[24-26] In the years that followed the introduction of EVAR, stent-graft design and materials have improved significantly and the success rate of EVAR both in the shorter and longer term have increased. EVAR has now been embedded in standard clinical practice in most of the western world and yearly thousands of aneurysm patients are treated by endovascular repair. Despite the attractive concept of less invasive surgery and the high initial success rate, EVAR remains a relatively new technique and durability problems such as kinking, thrombosis, endoleak, stent-graft disintegration and stent-graft migration have arisen. Most of these complications were unheard of after open aneurysm repair. These adverse events have been analyzed and have lead to the withdrawal of earlier types of stent-grafts, adjustments in stent-graft design and development of completely new, more durable, devices.

Although the stent-grafts were submitted to extensive preclinical laboratory and animal testing, newly introduced or redesigned stent-grafts showed varying defects during post-EVAR surveillance. These defects are caused by the hostile and demanding biomechanical environment of the aorta. Repetitive forces of the cardiac and respiratory cycle induce strain to the graft material leading to migration and fatigue. Currently, it is impossible to quantify the nature and extent of these three-dimensional dynamics of the stent-graft inside the aorta. Therefore, preclinical biomechanical modeling is difficult and has shown to have been insufficient in the past. This has lead to design shortcomings in stent-grafts that only became apparent after clinical introduction despite extensive but, in retrospect, insufficient pre-clinical testing. Reversed engineering of the circumstances to reproduce these types of stent-graft failure have led to improved understanding of previously unknown motion of the aorta, like torsion / rotation of the thoracic aorta. Increased knowledge of stent-graft dynamics after EVAR is essential to improve preclinical testing of new devices and to help detect deficiency of this type of testing early after initial clinical introduction of new stent-grafts.

Migration of the graft can result in disconnection between the stent-graft and the "landing zone", the relatively healthy part of the artery in which the stent-graft is positioned before bridging the aneurysm. This disconnection may lead to reestablishment of flow and / or repressurization of the aneurysm sac. Stent-graft migration has been reported to occur in over 50% in certain first generation devices.[27] Migration can have detrimental effects on patient safety.[28-30] Despite design changes like adding hooks and barbs to the graft to increase fixation

to the aortic wall,[31] stent-graft migration is still reported in currently marketed abdominal and thoracic devices between 1 and up to 66% and detailed analysis seems to reveal more cases of migration.[32-50]

Material fatigue can lead to stent fracture and / or stent-graft disintegration. Stent fracture can be harmless, but can also lead to perforation of the fabric or the aortic wall, with graft infection, bleeding or repressurization of the aneurysm as a result.[32,46,47] Disintegration of the graft, due to detachment of the fabric and the stents can also lead to repressurization of the AAA sac.[48] These forms of failure can ultimately lead to death of the patient.[39] The reported late aneurysm related mortality after EVAR is 1-2% per year and is largely explained by migration, endoleak and material fatigue.[28,30,33,35,37,51-53]

Surveillance after EVAR

Surveillance after EVAR aims at early detection of the described adverse events. In contrast to open repair, rigorous follow-up is required because long term results of the available stent-grafts are unknown and new or redesigned grafts are constantly introduced in clinical practice. Current surveillance protocols vary slightly but in general consist of intravascular contrast enhanced CT-scan investigation and plain radiography combined with duplex ultrasound. To date, intravascular contrast enhanced CT-scan is the clinical gold standard to detect stent-graft migration and AAA size.[54] The major disadvantages of this surveillance program are poor patient compliance, intravascular contrast requirement, logistical burden and healthcare cost.[30,55,56,57] Another disadvantage is the high cumulative radiation dose that results from frequent CT scanning.[58]

Patient compliance with the current follow-up regime is poor and this may explain part of the incidence of late rupture after EVAR.[30,57] A possible explanation for this incompliance is the cumbersome amount and intensity of investigations for an asymptomatic disease.[57] A less intensive surveillance schedule might increase patient compliance. This is an additional argument in favor of a more patient friendly alternative to CT surveillance in selected patients. The risk of limiting the intensity of surveillance is that adverse effects are identified too late. Therefore, it is paramount that alternative surveillance strategies are not only more patient friendly but also at least as accurate as current clinical strategies.

Optimal imaging using CT requires intravascular contrast enhancement. The major disadvantage of intravascular contrast use is its nephrotoxic side effect. This is especially relevant

considering the fact that reported rates of renal function impairment vary from 23% up to 83% in patients eligible for EVAR.[59-61]

Cost effectiveness of EVAR as compared to open aneurysm repair is mainly limited by the cost of the stent-graft, post EVAR surveillance and secondary interventions.[56] The introduction of a safe and accurate lower cost alternative to CT for surveillance in selected cases could therefore significantly improve this cost effectiveness balance.

Alternative to current surveillance modalities

Because surveillance aims at early detection of adverse events, the methods used need to be accurate enough to reliably detect abnormalities. The items that need to be identified are:

- Correct position and integrity of the stent-graft
- Exclusion of the AAA sac from the circulation

CT, duplex ultrasound and plain radiography, alone or in various combinations are currently used. The correct position and integrity of the stentgraft are currently assessed with CT and / or plain radiography. Both aim at identifying stent fractures, configuration changes and (pending) disconnection of components. The accuracy of both methods to determine stent-graft migration is not known but considered clinically adequate. An important factor in the accuracy of CT and plain radiography is the fact that the images have to be analyzed by hand. The clinical significance of the impact of human error on the accuracy of this kind of analysis is unknown. Furthermore, plain radiography produces a two dimensional image of a three dimensional situation. This may lead to projection errors due to the divergence of the X-ray beam (parallax). Most clinicians agree that technical problems may arise with reproducibility of plain radiographic imaging. CT is, next to the disadvantages of intravenous contrast requirement, high radiation dose and cost, a still image reconstructed from a relatively long exposure of a dynamic situation and therefore incorporates artefacts of varying degree.

Plain abdominal radiography is widely used as a method to detect stent-graft migration [62-64] and has been proposed to replace CT as a more cost effective and patient friendly method. The main difference between these modalities is that plain radiography uses the vertebral column as the point of reference to determine stent-graft position, whereas CT analysis uses the, more appropriate, branches of the aorta to detect changes in position of the graft.

Over the last years, the accepted length of the proximal landing zone in EVAR, the aneurysm neck, is continuously reported to be shorter.[65] Currently a length as short as 5mm is accepted in selected patients. With this ever decreasing neck length, the accuracy and precision of migration detection becomes increasingly important.

To ensure exclusion of the AAA sac from the systemic circulation, several strategies can be followed. AAA sac diameter or volume can be measured with CT and, in case of growth, additional diagnostics can be performed to determine and treat the cause of the sac growth. In case of significant (over 5mm) sac diameter shrinkage after EVAR, this change can be reliably detected and followed by ultrasound. Ultrasound seems inappropriate to accurately detect changes smaller than 5mm due to the inter- and intra-observer variability.[66] Alternatively, sac pressure measurement could be performed to determine trends in pressure changes.[67-73] The latter method is still under investigation and has considerable pitfalls.[74-77]

A significant reduction of aneurysm sac size is reported to occur in 50-73% after EVAR and appears to be a strong indicator for succes.[78-84] If this reduction is found after EVAR, it can be deduced that the pressure in the AAA sac, has been reduced.[85] In this case the only remaining issues of interest are stent-graft position and integrity. If a method can be developed to accurately determine these items at low cost in terms of logistics and healthcare budget, the indications for CT could be reduced and therefore the cost effectiveness and patient friendliness of EVAR could increase. In theory, Roentgen Stereophotogrammetric Analysis (RSA) may be the ideal tool to perform the surveillance of stent-graft position and integrity. The technique is described in further detail below. If RSA can be used for the purpose of surveillance of stent-grafts, follow-up intensity after EVAR in patients with a decreased AAA sac size could be reduced to ultrasound and RSA imaging without the risk of loss (or possibly even increase) of accuracy. This would result in significant reduction of cost, burden to hospital and patient and required doses of radiation and intravascular contrast.

Roentgen stereophotogrammetric analysis

Roentgen stereophotogrammetric analysis is a method that has been used in orthopedic surgery for many years.[86-88] It enables highly accurate detection of the position of joint prosthesis components relative to the bony structures. The technique is based on computer aided analysis of calibrated stereo images to determine the relative position of markers in space. The markers are placed on the prosthesis and reference markers are attached to the bone.

In endovascular surgery, the stent-graft markers that are used to position the graft during endovascular aneurysm repair can be used as graft markers. Additional markers need to be attached to the aortic wall to function as reference markers and enable detection of change of position of the graft. This means an additional procedure has to be performed during EVAR. Major assets of RSA are the fact that no intravascular contrast is required, its low cost and low burden to hospital logistics and its low radiation dose. Moreover, it may be a more accurate method than CT and plain radiography. There are several questions that need to be answered before RSA can be introduced into clinical practice. In short, they concern the accuracy and feasibility of RSA to detect stent-graft migration and the extent to which these are influenced by physiological motion due to the cardiac cycle. Furthermore, the nature and the number of aortic reference markers required for accurate analysis needs to be clarified.

Imaging of stent-graft motion in vivo using FRSA

As previously described, the forces of the cardiac cycle can have a detrimental effect on a stent-graft. To analyze these forces and enable accurate laboratory fatigue and biocompatibility modeling, detailed knowledge of stent-graft motion is mandatory. With current imaging techniques such as CT, MRI motion analysis is possible using cinematographic reconstruction with the help of "ECG-gating".[89-91] These methods have specific disadvantages to the patient in terms of intravascular contrast requirement, radiation dose (for CT) and limitation in analysis of stainless steel stent-grafts (MRI). Furthermore, there are technical difficulties in ECG gated analysis.

ECG gating is a technique that reconstructs a series of still images acquired over a short period of time according to the recorded ECG phase in which the image was acquired. The images are all reconstructed in the same plane respective to the position of the patient on the couch. This means that the cinematographic loop that is produced with this kind of imaging is actually a reconstruction that sequences images that are not acquired consecutively. The image loop is therefore a representation of a series of motions, not an exact image. Cardiac arrythmias can hinder this kind of image reconstruction.

The main disadvantage of cine-CT and cine-MRI is that reconstruction of images is limited to one single plane at a time. Therefore, quantification of out-of-plane motion is impossible with the current techniques.

In other words, cine-CT and cine-MRI can only quantify two-dimensional motion. The accuracy of this type of measurement is not validated. Out of plane motion can only be visualized. Complex, three-dimensional motion cannot be measured with current techniques.

With the knowledge of RSA available at our institution and the arrival of new, digital bi-plane fluoroscopy equipment, we will develop and validate Fluoroscopic Roentgen Stereophotogrammetric Analysis, FRSA. FRSA uses the same three-dimensional reconstruction technique as RSA, but a different method of calibration is required. Redesigning the available software and testing for accuracy will be required before introduction into clinical practice can take place.

Patient risk of radiation exposure due to imaging in EVAR

As mentioned above, there is considerable exposure of the patient to ionizing radiation due to different imaging modalities.[58] There is concern with regard to patient safety, since this type of radiation can induce malignancy. However, EVAR candidates are afflicted with other forms of systemic disease. This co-morbidity results in significant long term mortality.[92-95] There is no literature on the risk of radiation induced death due to imaging for (surveillance of) EVAR.

Aims of this research:

-   To develop, test for feasibility and validate roentgen stereophotogrammetric analysis to assess stent-graft migration in long-term surveillance studies, as an alternative to plain abdominal radiography and CT, the current clinical gold standard.

-   To develop, validate and clinically introduce fluoroscopic roentgen stereophotogrammetric analysis, a noninvasive tool that can be applied to assess real time three-dimensional stent-graft dynamics due to the cardiac and respiratory cycle.

Outline

The technique of RSA to determine stent-graft migration and FRSA to study stent-graft dynamics are explained in further detail in **CHAPTER 2**. **CHAPTER 3 and 4** concern the accuracy and feasibility of RSA to detect stent-graft migration in a static model and in a model with pulsatile motion. The results are compared to CT, the current clinical gold standard. RSA requires an aortic reference marker to detect stent-graft migration. A possible aortic reference marker is studied in **CHAPTER 4 and 5**. In **CHAPTER 5**, the feasibility of RSA in vivo is described. Furthermore, the position and the number of aortic reference markers required for accurate analysis needs to be clarified. These issues are discussed in **CHAPTERS 5 and 6**.

Plain abdominal radiography is widely used as a low cost method to determine stent-graft migration. In **CHAPTER 7,** a study on the accuracy and, therefore, clinical applicability of plain abdominal radiography to detect stent-graft migration is described.

In **CHAPTER 8** the feasibility of FRSA is studied in a model and the method is validated for accuracy and precision. In **CHAPTER 9**, the first clinical introduction of this technique is reported. To conclude this thesis, the risk of radiation due to imaging for EVAR is evaluated in **CHAPTER 10.**

References

1. Johnston KW, Rutherford RB, Tilson MD, Shah DM, Hollier L, Stanley JC. Suggested standards for reporting on arterial aneurysms, Ad Hoc Committee on Reporting Standards, Society of Vascular Surgery and North American Chapter, International Society for Cardiovascular Surgery. *J Vasc Surg* 1991;13:452-458)

2. United Kingdom Small Aneurysm Trial Participants. Long-term outcomes of immediate repair compared with surveillance of small abdominal aortic aneurysms. N Engl J Med 2002;346:1445–1452.

3. Baxter BT, Terrin MC, Dalman RL. Medical management of small abdominal aortic aneurysms. *Circulation* 2008 Apr 8;117(14):1883-9

4. Pleumeekers HJ, Hoes AW, van der Does E, van Urk H, Hofman A, de Jong PT, Grobbee DE. Aneurysms of the abdominal aorta in older adults. The Rotterdam study. *Am J Epidemiol* 1995;142:1291-1299.

5. Lederle FA, Johnson GR, Wilson SE, Chute EP, Littooy FN, Bandyk D, Krupski WC, Barone GW, Acher CW, Ballard DJ. Prevalence and associations of abdominal aortic aneurysm detected through screening. Aneurysm Detection and Management (ADAM) Veterans Affairs Cooperative Study Group. Ann Intern Med. 1997;126(6):441-9.

6. Akkersdijk GJ, Puylaert JB, de Vries AC. Abdominal aortic aneurysm as an incidental finding in abdominal ultrasonography. *Br J Surg* 1991;78(10):1261-3.

7. Best VA, Price JF, Fowkes FG. Persistent increase in the incidence of abdominal aortic aneurysm in Scotland, 1981-2000. *Br J Surg* 2003;90(12):1510-5.

8. Acosta S, Ogren M, Bengtsson H, Bergqvist D, Lindblad B, Zdanowski Z. Increasing incidence of ruptured abdominal aortic aneurysm: a population-based study. *J Vasc Surg.* 2006;44(2):237-43.

9. Reitsma JB, Pleumeekers HJ, Hoes AW, Kleijnen J, de Groot RM, Jacobs MJ, Grobbee DE, Tijssen JG. Increasing incidence of aneurysms of the abdominal aorta in The Netherlands. *Eur J Vasc Endovasc Surg* 1996;12(4):446-51.

10. Bengtsson H, Bergqvist D. Ruptured abdominal aortic aneurysm: a population-based study. *J Vasc Surg* 1993;18(1):74-80.

11. Heikkinen M, Salenius JP, Auvinen O. Ruptured abdominal aortic aneurysm in a well-defined geographic area. *J Vasc Surg* 2002;36(2):291-6.

12. Branchereau A, Jacobs M. Surgical and endovascular treatment of aortic aneurysms. 2000 Futura Publishing Company, Inc. Armonk, New York, USA. P1-9, 19, 27, 4346

13. Thompson RW, Baxter BT.MMP inhibition in abdominal aortic aneurysms. Rationale for a prospective randomized clinical trial. *Ann N Y Acad Sci* 1999;878:159-178.

14. Mosorin M, Juvonen J, Biancari F, Satta J, Surcel HM, Leinonen M, Saikku P, Juvonen T. Use of doxycycline to decrease the growth rate of abdominal aortic aneurysms: a randomized, double-blind, placebo-controlled pilot study. *J Vasc Surg* 2001;34:606-610.

15. Baxter BT, Pearce WH, Waltke EA, Littooy FN, Hallett JW Jr, Kent KC, Upchurch GR Jr, Chaikof EL, Mills JL, Fleckten B, Longo GM, Lee JK, Thompson RW. Prolonged administration of doxycycline in patients with small asymptomatic abdominal aortic aneurysms: report of a prospective (Phase II) multicenter study. *J Vasc Surg* 2002;36:1-12.

16. Abdul-Hussien H, Hanemaaijer R, Verheijen JH, van Bockel JH, Geelkerken RH, Lindeman JH. Doxycycline therapy for abdominal aneurysm: improved proteolytic balance through reduced neutrophil content. *J Vasc Surg, in press.*

17. Baxter BT, Terrin MC, Dalman RL. Medical management of small abdominal aortic aneurysms. *Circulation* 2008;117(14):1883-9.

18. Hollier LH, Taylor LM, Ochsner J. Recommended indications for operativetreatment of abdominal aortic aneurysms. *J Vasc Surg* 1992;15:1046-56.

19. The UK Small Aneurysm Trial Participants. Mortality results for randomized of early elective surgery or ultrasonographic surveillance of small abdominal aortic aneurysms. *Lancet* 1998;325:1649-1655.

20. Lederle FA, Wilson SE, Johnson GR, Reinke DB, Littooy FN, Acher CW, Ballard DJ, Messina LM, Gordon IL, Chute EP, Krupski WC, Busuttil SJ, Barone GW, Sparks S, Graham LM, Rapp JH, Makaroun MS, Moneta GL, Cambria RA, Makhoul RG, Eton D, Ansel HJ, Freischlag JA, Bandyk D; Aneurysm Detection and Management Veterans Affairs Cooperative Study Group. Immediate repair compared with surveillance for small abdominal aortic aneurysms. *N Eng J Med* 2002;346:1437-1444.

21. Lederle FA, Johnson GR, Wilson SE, Ballard DJ, Jordan WD Jr, Blebea J, Littooy FN, Freischlag JA, Bandyk D, Rapp JH, Salam AA; Veterans Affairs Cooperative Study #417 Investigators. Rupture rate of large abdominal aortic aneurysms in patients refusing or unfit for elective repair. *JAMA* 2002;287(22):2968-72.

22. Volodos NL, Karpovich IP, Troyan VI, Kalashnikova YuV, Shekhanin VE, Ternyuk NE, Neoneta AS, Ustinov NI, Yakovenko LF. Clinical experience of the use of self-fixing synthetic prostheses for remote endoprosthetics of the thoracic and the abdominal aorta and iliac arteries through the femoral artery and as intraoperative

endoprosthesis for aorta reconstruction. *Vasa Suppl* 1991;33:93-5.

23. Parodi JC, Palmaz JC, Barone HD. Transfemoral intraluminal graft implantation for abdominal aortic aneurysms. *Ann Vasc Surg* 1991;5(6):491-9.

24. Greenhalgh RM, Brown LC, Kwong GP, Powell JT, Thompson SG; EVAR trial participants. Comparison of endovascular aneurysm repair with open repair in patients with abdominal aortic aneurysm (EVAR trial 1), 30-day operative mortality results: randomised controlled trial. *Lancet* 2004;364(9437):843-8.

25. Prinssen M, Verhoeven EL, Buth J, Cuypers PW, van Sambeek MR, Balm R, Buskens E, Grobbee DE, Blankensteijn JD; Dutch Randomized Endovascular Aneurysm Management (DREAM)Trial Group. A randomized trial comparing conventional and endovascular repair of abdominal aortic aneurysms. *N Engl J Med* 2004;351(16):1607-18.

26. Lovegrove RE, Javid M, Magee TR, Galland RB. A meta-analysis of 21,178 patients undergoing open or endovascular repair of abdominal aortic aneurysm. *Br J Surg* 2008;95(6):677-84.

27. Alric P, Hinchliffe RJ, Wenham PW, Whitaker SC, Chuter TA, Hopkinson BR. Lessons learned from the long-term follow-up of a first-generation aortic stent graft. *J Vasc Surg* 2003;37(2):367-73.

28. Harris PL, Vallabhaneni SR, Desgranges P, Becquemin JP, van Marrewijk C, Laheij RJ. Incidence and risk factors of late rupture, conversion, and death after endovascular repair of infrarenal aortic aneurysms: the EUROSTAR experience. European Collaborators on Stent/graft techniques for aortic aneurysm repair. *J Vasc Surg* 2000;32(4):739-49.

29. Resch T, Ivancev K, Brunkwall J, Nyman U, Malina M, Lindblad B. Distal migration of stent-grafts after endovascular repair of abdominal aortic aneurysms. *J Vasc Interv Radiol* 1999;10(3):257-64

30. Fransen GA, Vallabhaneni SR Sr, van Marrewijk CJ, Laheij RJ, Harris PL, Buth J; EUROSTAR. Rupture of infra-renal aortic aneurysm after endovascular repair: a series from EUROSTAR registry. *Eur J Vasc Endovasc Surg* 2003;26(5):487-93.

31. Malina M, Lindblad B, Ivancev K, Lindh M, Malina J, Brunkwall J. Endovascular AAA exclusion: will stents with hooks and barbs prevent stent-graft migration? *J Endovasc Surg* 1998;5(4):310-7.

32. Greenberg RK, Chuter TA, Sternbergh WC 3rd, Fearnot NE; Zenith Investigators. Zenith AAA endovascular graft: intermediate-term results of the US multicenter trial. *J Vasc Surg* 2004;39(6):1209-18.

33. Leurs LJ, Hobo R, Buth J; EUROSTAR Collaborators. The multicenter experience with a third-generation endovascular device for abdominal aortic aneurysm repair. A report from the EUROSTAR database. *J Cardiovasc Surg (Torino)* 2004;45(4):293-300.

34. Sternbergh WC 3rd, Money SR, Greenberg RK, Chuter TA; Zenith Investigators. Influence of endograft oversizing on device migration, endoleak, aneurysm shrinkage, and aortic neck dilation: results from the Zenith Multicenter Trial. *J Vasc Surg* 2004 Jan;39(1):20-6.

35. van Marrewijk CJ, Fransen G, Laheij RJ, Harris PL, Buth J; EUROSTAR Collaborators. Is a type II endoleak after EVAR a harbinger of risk? Causes and outcome of open conversion and aneurysm rupture during follow-up. *Eur J Vasc Endovasc Surg* 2004;27:128–137.

36. Conners MS 3rd, Sternbergh WC 3rd, Carter G, Tonnessen BH, Yoselevitz M, Money SR.LinksEndograft migration one to four years after endovascular abdominal aortic aneurysm repair with the AneuRx device: a cautionary note. *J Vasc Surg* 2002;36(3):476-84.

37. Harris PL, Vallabhaneni SR, Desgranges P, Becquemin JP, van Marrewijk C, Laheij RJ. Incidence and risk factors of late rupture, conversion, and death after endovascular repair of infrarenal aortic aneurysms: the EUROSTAR experience. *J Vasc Surg* 2000;32:739–749.

38. Torsello G, Osada N, Florek HJ, Horsch S, Kortmann H, Luska G, Scharrer-Pamler R, Schmiedt W, Umscheid T, Wozniak G; Talent AAA Retrospective Longterm Study Group. Long-term outcome after Talent endograft implantation for aneurysms of the abdominal aorta: a multicenter retrospective study. *J Vasc Surg* 2006;43(2):277-84;

39. Abel DB, Dehdashtian MM, Rodger ST, Smith AC, Smith LJ, Waninger MS. Evolution and future of preclinical testing for endovascular grafts. *J Endovasc Ther* 2006;13(5):649-59.

40. Lee WA. Infrarenal aortic devices: failure modes and unmet needs. *Semin Vasc Surg* 2007;20(2):75-80.

41. Alric P, Hinchliffe RJ, MacSweeney ST, Wenham PW, Whitaker SC, Hopkinson BR. The Zenith aortic stent-graft: a 5-year single-center experience. *J Endovasc Ther* 2002;9(6):719-28.

42. Drury D, Michaels JA, Jones L, Ayiku L. Systematic review of recent evidence for the safety and efficacy of elective endovascular repair in the management of infrarenal abdominal aortic aneurysm. *Br J Surg* 2005;92(8):937-46.

43. Matsumura JS, Cambria RP, Dake MD, Moore RD, Svensson LG, Snyder S; TX2 Clinical Trial Investigators. International controlled clinical trial of thoracic endovascular aneurysm repair with the Zenith TX2 endovascular graft: 1-year results. *J Vasc Surg* 2008;47(2):247-257

44. Greenberg R, Resch T, Nyman U, Lindh M, Brunkwall J, Brunkwall P, Malina M, Koul B, Lindblad B, Ivancev

K. Endovascular repair of descending thoracic aortic aneurysms: an early experience with intermediate-term follow-up. *J Vasc Surg* 2000;31:147-56.

45. Zarins CK, Bloch DA, Crabtree T, Matsumoto AH, White RA, Fogarty TJ. Stent graft migration after endovascular aneurysm repair: importance of proximal fixation. *J Vasc Surg* 2003;38(6):1264-72.

46. Jacobs TS, Won J, Gravereaux EC, Faries PL, Morrissey N, Teodorescu VJ, Hollier LH, Marin ML. Mechanical failure of prosthetic human implants: a 10-year experience with aortic stent graft devices. *J Vasc Surg* 2003;37(1):16-26.

47. Böckler D, von Tengg-Kobligk H, Schumacher H, Ockert S, Schwarzbach M, Allenberg JR. Late surgical conversion after thoracic endograft failure due to fracture of the longitudinal support wire. *J Endovasc Ther* 2005;12(1):98-102.

48. Tiesenhausen K, Hessinger M, Konstantiniuk P, Tomka M, Baumann A, Thalhammer M, Portugaller H. Surgical conversion of abdominal aortic stent-grafts--outcome and technical considerations. *Eur J Vasc Endovasc Surg* 2006;31(1):36-41.

49. Lee JT,Lee J, Aziz I, Donayre CE, Walot I, Kopchok GE, Heilbron M, Lippmann M, White RA. Stent-graft migration following endovascular repair of aneurysms with large proximal necks: anatomical risk factors and long-term sequelae. *J Endovasc Ther* 9 (5):652-664, 2002.

50. Sun Z. Three-dimensional visualization of suprarenal aortic stent-grafts: evaluation of migration in midterm follow-up. *J Endovasc Ther* 2006;13:85–93.

51. Beebe HG, Cronenwett JL, Katzen BT, Brewster DC, Green RM; Vanguard Endograft Trial Investigators. Results of an aortic endograft trial: impact of device failure beyond 12 months. *J Vasc Surg* 2001;33(2 Suppl):S55-63.

52. Enzler MA, van Marrewijk CJ, Buth J, Harris PL. Endovaskuläre Therapie von Aneurysmen der Bauchaorta: Bericht über 4291 Patienten des Eurostar-Registers. *Vasa* 2002;31(3):167-72.

53. Peppelenbosch N, Buth J, Harris PL, van Marrewijk C, Fransen G; EUROSTAR Collaborators. Diameter of abdominal aortic aneurysm and outcome of endovascular aneurysm repair: does size matter? A report from EUROSTAR. *J Vasc Surg* 2004;39(2):288-97.

54. Wolf YG, Hill BB, Lee WA, Corcoran CM, Fogarty TJ, Zarins CK. Eccentric stent graft compression: an indicator of insecure proximal fixation of aortic stent graft. *J Vasc Surg* 2001;33:481–487.

55. Jones WB, Taylor SM, Kalbaugh CA, Joels CS, Blackhurst DW, Langan EM 3rd, Gray BH, Youkey JR. Lost to follow-up: a potential under-appreciated limitation of endovascular aneurysm repair. *J Vasc Surg* 2007;46(3):434-40.

56. Prinssen M, Buskens E, de Jong SE, Buth J, Mackaay AJ, van Sambeek MR, Blankensteijn JD; DREAM trial participants. Cost-effectiveness of conventional and endovascular repair of abdominal aortic aneurysms: results of a randomized trial. *J Vasc Surg* 2007;46(5):883-890.

57. Jones WB, Taylor SM, Kalbaugh CA, Joels CS, Blackhurst DW, Langan EM 3rd, Gray BH, Youkey JR. Lost to follow-up: a potential under-appreciated limitation of endovascular aneurysm repair. *J Vasc Surg* 2007;46(3):434-40.

58. Weerakkody RA, Walsh SR, Cousins C, Goldstone KE, Tang TY, Gaunt ME. Radiation exposure during endovascular aneurysm repair. *Br J Surg* 2008 Jun;95(6):699-702.

59. Vasquez J, Rahmani O, Lorenzo AC, Wolpert L, Podolski J, Gruenbaum S, Gallagher JJ, Allmendinger P, Hallisey MJ, Lowe R, Windels M, Drezner AD. Morbidity and mortality associated with renal insufficiency and endovascular repair of abdominal aortic aneurysms: a 5-year experience. *Vasc Endovascular Surg* 2004;38(2):143-8.

60. van Eps RG, Leurs LJ, Hobo R, Harris PL, Buth J; EUROSTAR Collaborators. Impact of renal dysfunction on operative mortality following endovascular abdominal aortic aneurysm surgery. *Br J Surg* 2007;94:174–178.

61. Azizzadeh A, Sanchez LA, Miller CC 3rd, Marine L, Rubin BG, Safi HJ, Huynh TT, Parodi JC, Sicard GA. Glomerular filtration rate is a predictor of mortality after endovascular abdominal aortic aneurysm repair. *J Vasc Surg* 2006;43:14–18.

62. Fearn S, Lawrence-Brown MM, Semmens JB, Hartley D. Follow-up after endoluminal grafting: the plain radiograph has an essential role in surveillance. *J Endovasc Ther* 2003;10:894–901.

63. Hodgson R, McWilliams RG, Simpson A, Gould DA, Brennan JA, Gilling-Smith GL, Harris PL. Migration versus apparent migration: the importance of errors due to positioning variation in plain radiographic follow-up of aortic stentgrafts. *J Endovasc Ther* 2003;10:902–910.

64. Murphy M, Hodgson R, Harris PL, McWilliams RG, Hartley DE, Lawrence-Brown MM. Plain radiographic surveillance of abdominal aortic stent-grafts: the Liverpool/Perth protocol. *J Endovasc Ther* 2003;10:911–912.

65. Kapma, MR, Groen, H, Oranen, BI, van der Hilst, CS, Tielliu, IF, Zeebrechts, CJ, Prins, TR, van den Dungen, J, Verhoeven EL. Emergency abdominal aortic aneurysm repair with a preferential endovascular strategy: mortality and cost-effectiveness analysis. *J Endovasc Ther* 2007;14:777-784.

66. Singh K, Bønaa KH, Solberg S, Sørlie DG, Bjørk L. Intra- and interobserver variability in ultrasound measurements of abdominal aortic diameter. The Tromsø Study. *Eur J Vasc Endovasc Surg* 1998;15(6):497-504.

67.	Gawenda M, Heckenkamp J, Zaehringer M, Brunkwall J. Intra-aneurysm sac pressure--the holy grail of endoluminal grafting of AAA. *Eur J Vasc Endovasc Surg* 2002;24(2):139-45.

68.	Sonesson B, Dias N, Malina M, Olofsson P, Griffin D, Lindblad B, Ivancev K. Intra-aneurysm pressure measurements in successfully excluded abdominal aortic aneurysm after endovascular repair. *J Vasc Surg* 2003;37(4):733-8.

69.	Dias NV, Ivancev K, Malina M, Hinnen JW, Visser M, Lindblad B, Sonesson B. Direct intra-aneurysm sac pressure measurement using tip-pressure sensors: in vivo and in vitro evaluation. *J Vasc Surg* 2004;40(4):711-6.

70.	Ellozy SH, Carroccio A, Lookstein RA, Minor ME, Sheahan CM, Juta J, Cha A, Valenzuela R, Addis MD, Jacobs TS, Teodorescu VJ, Marin ML. First experience in human beings with a permanently implantable intrasac pressure transducer for monitoring endovascular repair of abdominal aortic aneurysms. *J Vasc Surg* 2004;40(3):405-12.

71.	Ohki T, Ouriel K, Silveira PG, Katzen B, White R, Criado F, Diethrich E. Initial results of wireless pressure sensing for endovascular aneurysm repair: the APEX Trial--Acute Pressure Measurement to Confirm Aneurysm Sac EXclusion. *J Vasc Surg* 2007;45(2):236-42.

72.	Hinnen JW, Koning OH, Van Bockel HJ, Hamming JF. Regarding "Initial results of wireless pressure sensing for endovascular aneurysm repair: The APEX trial--Acute Pressure Measurement to Confirm Aneurysm Sac EXclusion". *J Vasc Surg* 2007;46(2):403.

73.	Dias NV, Ivancev K, Resch TA, Malina M, Sonesson B. Endoleaks after endovascular aneurysm repair lead to nonuniform intra-aneurysm sac pressure. *J Vasc Surg* 2007 Aug;46(2):197-203.

74.	Hinnen JW, Koning OH, Visser MJ, Van Bockel HJ. Effect of intraluminal thrombus on pressure transmission in the abdominal aortic aneurysm. *J Vasc Surg* 2005;42(6):1176-82.

75.	Hinnen JW, Koning OH, Visser MJ, Van Bockel HJ. Effect of intraluminal thrombus on pressure transmission in the abdominal aortic aneurysm. *J Vasc Surg* 2005;42(6):1176-82.

76.	Hinnen JW, Koning OH, Vlaanderen E, van Bockel JH, Hamming JF. Aneurysm sac pressure monitoring: effect of pulsatile motion of the pressure sensor on the interpretation of measurements. *J Endovasc Ther* 2006;13(2):145-51.

77.	Hinnen JW, Rixen DJ, Koning OH, Van Bockel HJ, Hamming JF. Aneurysm sac pressure monitoring: does the direction of pressure measurement matter in fibrinous thrombus? *J Vasc Surg* 2007;45(4):812-6.

78.	Lee JT, Aziz IN, Lee JT, Haukoos JS, Donayre CE, Walot I, Kopchok GE, Lippmann M, White RA. Volume regression of abdominal aortic aneurysms and its relation to successful endoluminal exclusion. *J Vasc Surg* 2003;38(6):1254-63.

79.	Sternbergh WC 3rd, Conners MS 3rd, Tonnessen BH, Carter G, Money SR. Aortic aneurysm sac shrinkage after endovascular repair is device-dependent: a comparison of Zenith and AneuRx endografts. Ann Vasc Surg 2003;17(1):49-53.

80.	Long-term outcome after Talent endograft implantation for aneurysms of the abdominal aorta: A multicenter retrospective study. Torsello G, Osada N, Florek HJ, Horsch S, Kortmann H, Luska G, Scharrer-Pamler R, Schmiedt W, Umscheid T, Wozniak G; Talent AAA Retrospective Longterm Study Group. J Vasc Surg 2006;43:277-84.

81.	Fairman RM, Nolte L, Snyder SA, Chuter TA, Greenberg RK; Zenith Investigators. Factors predictive of early or late aneurysm sac size change following endovascular repair. J Vasc Surg 2006;43:649-56.

82.	Haider SE, Najjar SF, Cho JS, Rhee RY, Eskandari MK, Matsumura JS, Makaroun MS, Morasch MD. Sac behavior after aneurysm treatment with the Gore Excluder low-permeability aortic endoprosthesis: 12-month comparison to the original Excluder device. J Vasc Surg 2006;44(4):694-700.

83.	Tanski W 3rd, Fillinger M. Outcomes of original and low-permeability Gore Excluder endoprosthesis for endovascular abdominal aortic aneurysm repair. J Vasc Surg 2007;45(2):243-9.

84.	Sternbergh WC 3rd, Greenberg RK, Chuter TA, Tonnessen BH; Zenith Investigators. Redefining postoperative surveillance after endovascular aneurysm repair: recommendations based on 5-year follow-up in the US Zenith multicenter trial. J Vasc Surg 2008;48(2):278-84.

85.	Dias NV, Ivancev K, Malina M, Resch T, Lindblad B, Sonesson B. Intra-aneurysm sac pressure measurements after endovascular aneurysm repair: differences between shrinking, unchanged, and expanding aneurysms with and without endoleaks. *J Vasc Surg* 2004;39(6):1229-35.

86.	Kärrholm J, Gill RH, Valstar ER. The history and future of radiostereometric analysis. *Clin Orthop Relat Res* 2006;448:10-21.

87.	Valstar ER. Digital roentgen stereophotogrammetry. Development, validation, and clinical application. Thesis, Leiden University. Den Haag, The Netherlands: Pasmans BV, 2001.

88.	Vrooman HA, Valstar ER, Brand GJ, Admiraal DR, Rozing PM, Reiber JH. Fast and accurate automated measurements in digitized stereophotogrammetric radiographs. *J Biomech* 1998;31:491-498.

89. Verhagen, HJ, Teutelink A, Olree M, Rutten A, de Vos AM, Raaijmakers R, Prokop M, Moll F. Dynamic CTA for cutting edge AAA imaging: Insights into aortic distensibility and movement with possible consequences for endograft sizing and stentdesign *J Endovasc Ther* 2005;12:I-45.

90. Teutelink A, Rutten A, Muhs BE, Olree M, van Herwaarden JA, de Vos AM, Prokop M, Moll FL, Verhagen HJ. Pilot study of dynamic cine CT angiography for the evaluation of abdominal aortic aneurysms: implications for endograft treatment. *J Endovasc Ther* 2006;13(2):139-44.

91. Vos AW, Wisselink W, Marcus JT, Vahl AC, Manoliu RA, Rauwerda JA. Cine MRI assessment of aortic aneurysm dynamics before and after endovascular repair. *J Endovasc Ther* 2003;10:433-9.

92. Biancari F, Ylönen K, Anttila V, Juvonen J, Romsi P, Satta J, Juvonen T. Durability of open repair of infrarenal abdominal aortic aneurysm: a 15-year follow-up study. *J Vasc Surg* 2002;35(1):87-93.

93. Torsello G, Osada N, Florek HJ, Horsch S, Kortmann H, Luska G, Scharrer-Pamler R, Schmiedt W, Umscheid T, Wozniak G; Talent AAA Retrospective Longterm Study Group. Long-term outcome after Talent endograft implantation for aneurysms of the abdominal aorta: a multicenter retrospective study. *J Vasc Surg* 2006;43(2):277-84.

94. Zarins CK, Crabtree T, Bloch DA, Arko FR, Ouriel K, White RA. Endovascular aneurysm repair at 5 years: Does aneurysm diameter predict outcome? *J Vasc Surg* 2006;44(5):920-29.

95. Schermerhorn ML, O'Malley AJ, Jhaveri A, Cotterill P, Pomposelli F, Landon BE. Endovascular vs. open repair of abdominal aortic aneurysms in the Medicare population. *N Engl J Med* 2008;358(5):464-74.

2

Technique of RSA and FRSA

History of RSA

Roentgen Stereophotogrammetric Analysis (RSA) has a long and success-ful history in orthopedic surgery. It is used to evaluate joint prostheses for signs of aseptic mechanical loosening, the most common cause for revi-sion surgery in long term follow-up.[1-3] A highly accurate measurement method is required to detect this detrimental effect at an early stage. Early detection allows for early evaluation of new implants, coatings and cement in small patient groups before large scale introduction in clinical practice.[4,5] RSA has a very high accuracy and digitization of the technique with specialized RSA software enabled easy, fast and accurate analysis of stereo images. For this reason, RSA has evolved to become the gold standard for evaluation of micro-motion of the prosthesis with respect to the bone after joint replacement surgery.[6-11]

Principles of RSA

The essence of RSA can be compared to stereo vision of human eye sight: two images of an object are simultaneously acquired by the eyes. Each image is taken from a different angle. The brain compares these images and is able to determine the position of the object in space as compared to the human body. "Calibration" of the brain to determine the position of the object is done by trial-and-error experience.

RSA also uses two simultaneously acquired, calibrated images to determine the three dimen-sional position of markers in the human body. During surgery, reference markers are placed inside the body. The prosthesis is inserted and the relative position and orientation of the prosthesis can be assessed by comparing its position and orientation to that of the reference markers. When comparing consecutive RSA images over time, a change of position of the prosthesis as compared to the reference markers can be detected. This way, migration of the prosthesis can be detected.

RSA uses two still images to perform this reconstruction. It is therefore ideal for follow-up after surgery, to determine position changes of prostheses. Obviously, this technique with still images cannot be used to assess a dynamic, rapidly changing position that occurs in the pulsatile environment of the vascular system. Analysis of a dynamic situation requires rapid sequence (calibrated) imaging.

Technique of RSA

Markers

As discussed previously, distinct prosthesis markers and reference markers are required to perform RSA. To apply RSA to the endovascular surgery environment, the stentgraft and the aorta have to be marked accordingly. The stentgraft markers used to position the graft during placement can be utilized for this purpose. Reference markers need to be attached to the aortic wall to serve as reference markers. In **CHAPTERS 4, 5 and 6** the issue of aortic reference markers will be addressed in more detail.

The RSA set-up

To acquire a stereo image for RSA, two roentgen films or detectors, positioned under the patient, are exposed by two synchronized roentgen tubes. A calibration box is positioned between the patient and the films to produce a coordinate system and enable measurements (Figure 1).
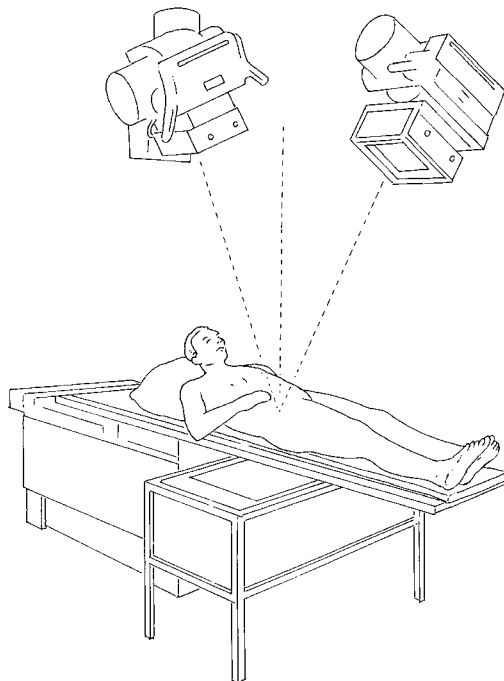

Figure 1. RSA imaging setup. The reference and control markers are in the box under the patient. The radiographic films are placed directly under the box.

Two synchronized Roentgen tubes

Two standard hospital roentgen tubes are used to acquire the images. The two roentgen tubes are positioned approximately 1.60 m above the film and at a 20º angle to the vertical (Figure 1 and 2). The exposure of the films is synchronized by simply pressing the exposure buttons of the two machines at the same time. Because this is done by hand, exact simultaneous exposure of the films may not be achieved. This could lead to motion artifacts and result in inaccurate measurements. This type of error is especially possible in an endovascular surgery setting where the markers are continuously displaced by the pulsatile motion of the blood vessels. This issue is further addressed in **CHAPTER 4**.

Calibration box

Since it is the goal of RSA to perform measurements to determine the three dimensional position of markers, the images have to be calibrated. This enables three important steps in the image analysis: a) the position of the images (films / detectors) as compared to each other has to be determined; b) a laboratory coordinate system has to be added to the image to define distance in the image; c) the position of the two roentgen tubes has to be determined as compared to the films. After these steps have been performed the position of all components of the set-up is known including their relation to each other. These steps will be discussed separately below.

Image calibration is performed with the help of a calibration box positioned between the patient and the films (Figure 1). The box is made of carbon fiber sandwich plates. This material is chosen because it is insensitive to changes in room temperature and humidity. Furthermore, carbon fiber plates are radiolucent. The dimensions of the box are 70 x 46 x 24 cm. The top and bottom layers of the box contain tantalum markers to perform the calibration. These markers are positioned with a computer controlled device and the position of these markers is known within a few micrometers. The bottom layer contains *fiducial* markers. The top layer of the box contains the *control* markers. The use of the calibration box markers will be elucidated below.

Scatter grids

As the roentgen beam passes through the body, it is partially absorbed by the tissues. The X-rays that pass through the body (the primary bundle) generate the image. Some X-rays however, are neither absorbed nor pass straight through the body but only change direction and scatter. These X-rays produce a grey mist in the image and therefore reduce the image quality. To reduce this effect, a scatter grid can be used to filter out these scattered X-rays.

Roentgen tube setting and radiation dose

The roentgen tubes are set to maximize contrast of the metal graft and reference markers. Next to RSA, the images can be used for stent fracture detection. Soft and bony tissues are of less interest in the image. The radiation dose for a stereo RSA image of an abdominal aortic stentgraft is 0.3 mSv, which is roughly one sixth of the yearly natural background radiation. This amount of radiation is dwarfed by the radiation dose received for a standard 3-phase contrast enhanced CT used for regular follow-up after endovascular aneurysm repair, which is approximately 17 mSv.

Digital RSA

After acquisition of the stereo image, the films are digitized and loaded into the RSA software (Model Based RSA software, MEDIS Specials BV, Leiden, The Netherlands) on a personal computer. Digitally acquired images are loaded directly into the software.

The software automatically detects the markers and performs the calibration and analysis steps. Every step in the marker recognition process can be verified manually in a user friendly way. This method has been validated and was described previously in mathematical detail.[8-12]

Calibration of the set-up

First the *fiducial* and *control* markers of the calibration box are detected. With the known positions of these markers the two images can be virtually repositioned next to each other in the same way as they were positioned under the patient. The *fiducial* markers on the bottom of the box are used to define the laboratory coordinate system. Furthermore, these markers are used to virtually transform the image from the plane of the film to the lower plane of the box. Now that the position of the two films is known relative to each other and the transformation of the films has been calculated as well as the laboratory coordinate system for the image pairs, the position of the two roentgen foci can be reconstructed.

The known positions of the *control* markers (Figure 2 thin arrow, top of the box) can be matched to the projections of these markers on the film (Figure 2 thick arrow). The marker and its image on the film are, by definition, in one line with the roentgen focus. These lines are called projection lines (Figure 2 thick lines). By calculating the point of intersection of different projection lines through the control markers and their images, the position of the roentgen focus is determined (Figure 2 top right).

Now that the position of the films and the roentgen foci is known as well as their relation to each other, the set-up calibration is complete.
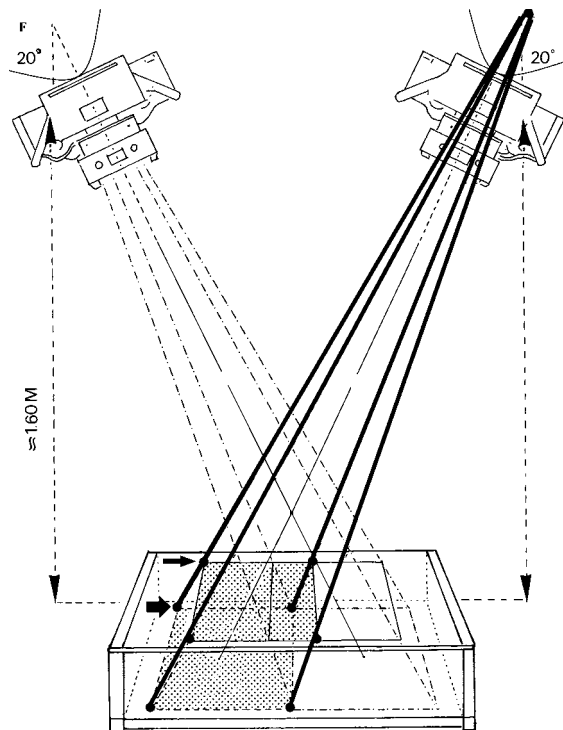
Figure 2. Reconstruction of the position of the Roentgen foci (F). The control markers (thin arrow, top layer of the box) project an image on the film (thick arrow). The point of intersection of the projection lines of the control markers (thick lines) defines the Roentgen focus (F).

Calculation of three-dimensional marker position

After calibration of the set-up, calculation of the position of a marker relative to other markers in the body becomes an equation with one unknown value: the position of the foci and the films is known, and therefore the position of the marker can be calculated.

To determine the three-dimensional position of a stentgraft marker or reference marker, a projection line is calculated through (the now known position of) the roentgen focus (Figure 3: F) and the projection of the marker on the film (Figure 3 projection B and C). This is done for both projections on the two films (Figure 3 line 1 and 2). By calculating the point of intersection of the two lines(Figure 3: A), the three-dimensional coordinates of the marker becomes clear, relative to the laboratory coordinate system. In reality, the projection lines do not intersect but cross, due to minute measurement errors. Therefore, the marker is positioned in the middle of the shortest distance between the two projection lines. This phenomenon of crossing instead of intersection is called the crossing line error and is given by the software for each calculated three dimensional marker position. It can be used as an internal control for measurement error:
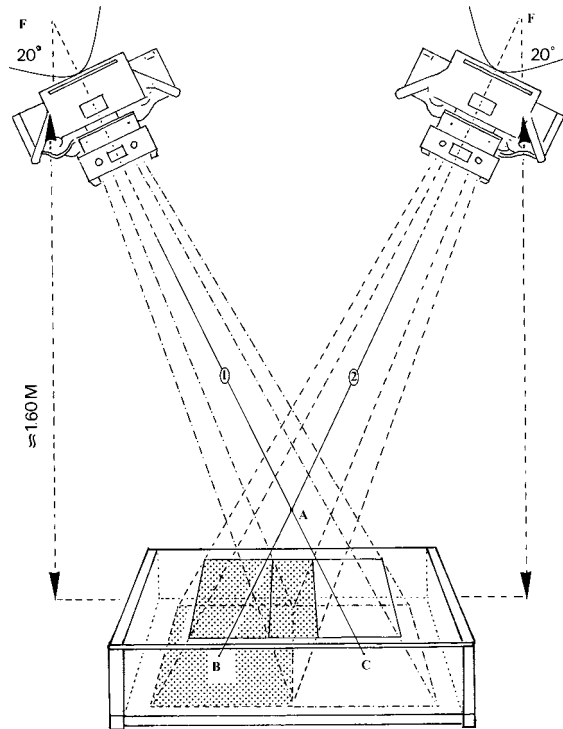
Figure 3. Schematic drawing of the RSA technique. Graft marker A gives projections B and C on the films. With a known focus position, projection lines 1 and 2 can be reconstructed. The calculation of intersection of 1 and 2 in space gives the position of A.

the smaller the crossing line error, the more accurate the calibrated set-up and measurement. A typical crossing line error is 0.02 mm.

Because the calibration is performed with the aid of the box under the patient, each new image is calibrated according to its laboratory coordinate system. Positioning of the patient does not influence the measurement because the distance between reference marker and graft marker is determined according to the coordinate system.

FRSA

Fluoroscopic roentgen stereophotogrammetric analysis (FRSA) is a novel application of RSA principles and technique to high definition digital stereo fluoroscopy with a high frame rate (images per second). This enables imaging and quantification of marker motion, for instance during the cardiac cycle. Until recently, equipment with these specifications was not available. In June 2005 a Siemens Axiom Artis dBc imaging system was placed in the Leiden University Medical Center, and we developed and validated a method to accurately quantify three

dimensional marker motion at a high frame rate.[13] This has been impossible up to now, despite advanced imaging systems like (ECG-gated) CT and MRI. FRSA could therefore be of great value to the knowledge of stentgraft motion and stentgraft improvement.

As explained above, RSA with still images is constrained to longer term follow-up because only one image can be produced at a time. In order to quantify marker motion, several images need to be acquired per second, comparable to cinematography. These images need to be calibrated in a similar way as RSA images.

The FRSA set-up and calibration process is different from regular RSA at several points in the process.

The FRSA set-up

The set-up consists of two C-arms with digital flat panel detectors (Siemens Axiom Artis dBc imaging system, Siemens, Forcheim, Germany). The C-arms are positioned at a 90º angle, producing a lateral and a postero-anterior (PA) image (Figure 4). In contrast to standard RSA, the 90º angle is chosen for two reasons: a) practical reasons, since this is a standard setting in the machine; b) for maximum accuracy, since on theoretical grounds a 90º angle will result
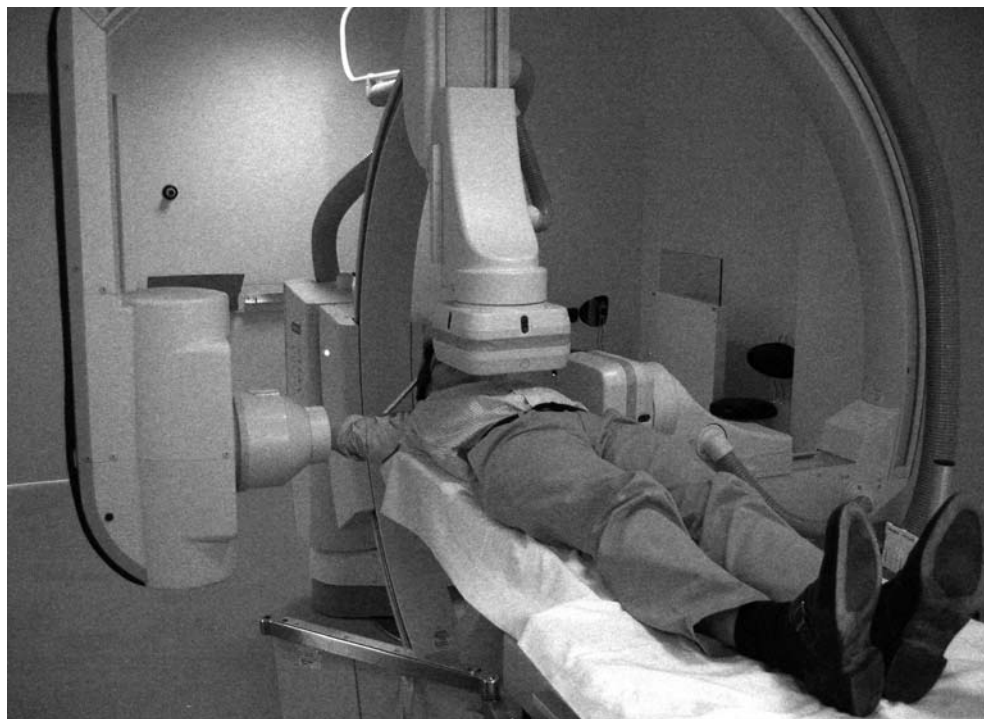
Figure 4. Clinical set-up of the bi-plane fluoroscope.

in a maximum angle of the imaging on the direction of the marker motion (as little out of plane motion as possible). To maximize the field of view, the detectors are placed as close to the patient as possible. The set-up acquires high definition digital stereo images of the body at a frame rate of 30 bi-directional frames per second. The stereo images are acquired as two alternate single images (i.e. 60 single frames per second). The exposure time of each image is approximately 4 ms. The pause between the PA and the lateral image is approximately 12.7 ms.

The image pairs are analyzed using Model-based RSA software (MB-RSA, MEDIS specials, Leiden, The Netherlands) to calculate the relative 3-D marker positions.[8-11] No image reconstruction is required before analyzing the image pairs.

Calibration of the FRSA set-up

To calibrate the set-up, an acrylic block is used with markers at precisely known positions (Figure 5). A FRSA (stereo) image of this block is acquired with the set-up. Afterwards, the process, as described above, of calculation of the position of markers with the MB-RSA software is reversed. This time the position of the markers is known and therefore the position of the foci and the detectors can be calculated, as well as their position in relation to each other. The patient is positioned in the set-up without changing the C-arm positions. Once the position of the foci and the detectors is known, this can be fed into the software and images of the patient can be analyzed in the standard way as described for RSA, revealing the positions of the markers on the stent-graft.

Figure 5. Calibration object. Acryllic block, dimensions w x d x h: 8 x 8 x 5 cm. In every corner one tantalum marker, diameter 1mm. In the top layer three extra markers, diameter 2mm for ease of identification of the different markers.

References

1. Sundfeldt M, Carlsson LV, Johansson CB, Thomsen P, Gretzer C. Aseptic loosening, not only a question of wear: a review of different theories. Acta Orthop. 2006 Apr;77(2):177-97.
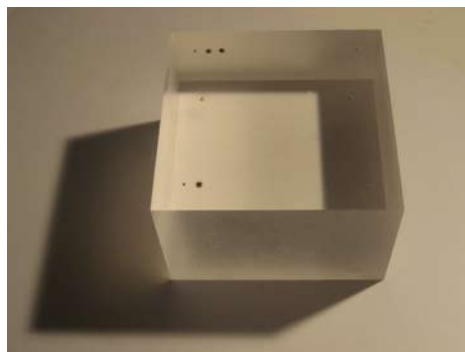
2. Herberts P, Malchau H. Long-term registration has improved the quality of hip replacement: a review of the Swedish THR Register comparing 160,000 cases. Acta Orthop Scand 2000; 71 (2): 111-21.

3. Robertsson O, Knutson K, Lewold S, Lidgren L. The Swedish Knee Arthroplasty Register 1975-1997: an update with special emphasis on 41,223 knees operated on in 1988-1997. Acta Orthop Scand 2001; 72 (5): 503-13.

4. Kärrholm J, Borssen B, Lowenhielm G, Snorrason F. Does early micromotion of femoral stem prostheses matter? 4–7-year stereoradiographic follow-up of 84 cemented prostheses. J Bone Joint Surg Br. 1994;76:912–917.

5. Ryd L, Albrektsson BE, Carlsson L. F. Dansgard F, Herberts P, Lindstrand A, Regner L, and S. Toksvig-Larsen. Roentgen stereophotogrammetric analysis as a predictor of mechanical loosening of knee prostheses. J Bone Joint Surg Br. 1995;77:377–383.

6. Kärrholm J. Roentgen stereophotogrammetry. Review of orthopedic applications. Acta Orthop Scand. 1989;60:491–503.

7. Kärrholm J, Gill RH, Valstar ER. The history and future of radiostereometric analysis. Clin Orthop Relat Res. 2006 Jul;448:10-21.

8. Valstar ER, Vrooman HA, Toksvig-Larsen S, et al. Digital automated RSA compared to manually operated RSA. J Biomech. 2000;33:1593–1599.

9. Vrooman HA, Valstar ER, Brand GJ, et al. Fast and accurate automated measurements in digitized stereophotogrammetric radiographs. J Biomech. 1998;31:491–498.

10. Valstar ER, de Jong FW, Vrooman HA, et al. Model-based Roentgen stereophotogrammetry of orthopaedic implants. J Biomech. 2001;34: 715–722.)

11. Kaptein BL, Valstar ER, Stoel BC, Rozing PM, Reiber JAC. A new model-based RSA method validated using CAD models and models from reversed engineering. *J Biomech*. 2003;36:873-882.

12. Valstar ER. Digital roentgen stereophotogrammetry. Development, validation, and clinical application. Thesis, Leiden University. Den Haag, The Netherlands: Pasmans BV, 2001.

13. Koning OH, Kaptein BL, Garling EH, Hinnen JW, Hamming JF, Valstar ER, Bockel JH. Assessment of three-dimensional stent-graft dynamics by using fluoroscopic roentgenographic stereophotogrammetric analysis. J Vasc Surg. 2007 Oct;46(4):773-779. Epub 2007 Aug 30.

PART

I

Surveillance of stent-graft migration after EVAR

C H A P T E R

3

Roentgen Stereophotogrammetric Analysis: An Accurate Tool to Assess Stent-Graft Migration

Olivier H.J. Koning

Olivier R. Oudegeest

Edward R. Valstar

Eric H. Garling

Edwin van der Linden

Jan-Willem Hinnen

Jaap F. Hamming

Albert M. Vossepoel

and J. Hajo van Bockel

Abstract

Purpose: To evaluate in an in vitro model the feasibility and accuracy of Roentgen stereo-photogrammetric analysis (RSA) versus computed tomography (CT) for the ability to detect stent-graft migration.

Methods: An aortic model was constructed from a 22-mm-diameter Plexiglas tube with 6-mm polytetrafluoroethylene inlays to mimic the renal arteries. Six tantalum markers were placed in the wall of the aortic tube proximal to the renal arteries. Another 6 markers were added to a Gianturco stent, which was cast in Plexiglas and placed inside the aorta and fixed to a micromanipulator to precisely control displacement of the stent along the longitudinal axis. Sixteen migrations were analyzed with RSA software and compared to the micromanipulator. Thirty-two migrations were measured by 3 observers from CT images acquired with 16×0.5-mm beam collimation and reconstructed with a 0.5-mm slice thickness and a 0.4-mm reconstruction interval. Measurements were made with Vitrea postprocessing software using a standard clinical protocol and central lumen line reconstruction. Results of CT were also compared to the micromanipulator.

Results: The mean RSA measurement error compared to the micromanipulator was 0.002 ± 0.044 mm, and the maximum error was 0.10 mm. There was no statistically significant interobserver variability for CT ($p=0.17$). The pooled mean (maximum) measurement error of CT was 0.14 ± 0.29 (1.00) mm, which was significantly different from the RSA measurement error ($p<0.0001$).

Conclusion: Detection of endograft migration by RSA is feasible and was significantly more accurate than CT in this nonpulsatile in vitro model.

Introduction

Endograft migration is a well recognized complication after endovascular aneurysm repair (EVAR) of an abdominal aortic aneurysm (AAA).[1,2] Contrast-enhanced computed tomographic angiography (CTA) is the current gold standard to detect endograft migration.[3] However, CT has several adverse effects, including high radiation dose and the use of nephrotoxic intravascular contrast. With the widespread use of EVAR, CT surveillance also places increasingly high logistical and economical burdens on hospitals,[4] considerations that have led many centers to reduce the frequency of CT after EVAR, especially if there is evidence of sac shrinkage.[5] Less frequent CT scans may be feasible; however, there is the risk of unnoticed migration. Clearly, there is a need for another type of imaging modality to follow the thousands of patients with aortic endografts.

Roentgen stereophotogrammetric analysis (RSA) was introduced by Selvik[6] in 1974 and became the gold standard for assessing micromotion of orthopedic implants[7-10]; the technique now is used widely across northern Europe. RSA is based on calculating the 3-dimensional (3D) position of markers from stereo images.[9] The technique is relatively simple, requiring only 2 standard Roentgen tubes, a calibration box with markers, and computer software for the analysis. The major advantages of RSA are the fact that intravascular contrast is not required and the radiation dose is only 0.3 mSv. Furthermore, RSA is a low-cost and time efficient method that can be performed by a trained technician.

Georg et al.[11] recently described the use of RSA to detect stent-graft migration in a model. However, they showed only reproducibility of marker position measurement with RSA in an endovascular setting. The accuracy of RSA to detect stent-graft migration is still unknown. To evaluate the possible role of RSA in the follow-up after EVAR, we tested the feasibility and accuracy of RSA in an in vitro model of endograft migration.

Methods

Aortic Model With Stent-Graft

An aortic model (Figure 1) was constructed from a 22-mm-diameter Plexiglas tube to simulate the aorta. The tube had 2 6-mm-diameter polytetrafluoroethylene tubes inserted to mimic the renal arteries with intravascular contrast, used for CT analysis. RSA requires the use of markers, so 6 1-mm-diameter tantalum markers were placed in the wall of the aortic tube proximal to the renal arteries. Another 6 tantalum markers were added to a Gianturco stent (Cook Inc.,

I RSA: Accurate tool to assess S-G migration

3

I   RSA: Accurate tool to assess S-G migration

Figure 1. Model used in the experiments. The micromanipulator can displace the stent in a highly controlled manner along the axis of the aorta. Markers are placed on the stent and inside the aorta for RSA analysis. Renal arteries (arrow) are mimicked by polytetrafluoroethylene inlays in the wall of the aorta for CT analysis.
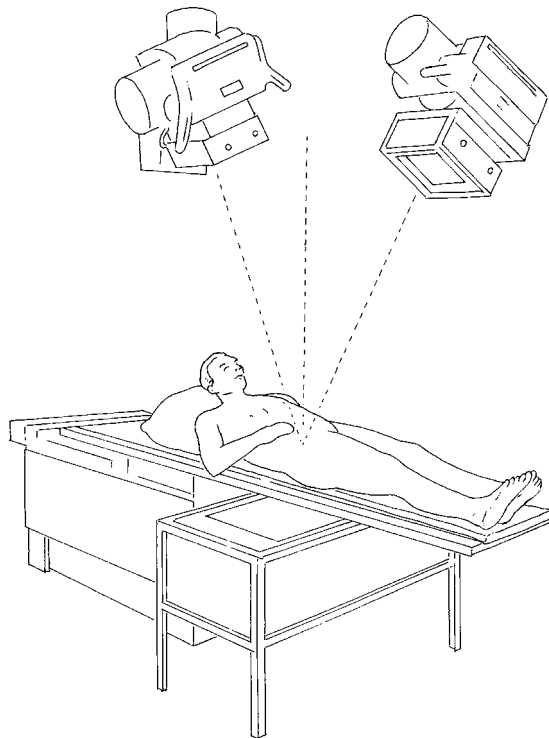

Figure 2. RSA imaging setup. The reference and control markers are in the box under the patient. The radiographic films are placed directly under the box.
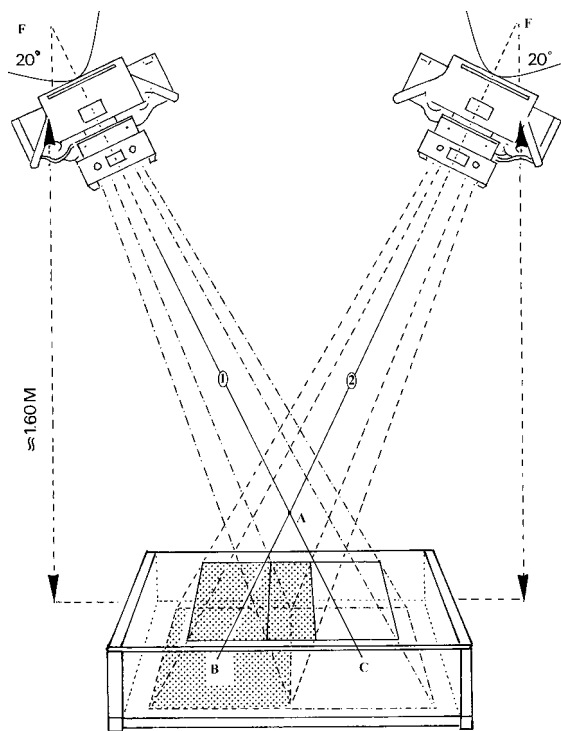
Figure 3. Schematic drawing of the RSA technique. The projection of the calibration box markers on the film is used to reconstruct the position of the Roentgen foci (F). Graft marker A gives projections B and C on the films. With a known focus position, projection lines 1 and 2 can be reconstructed. The calculation of intersection of 1 and 2 in space gives the position of A.

Bjaeverskov, Denmark), which was then cast in Plexiglas, making rotational movement and stent distortion impossible. The encased stent was placed inside the aorta and fixed to a micro-manipulator (Thesa, Veenendaal, The Netherlands) to precisely control displacement of the stent along the longitudinal axis of the aorta. The increments of the micromanipulator were accurate up to 0.01 mm according to the manufacturer, which was confirmed by laboratory testing at our institution. To simulate soft tissue, 22 cm of Plexiglas was placed on top of the model during RSA imaging.[12]

RSA Imaging Technique

The RSA setup (Figure 2), identical to that used for orthopedic evaluation,[13] consisted of 2 Roentgen tubes (Philips Rotalix, 90 kV/100 mAs and a Philips Practix 2000, 90 kV/60 mAs; Philips Medical Systems Europe, Amsterdam, The Netherlands) positioned 1.5 meters above a

pair of 35×43-cm Roentgen cassettes (Kodak, Amsterdam, The Netherlands) at a 20° angle to the vertical. To define a 3D laboratory coordinate system, 50 1-mm-diameter tantalum reference markers were positioned in the lower plane of a calibration box. In order to calculate the Roentgen focus position, 24 1-mm tantalum control markers were positioned in the upper plane of the box. The films were placed directly under the box (Figure 3).

First, a reference RSA image was taken by simultaneously exposing the films, and then the stent was moved longitudinally in 0.1-mm increments up to 15 mm using the micromanipulator. One migration of 20 mm was also created. After each migration, an RSA image was taken. The 16 images were randomly numbered, and the reviewer was blinded as to the distance of migration induced. The RSA software determined the distance between the aortic markers and the stent markers. It then compared this distance to the reference image to determine the extent of migration. This measurement was then compared to the micromanipulator to calculate the measurement error of the technique. Figure 4 shows the RSA software reconstruction of the marker and x-ray focus positions in space in relation to the 2 images.

Subsequently, the radiographs were digitized by scanning with a Vidar VXR-12 scanner (Vidar, Lund, Sweden) at a 150-dots/inch, 8-bit grayscale resolution. The RSA-CMS software (MEDIS,
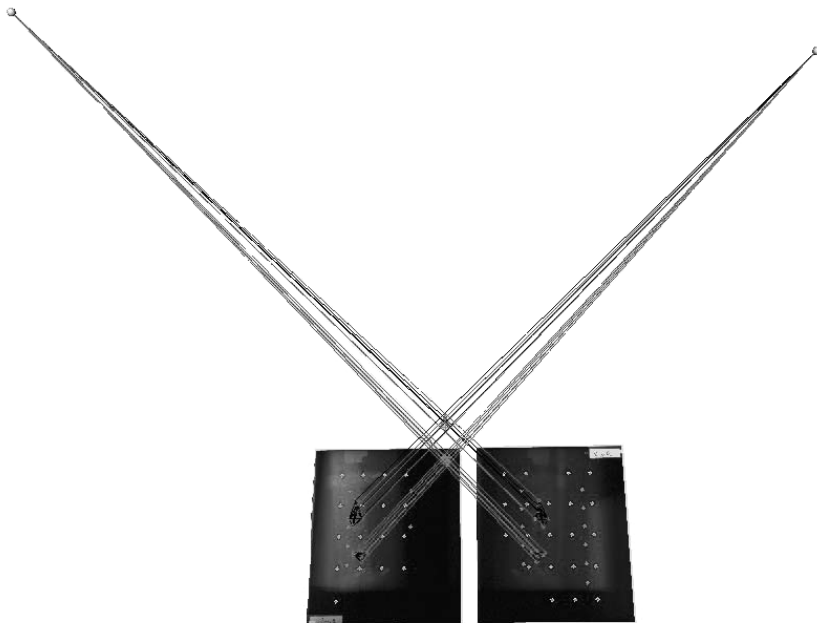

Figure 4. RSA software reconstruction of the position of the 2 Roentgen foci, the stent-graft markers, and reference markers in space (crossing lines). These positions were reconstructed from the 2 radiographs (black).

Leiden, The Netherlands) automatically measured the marker coordinates in the digitized radiographs from the 3D reconstruction of the marker positions to measure micromotion.[8-10]

CTA

The same techniques for acquiring, postprocessing, and analyzing CT data to measure endograft position were the same as those used for EVAR surveillance in our clinic The images were acquired with a Toshiba Aquilion 16 multidetector CT scanner (Toshiba Medical Systems Europe, The Netherlands) set to the following parameters: 80 kV, 200 mAs, 1-second rotation, pitch 0.7, and 0.5-mm collimation; images were reconstructed with a 0.5-mm slice thickness and a 0.4-mm reconstruction interval. A reference scan was made, and then the stent was moved longitudinally in 0.5-mm increments up to 15 mm using the micromanipulator. One migration of 20 mm was also created. After each migration, a CT scan was made, for a total of 32 CT scans. Because CT involves human action and possible interpretation error, the number of CTs created was double that of the RSA setup. The CT images were randomly numbered, and the observers were blinded to the amount of migration induced. Using the Vitrea2 postprocessing software (Vital Images Inc., Plymouth, MN, USA), the images were reconstructed along the central lumen line. The distance was measured from just below the most caudal renal artery to the level where the first circumferential view of the stent was obtained. The struts of the stent were used for orientation. No special markers were used for CT measurement. To correct for interobserver variability, the CT scans were evaluated by 3 medical specialists (2 interventional radiologists and a vascular surgeon who were all experienced with this protocol). The distances measured in the 32 CT images were compared to the reference image. The migration thus measured was compared to the micromanipulator to determine the measurement error of the technique.

Statistical Analysis

Levene's test for variance was used to detect statistically significant interobserver variability between the measurement errors of the 3 CT readers. An F-test was used to compare the pooled CT measurement errors to the measurement error of RSA. $P < 0.05$ represented a statistically significant difference. The tests were performed using SPSS for Windows (version 11.0; SPSS Inc., Chicago, IL, USA).

Results

The mean measurement error for RSA compared to the micromanipulator was 0.002 ± 0.044 mm, and the maximum error was 0.10 mm. Three observers measured endograft migration (Figure

5) in 32 CTA scans. Compared to the micromanipulator (Figure 6), the mean (maximum) errors were 0.15±0.26 (0.70) mm for observer A, 0.25±0.36 (1.00) mm for observer B, and 0.02±0.23 (0.70) mm for observer C. There appeared to be no significant interobserver variability (p=0.17). Pooling the CT measurement errors of the 3 observers resulted in a pooled mean (maximum) error of 0.14±0.29 (1.00) mm, which was significantly different from the 0.002±0.044-mm RSA measurement error (p<0.0001).
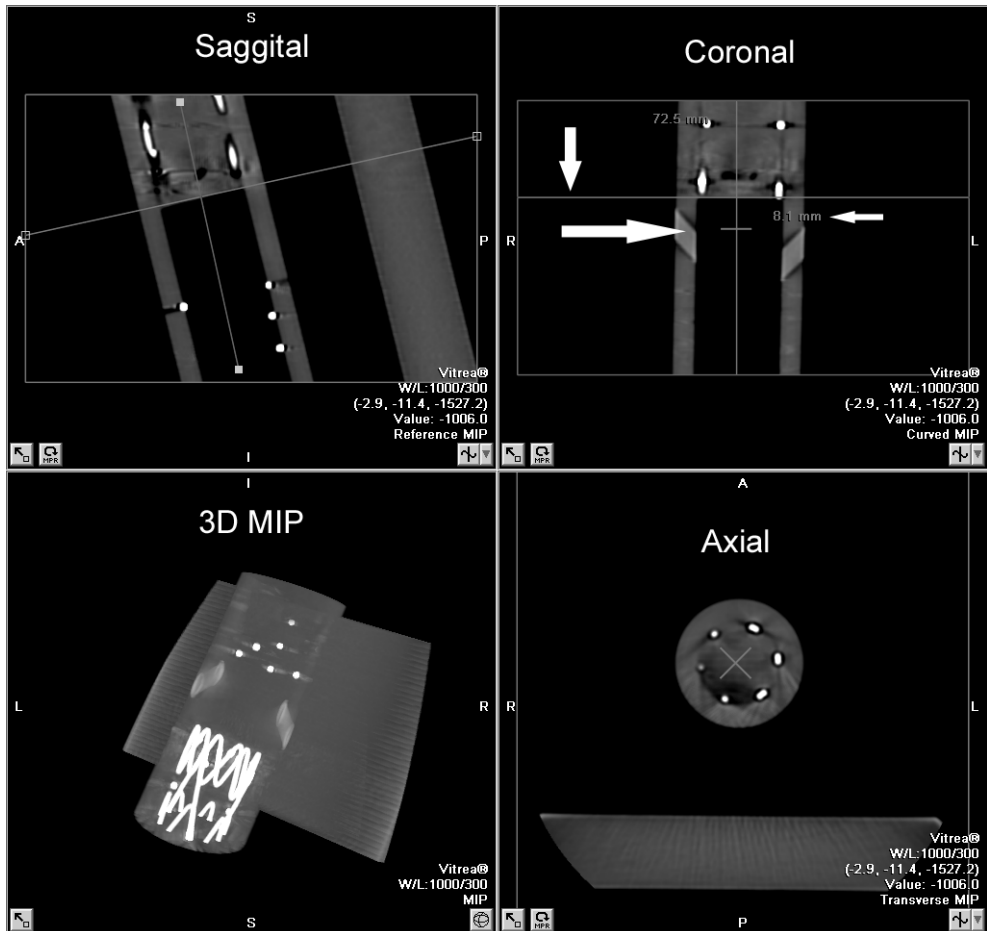

Figure 5. CT image reconstruction with Vitrea2 software. The caudal margin of the renal artery is identified (coronal image, largest arrow) on the axial image and the "ruler" is set to 0 mm. Afterward, the axial image is used to determine the first image with a circumferential view of the stent (axial image and coronal image, vertical arrow). The measurement is now taken (coronal image, smallest arrow).
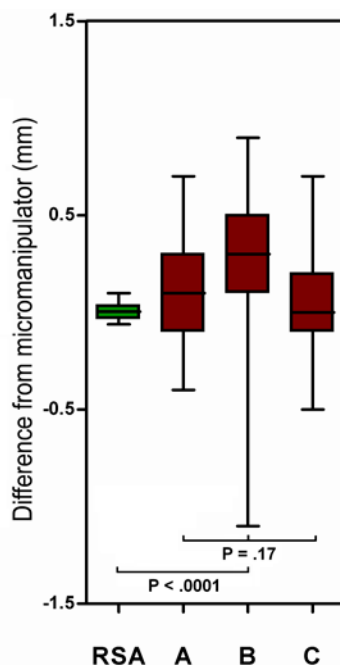
Figure 6. Box plot of the measurement errors of RSA and CT (observers A, B, and C) compared to the micromanipulator. The median, 10th, 25th, 75th, and 90th percentiles are given in mm.

Discussion

The use of RSA to evaluate endograft migration is promising for several reasons. Perhaps the most important advantage of RSA is that it does not require intravascular contrast to accurately determine stent-graft position, which is an asset in a patient population with a significant incidence of renal dysfunction. Plain CT without contrast enhancement may be used for stent-graft migration assessment, but it is likely that this reduces the accuracy of identifying the renal arteries consistently in consecutive scans.

Comparing radiation doses, RSA results in a radiation dose of only 0.3 mSv. In contrast, the radiation dose of CT is much higher, ~17 mSv for a complete triple-phase scan: 6.8 mSv for the unenhanced phase and 6.8 mSv for the early contrast-enhanced phase to measure stent-graft position. The RSA images can also be used to identify other adverse effects, such as possible stent fractures, so that RSA could replace the plain abdominal radiographs that are part of current routine follow-up in most centers.

RSA is a simple technique to use and does not require a large investment in special equipment. The imaging as well as the computerized postprocessing and migration measurement can be

performed by a trained technician instead of a dedicated medical specialist, which makes the investigation far less expensive in terms of logistical burden and healthcare cost. It could thus increase the cost effectiveness of EVAR by reducing the need for serial CTs.

Furthermore, there is the high accuracy of RSA. To our knowledge, no data exist in the literature about the accuracy of CT measurement of stent-graft migration. We used thin 0.5-mm slices for CT and 3D image reconstruction, which resulted in a significantly less accurate migration measurement by CT than by RSA. Thicker CT slices, as are the current practice in follow-up protocols, will undoubtedly result in larger errors of measurement by CT.

Another possible advantage of RSA is that it uses a single 90-ms exposure for the entire field of interest, which is minimally affected by the cardiac cycle and produces a high-definition image with high spatial resolution. Pulsatile changes in the aorta–stent-graft complex[14,15] will result in minimal measurement error due to this short acquisition time.

In terms of image postprocessing, RSA uses digital image processing that will distinguish the points of reference automatically with the help of a computer. To the contrary, CT requires observer-assigned reference points for measurement, which are sensitive to human variance. RSA reference points are constant, inherent metal markers, so accuracy of measurement is higher due to this consistent position.

Finally, there is the measurement of CT itself that can be performed in different ways, varying from workstation "image counting" multiplied by slice thickness to advanced postprocessing software, as used in our study. RSA is a consistent method using one well-established protocol for measuring the distance between reference points. In RSA analysis, the relative positions of markers do not change in the absence of migration. Any change in relative position indicates movement between the markers. Patient position is not critical, as the calibration box will facilitate the calculation of marker coordinates each time an RSA image is taken.

A potentially significant disadvantage of RSA compared to CT with intravascular contrast is the fact that at least one marker is required in the aortic wall as a reference point. Theoretically, one marker is sufficient to accurately measure axial migration. This marker would have to be placed as an additional procedure, preferably during EVAR. After secure fixation, migration of a reference marker is unlikely, as there is no significant dislocating force acting on it. The markers used to identify the endograft could be incorporated during manufacture of the stent-graft without many modifications. Certain endografts already have welding points that might function as markers.

In theory, remodeling of the aorta could lead to erroneous detection of migration. However, the amount of error will be minimal as the reference markers will be placed directly proximal to the stent-graft and renal arteries. The distance between the aortic markers and the stent-graft markers

will therefore be small, and slight changes in the aortic wall in this area will subsequently have minimal significance. The amount and design of the endovascular marker(s) needed for this application is subject to further study at our institution. We are confident that this issue can be resolved.

Currently, plain abdominal radiography may be used to detect endograft migration as an alternative to CT. In this investigation, the lumbar spine is used as a reference. Based on the protocol published by Murphy et al.,[16] a 2-mm margin of error has been reported by Hodgson et al.[17] in an experimental static model that eliminated any pulsatile axial movement of the aorta relative to the spine. Flora et al.[18] measured a pulsatile movement up to 1 mm in just 4 patients,[18] while Vos et al.[14] reported craniocaudal movement of up to 1.99 mm in 7 patients,[14] indicating that a wider range of movement is likely. The measurement error in a static situation versus the pulsatile motion of the aorta–stent-graft complex could significantly impair the accuracy of stent-graft migration assessment with plain radiography.

Other possible errors in the analysis of plain abdominal radiographs are changes in the vertebral column, e.g., due to osteoporosis or fractures, and possibly changes in neck angulation due to AAA shrinkage. RSA uses reference markers in the aorta and is therefore, in theory, not susceptible to pulsatile movement or changes in, or relative to, the vertebral column. Georg et al.[11] described the use of the transverse process of a vertebral body as a reference point to measure stent-graft migration. We believe that this will provide a significant source of error due to the pulsatile movement of the aorta.

When considering our model, it is obvious that all motion artifacts were eliminated in this static setup. To assess the impact of pulsatile motion on the accuracy of RSA, further studies are necessary. Axial movement of the aorta-endograft complex, as well as rotational movement, will probably have insignificant impact on RSA accuracy; endovascular reference markers are placed directly proximal to the endoprosthesis, which eliminates any significant movement between the two. With the use of endovascular reference markers, the vertebral column is no longer required as a reference, and all the abovementioned confounders regarding this structure and its relation to the endoprosthesis can be avoided.

Conclusion

Detection of stent-graft migration by RSA was feasible and significantly more accurate than CT in this nonpulsatile in vitro study. RSA combines high accuracy with low cost in terms of radiation, healthcare cost, and logistics. The absence of intravascular contrast is an additional asset of this method. Further studies are necessary to investigate the application of RSA markers in endovascular surgery and to investigate the influence of pulsatile motion on the accuracy of RSA.

Acknowledgments

References

1. van Marrewijk CJ, Fransen G, Laheij RJ, et al. Is a type II endoleak after EVAR a harbinger of risk? Causes and outcome of open conversion and aneurysm rupture during follow-up. *Eur J Vasc Endovasc Surg*. 2004;27:128-137.

2. Harris PL, Vallabhaneni SR, Desgranges P, et al. Incidence and risk factors of late rupture, conversion, and death after endovascular repair of infrarenal aortic aneurysms: the EUROSTAR experience. *J Vasc Surg*. 2000;32:739-749.

3. Wolf YG, Hill BR, Lee WA, et al. Eccentric stent graft compression: an indicator of insecure proximal fixation of aortic stent graft. *J Vasc Surg*. 2001;33:481-487.

4. Prinssen M, Buskens E, Jong SECA de, et al. Cost-effectiveness of endovascular versus conventional abdominal aortic aneurysm repair at one year. Results of a randomized trial. In: Prinssen M, ed. DREAM. Oud-Beijerland, The Netherlands: As BV; 2005:89-103.

5. Verhoeven EL, Tielliu IF, Prins TR, et al. Frequency and outcome of re-interventions after endovascular repair for abdominal aortic aneurysm: a prospective cohort study. *Eur J Vasc Endovasc Surg*. 2004;28:357-364.

6. Selvik G. Roentgen stereophotogrammetry. A method for the study of the kinematics of the skeletal system. *Acta Orthop Scand Suppl*. 1989;232:1-51.

7. Karrholm J. Roentgen stereophotogrammetry. Review of orthopedic applications. *Acta Orthop Scand*. 1989;60:491-503.

8. Valstar ER, Vrooman HA, Toksvig-Larsen S, et al. Digital automated RSA compared to manually operated RSA. *J Biomech*. 2000;33:1593-1599.

9. Vrooman HA, Valstar ER, Brand GJ, et al. Fast and accurate automated measurements in digitized stereophotogrammetric radiographs. *J Biomech*. 1998;31:491-498.

10. Valstar ER, de Jong FW, Vrooman HA, et al. Model-based Roentgen stereophotogrammetry of orthopaedic implants. *J Biomech*. 2001;34:715-722.

11. Georg C, Welker V, Eidam H, et al. Aortic stent-graft movement detection using digital roentgen stereophotogrammetric analysis on plane film radiographs – initial results of a phantom study. *Rofo*. 2005;177:321-325.

12. Martin CJ, Sutton DG, Workman A, et al. Protocol for measurement of patient entrance surface dose rates for fluoroscopic x-ray equipment. *Br J Radiol*. 1998;71:1283-1287.

13. Valstar ER. Digital roentgen stereophotogrammetry. Development, validation, and clinical application. Thesis, Leiden University. Den Haag, The Netherlands: Pasmans BV, 2001.

14. Vos AW, Wisselink W, Marcus JT, et al. Cine MRI assessment of aortic aneurysm dynamics before and after endovascular repair. *J Endovasc Ther*. 2003;10:433-439.

15. Verhagen HJ, Teutelink A, Olree M, et al. Dynamic CTA for cutting edge AAA imaging: insights into aortic distensibility and movement with possible consequences for endograft sizing and stent design [Abstract]. *J Endovasc Ther*. 2005;12(suppl I):I-45.

16. Murphy M, Hodgson R, Harris PL, et al. Plain radiographic surveillance of abdominal aortic stent-grafts: the Liverpool/Perth protocol. *J Endovasc Ther*. 2003;10:911-912.

17. Hodgson R, McWilliams RG, Simpson A, et al. Migration versus apparent migration: importance of errors due to positioning variation in plain radiographic follow-up of aortic stent-grafts. *J Endovasc Ther*. 2003;10:902-910.

18. Flora HS, Woodhouse N, Robson S, et al. Micromovements at the aortic aneurysm neck measured during open surgery with close-range photogrammetry: implications for aortic endografts. *J Endovasc Ther*. 2001;8:511-520

C H A P T E R

4

Accurate Detection of Stent-Graft Migration in a Pulsatile Aortic Model Using Roentgen Stereophotogrammetric Analysis

---

Olivier H.J. Koning

Eric H. Garling

Jan-Willem Hinnen

Lucia J.M. Kroft

Edwin van der Linden

Jaap F. Hamming

Edward R. Valstar

and J. Hajo van Bockel

Abstract

Purpose: To evaluate the feasibility and accuracy of Roentgen stereophotogrammetric analysis (RSA) versus computed tomography (CT) for detecting stent-graft migration in an in vitro pulsatile circulation model and to study the feasibility of a nitinol endovascular clip (NEC) as an aortic wall reference marker for RSA.

Methods: An aortic model with stent-graft was constructed and connected to an artificial circulation with a physiological flow and pressure profile. Tantalum markers and NECs were used as aortic reference markers for RSA analysis. Stent-graft migrations were measured during pulsatile circulation with RSA and CT. CT images acquired with 64×0.5-mm beam collimation were analyzed with Vitrea postprocessing software using a standard clinical protocol and central lumen line reconstruction. RSA in the model with the circulation switched off was used as the reference standard to determine stent-graft migration. The measurement errors of RSA and CT were determined during pulsatile circulation.

Results: The mean measurement error ± standard deviation (maximum) of RSA during pulsatile circulation using the tantalum markers was –0.5±0.16 (0.7) mm. Using the NEC, the mean (maximum) measurement error was –0.4±0.25 (1.1) mm. The mean (maximum) measurement error of CT was –1.1±1.17 (2.8) mm.

Conclusion: RSA is an accurate and feasible tool to measure stent-graft migration in a pulsatile environment. Migration measurement with RSA was more accurate than CT in this experimental setup. The nitinol clip tested in this study is potentially feasible as an aortic reference marker in patients after endovascular repair.

Introduction

Stent-graft migration is a potential complication after endovascular aneurysm repair (EVAR) of an abdominal aortic aneurysm (AAA) .[1-3] Periodic surveillance is necessary to detect migration and other complications.[4,5] The current gold standard for follow-up after EVAR is contrast-enhanced computed tomography (CT).[6] However, this modality requires intravascular contrast, a high radiation dosage, and significant logistical consequences and costs, making EVAR less cost effective.[7] For these reasons, the use of CT for routine surveillance after EVAR is less attractive. Reducing the frequency of CT imaging in EVAR surveillance may be possible, especially if there is evidence of sac shrinkage.[8] However, stent-graft migration may go unnoticed as a result of this reduced imaging frequency.

Roentgen stereophotogrammetric analysis (RSA) may be a valuable alternative to identify stent-graft migration.[9] This technique is a well established and highly accurate tool to detect 3-dimensional micromotion of orthopedic implants in relation to tantalum reference markers in the bone.[9-13] The potential benefits of RSA are low costs, low radiation dose, and no intravenous contrast enhancement. In addition to these potential benefits of RSA, its highly accurate method of measurement could be of great advantage in detecting migration in the early period after introduction of new endografts.

Furthermore, RSA data acquisition and analysis is simple and fast and can be performed by a trained technician. Since RSA images are stereo plain abdominal radiographic images, they can also be used to detect stent fractures. In a static model for stent-graft migration, RSA was found to be more accurate than CT.[9]

A disadvantage of RSA is that aortic wall reference markers are required to assess the relative motion of the stent compared to the aorta.[9] The pulsatile change of the aortic diameter results in movement of both the aortic markers and stent-graft markers during the cardiac cycle, which could induce a measurement error in RSA.

In this study, we evaluated the effect of pulsatile motion on the accuracy of RSA and CT in stent-graft migration measurement in an in vitro model for endograft migration with physiological flow and pressure profiles. Furthermore, we tested the feasibility of a nitinol endovascular clip (NEC) as an aortic reference marker for RSA.

Methods

Pulsatile Aortic Model With Stent-Graft

A pulsatile flow model was developed to simulate migration of a stent-graft in the pulsating aorta. A human cadaver spine was obtained from the anatomical department and used according to the standard consent procedures of our Institutional Review Board. A fresh specimen of a pig thoracic aorta was attached to the cadaver spine, replacing the cadaveric aorta. The spine, including the surrounding soft tissues, was conserved in a solution of formaldehyde, ethanol, glycerin, and phenol (Figure 1). Since accurate CT analysis requires a reference point (usually a renal artery), a side branch was anastomosed to the aorta at the level of the cadaver's renal artery. The model was placed in a Plexiglas box, topped off with water to simulate soft tissue.

The perfusate of this artificial circulation was starch solution with the same viscosity as blood. To enable CT analysis, the perfusate was enhanced with intravascular contrast [iomeprol 816.5 mg/mL (Iomeron 400); Altana Pharma, Hoofddorp, The Netherlands) to a level of 250 Hounsfield units, which is similar to the attenuation in a normal abdominal CT scan. The

Figure 1. The porcine aorta fixed to the human cadaveric spine. A side branch was attached to the aorta at the site of the original renal artery. Cranial side to the left.

contrast was washed out by changing the perfusate after each CT acquisition, so RSA imaging was not disturbed by the contrast medium.

To generate pulsatility, the model was connected to an artificial circulation set at 70 beats per minute with a 75 mL/s flow rate, which produced a physiological flow and pressure profile (Figure 2 and 3).[14] The pulsatility resulted in a luminal diameter change from 20.0 to 21.5 mm, as recorded in M-mode ultrasound with a 7.5-MHz linear array probe (ProSound SSD-5500; ALOKA, Tokyo, Japan). This diameter change was induced to simulate aortic diameter changes measured in vivo.[16-18]
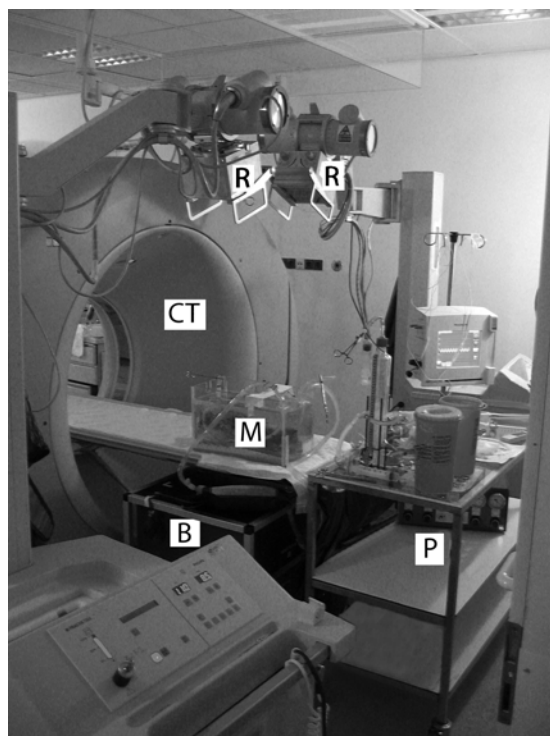
Figure 2. Experimental setup. The model (M) is placed on the CT table. Imaging can be switched between RSA and CT without disturbing the model. The physiological flow and pulsatility is generated with an artificial circulation (P). The RSA setup is positioned next to the CT gantry (CT). Two crossing X-ray beams from the 2 Roentgen foci (R) expose the films under the calibration box (B).

A Gianturco stent (Cook, Bjaeverskov, Denmark) was placed inside the aorta (Figure 4). A stent rather than a stent-graft was used to model migration since radiological imaging techniques use the stents of the stent-graft for analysis. Furthermore, deleting the fabric from the model facilitated the induction of migration. The stent could be "migrated" along the aorta by pulling
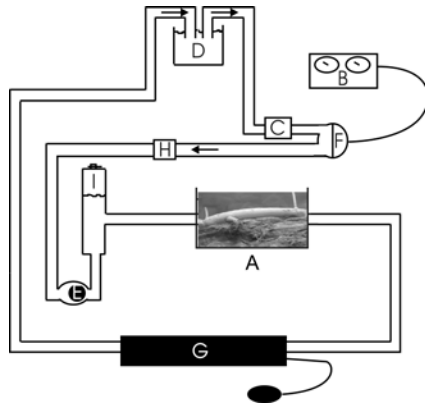
Figure 3. Schematic representation of the model, which consists of the aortic model with stent-graft (A), an artificial heart driver (B), a valve (C), an open reservoir (D), a ball valve (E), left ventricle (F), a blood pressure cuff (G), a flow transducer (H), and an air chamber (I). Fluid pressures were measured at the entrance of the aortic model.

Figure 4. 3D maximum intensity projection of the CT image of the model. Short arrow lower left: tantalum marker; short arrow upper left: nitinol clip; long arrow lower right: renal artery. Cranial side to the left.

on monofilament fishing wire (Spro, Vianen, The Netherlands), which was attached to each side of the stent. To prevent unintended migration, the fishing wire was fixed to the box during the measurements.

For RSA analysis, markers were added at the cranial and caudal corners of the stent (i.e., *stent-graft markers*), and reference markers were attached to the aorta (i.e., *aortic markers*). Two sets of *aortic markers* were tested: (1) 3 clusters of 1-mm-diameter tantalum markers glued to the aortic adventitia with Histoacryl (B. Braun Aesculap, Tuttlingen, Germany), representing the standard clinical RSA situation used in orthopedics (Figure 4), and (2) 3 Anson Refix nitinol endovascular clips (NEC; Figure 5) (Lombard Medical, Didcot, UK) placed in the aortic wall by an endovascular technique to mimic the clinical situation (Figure 4).

Three stent-graft positions were analyzed with RSA and CT: the initial or reference position and 2 migrations. The stent-graft was migrated caudally under visual control provided by an image intensifier (Philips BV300 plus; Philips Medical Systems Europe, The Netherlands).

Figure 5. Nitinol endovascular clip.

RSA Imaging Technique

Two manually synchronized, standard, mobile Roentgen tubes (Philips Practix 2000; Philips Medical Systems Europe) were set to 110 kV/8.5 mAs, resulting in an exposure time of 78 ms for all RSA images. A calibration box was positioned between the model and the radiographic films to define a 3D laboratory coordinate system and to determine the position of the Roentgen foci (Figure 6 and 7).[9] Defining the 3D laboratory coordinate system in each RSA image eliminates any influence of model (or patient) positioning on the outcome of RSA measurements (Figure 8). After digitizing the films, image postprocessing was performed on a personal computer with the help of RSA-CMS software[11-13,15] (MEDIS, Leiden, The Netherlands).[9] The RSA images were randomly numbered, and the reviewer was blinded to the degree of induced migration. Using this technique, it was possible to calculate the distance between 2 groups of markers. Migration was determined by comparing an initial reference RSA image to the follow-up RSA image.
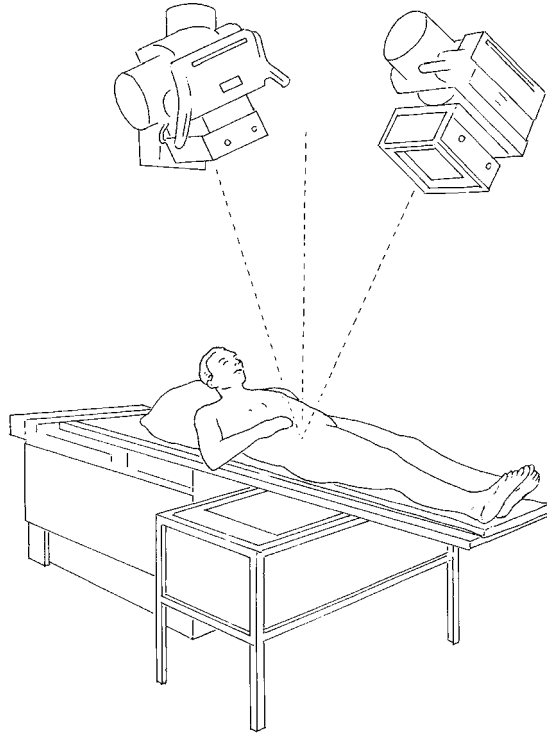
Figure 6. RSA imaging setup. The box under the patient contains markers that are used to define the Roentgen setup and measurement coordinates. The radiographic films are placed directly under the box.

Since RSA is proven to be highly accurate in a static environment,[9-13] RSA of the model without pulsatile circulation was used as the reference standard to determine actual stent-graft migration,[9] using the tantalum aortic reference markers for the analysis. Five RSA images of the reference position and 3 images of each stent-graft position after migration were acquired. These results would later be compared to RSA and CT analysis with pulsatile circulation in the model to determine the measurement error of the 2 techniques. The migration was assessed using cross-table analysis, comparing each of the 5 reference images to all 3 follow-up images, producing 15 measurements per migration.

To determine the influence of pulsatility on RSA migration measurement, 11 RSA images were acquired of each stent-graft position at a random point in the pulsatile circulation cycle. Migration was determined by cross-table analysis, comparing each of the 11 reference images to all 11 follow-up images, resulting in 121 measurements per migration or 121 possible clinical combinations of RSA images. The measurements were performed using tantalum markers as well as NECs. The measured migration with RSA was compared to the actual migration to determine the measurement error of RSA with both types of aortic reference markers.
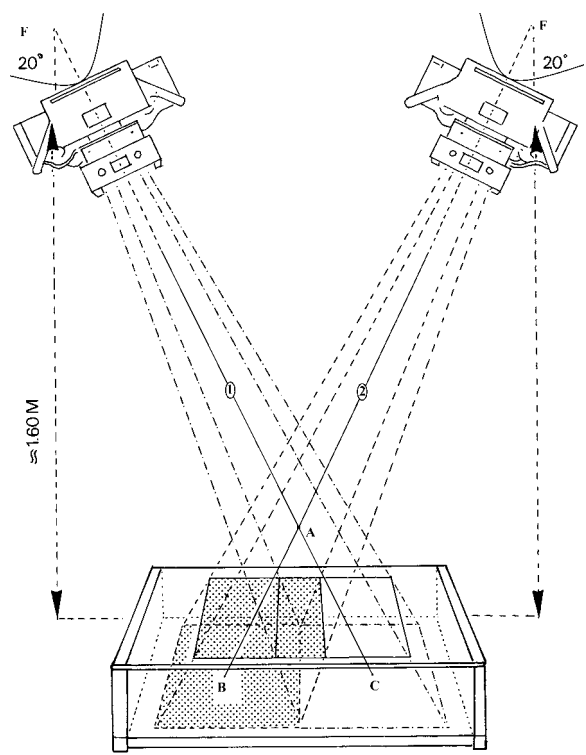
Figure 7. Schematic drawing of the RSA technique. The projection of the calibration box markers on the film is used to reconstruct the position of the Roentgen foci (F). Graft marker A gives projections B and C on the films. With known focus position, projection lines 1 and 2 can be reconstructed; calculating the intersection of 1 and 2 in space gives the position of A.
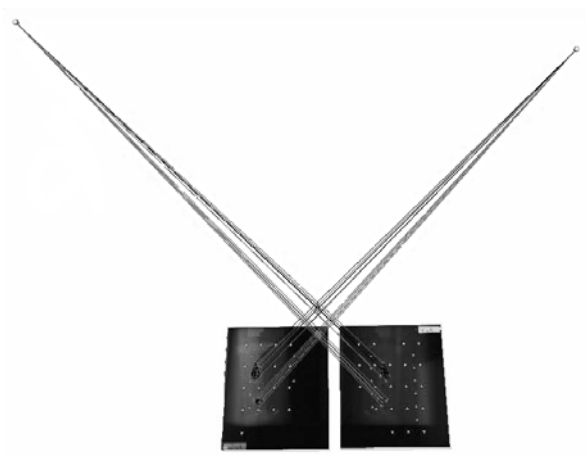

Figure 8. RSA software reconstruction of the position of the 2 Roentgen foci and the stent-graft markers and reference markers in space (crossing lines). These positions were reconstructed from the 2 radiographic images (black).

Computed Tomography

To compare the results of RSA to those of CT, the accuracy of CT measurement with 3D image reconstruction was determined using the same technique for postprocessing and analysis to measure stent-graft position as the one used for CT surveillance in our clinic. The CT images were acquired with a Toshiba Aquilion 64 CT scanner (Toshiba Medical Systems, Otawara, Japan), which was set to 120 kV, 250 mA, 400-ms rotation, pitch factor 0.84, 0.5-mm beam collimation, and 64 detector rows during pulsatile flow in the model. The images were reconstructed with a 0.5-mm thickness and 0.4-mm reconstruction interval.

A reference CT scan was made of the initial stent-graft position. After each migration, a follow-up CT scan was produced. The CT images were randomly numbered, and the observers were blinded to the amount of migration induced. Using Vitrea2 postprocessing software (Vital Images Inc., Plymouth, MN, USA), the amount of migration was measured on 3D curved multiplanar reconstructions along the aortic central lumen line to evaluate the aorta in 2 perpendicular longitudinal directions as well as the perpendicular axial direction. Using automatic calipers, the distance was measured between the lower margin of the renal artery (reference point) and the stent at the level where the first circumferential view of the stent was observed (in perpendicular axial direction). The struts of the stent were used for orientation; no special markers were used for CT measurement.

The CT scans were evaluated by 5 observers: 4 interventional radiologists and a vascular surgeon, all experienced users of this technique. Migration was determined by comparing the distance measured by the same observer in the follow-up CT images to the distance in the reference CT. The resulting migration was compared to the actual migration to determine the measurement error of CT.

Statistical Analysis

Data are presented as the mean ± standard deviation (SD) and maximum. Levene's test for variance was used to detect statistically significant interobserver variability between the measurement errors of the 5 CT readers. The tests were performed using SPSS for Windows (version 11.0; SPSS Inc., Chicago, IL, USA).

Results

The actual migration of the stent-graft as determined by RSA without pulsatile circulation was 7.0±0.02 mm for the first migration (n=15) and 13.9±0.03 mm for the second migration (n=15). For the first migration measured during pulsatile flow (n=121), the mean distance was 6.5±0.08

mm measured by RSA using the tantalum aortic reference markers, which gave a mean (maximum) measurement error of –0.5±0.08 (0.7) mm. For the second migration measured during pulsatile flow (n=121), the mean measured distance was 13.4±0.21 mm, for a mean (maximum) measurement error of –0.5±0.21 (0.7) mm. The pooled error of all migration measurements by RSA in the pulsatile situation using tantalum aortic markers (n=242) was –0.5±0.16 mm (maximum error 0.7 mm). (Figure 9)

Using the NECs as aortic reference markers, the mean distance of the first migration (n=121) measured by RSA was 6.7±0.19 mm [–0.3±0.19 (0.7) mm mean (maximum) measurement error]. The mean distance of the second migration (n=121) was 13.3±0.24 mm [—0.6±0.24 (1.1) mm mean (maximum) measurement error]. The pooled measurement error of all migration measurements by RSA in the pulsatile situation using NECs as reference markers (n=242) was –0.4±0.25 mm (maximum error 1.1 mm). (Figure 9)
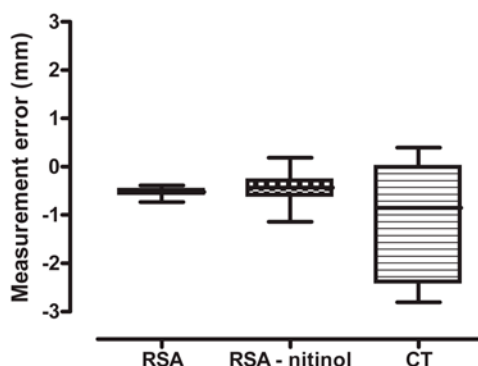

Figure 9. Box plot of the measurement errors of RSA with tantalum aortic markers (RSA), RSA with nitinol endovascular clips as aortic markers (RSA-nitinol), and CT using the renal artery as a reference (CT) compared to the measurement with RSA in a static situation. Median (line), 25th and 75th percentiles (boxes), and range (whiskers) are plotted.

Stent-graft migration was measured with CT under pulsatile flow in the model using the renal artery as a reference. The mean distance of the first migration (n=5) was 6.2±1.22 mm, for a mean (maximum) measurement error of –0.8±1.37 (2.7) mm versus the actual migration. The mean distance of the second migration (n=5) was 12.5±0.88 mm, which gives a mean (maximum) measurement error of –1.4±0.98 (2.8) mm. The pooled measurement error of all migration measurements by CT (n=10) was –1.1±1.17 mm (maximum error 2.8 mm; Figure 9). There appeared to be no significant interobserver variability (p=0.27).

Discussion

This study shows that roentgen stereophotogrammetric analysis is an accurate tool for the measurement of stent-graft migration despite pulsatile motion of the stent-graft and the aortic markers. RSA, with either tantalum or NEC aortic markers, was more accurate than CT with 3D image reconstruction in determining stent-graft migration in our model with physiological pulsatile flow.

The accuracy of CT and RSA in detecting stent-graft migration has been previously assessed in a static plastic model.[9] The measurement error of RSA was 0.002±0.044 mm versus 0.14±0.29 mm for CT with 3D image reconstruction. When comparing these results to the present study, pulsatile movement caused by a simulated cardiac cycle apparently reduces the accuracy of RSA and CT to a measurement error of –0.5±0.16 mm and 1.1±1.17 mm, respectively. Furthermore, in the present study, RSA in the situation with pulsatile motion was less consistent in migration measurement (SD=0.16 mm) compared with RSA in the static situation (SD=0.02/0.03 mm). This may be explained by the limited temporal resolution in imaging. While the RSA images are acquired, the stent and the aorta will have moved slightly, including the renal arteries, the stent-graft markers, and the aortic markers in the wall of the aorta. This results in an image blurring of markers that may lead to less accurate measurement (Figure 10A,B). Furthermore, the stereo RSA images are taken with manually synchronized X-ray tubes; a delay between the 2 roentgen tubes may cause an additional measurement error because of a slight change in marker position between the stereo images (Figure 10C). Nevertheless, this study shows that RSA measurement errors remain extremely small despite pulsatile movement.

The pulsatile movement also occurs during CT acquisition and could partially explain the decrease in accuracy compared to the static experiments as previously described. In the clinical situation, vessel distention (1- to 2-mm diameter change) and craniocaudal (up to 1.5 mm) and rotational (up to 0.59 mm) movements have been described.[16-19] For both the RSA and CT techniques, image acquisition was performed at random time points during the pulsatile cycle. These pulsatile movements may have influenced the accuracy of stent-graft position measurements for both techniques. Electrocardiographically-gated CT has the potential to significantly reduce the measurement error caused by the cyclic motion of the aorta and stent-graft. However, the disadvantages of CT for follow-up after EVAR, such as the high cost and radiation dose, contrast, and logistical burden, remain or may even increase.

An increasing distance between the aortic and stent-graft markers due to migration caused a slight increase in the error of measurement in our study, which is in accord with orthopedic RSA literature.[20] This implies that for the most accurate RSA measurement of stent-graft migration,
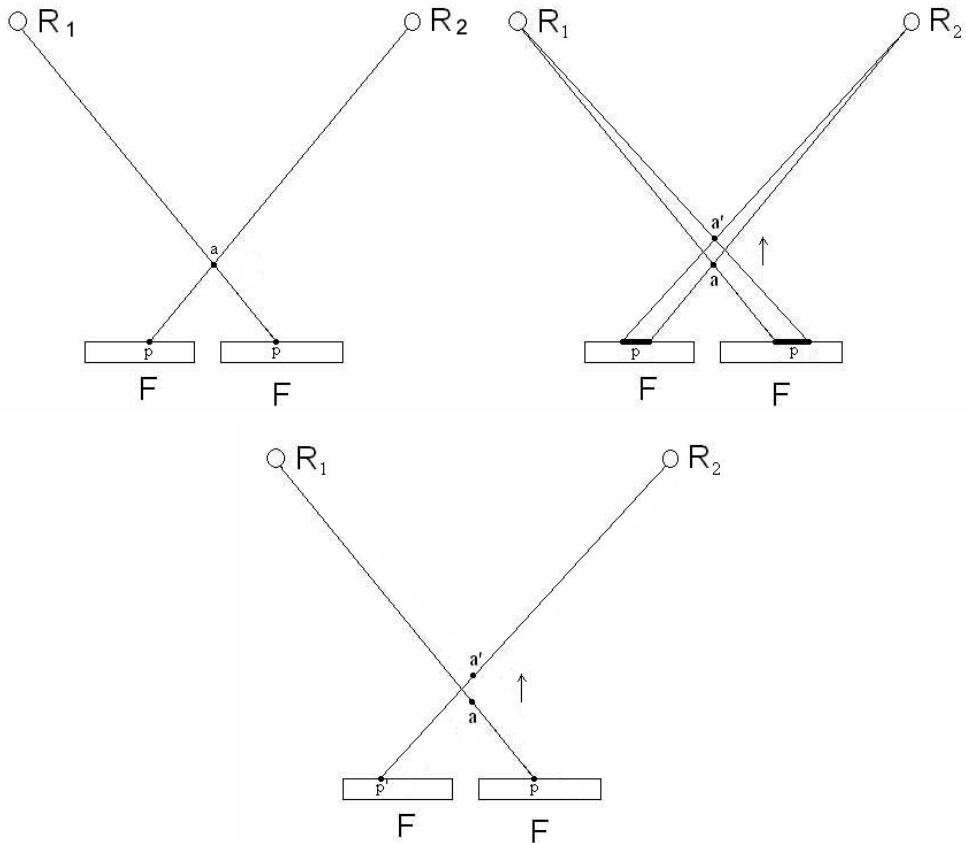
Figure 10. Sources of measurement error in RSA for markers in pulsatile motion versus (**A**) the static situation: marker *a* gives projection *p* on both films *F* after exposure by X-ray foci R$_1$ and R$_2$. (**B**) Movement of the marker *a* to *a'* during image acquisition will blur *p*, resulting in less accurate measurement. (**C**) Delay between the exposures of the 2 films *F* will produce 2 different projections, *p* and *p'*, resulting in less accurate measurement.

the aortic markers need to be positioned as close to the stent-graft as possible. Despite the reduction of accuracy after the 13.9-mm migration reported in our study, RSA is still more accurate than CT. A reason for this finding may be the combination of a higher spatial resolution and a shorter acquisition time of an RSA image compared to CT. For these reasons, using a CT scan with less than 64 detectors could further increase the measurement error of CT.

In the present study, we tested an NEC available for use in endovascular surgery for feasibility of use as an aortic marker. The measurement of stent-graft migration using this clip was also accurate but less precise than the standard tantalum markers. This could be explained by the fact that tantalum markers are spherical and have a smaller diameter (Figure 3), which may

be more accurately detected. Despite this decreased accuracy, RSA with NEC aortic markers remained more accurate than CT. Automatic detection of the NECs by the RSA software was not possible due to their non-spherical shape. Manual identification of the center of the marker could be performed without difficulty using the RSA software, from which the position of the marker could be determined. Marker detection is done at a different phase in the processing of RSA images than the migration measurement, and the reviewer was blinded to the amount of migration. Therefore, manual detection of the clip could not interfere with the outcome of measurement. Despite this potential source of error, the RSA measurements using the NEC were accurate. Therefore, the NEC could potentially be used as an aortic marker for RSA measurement in patients. The NEC requires further testing for its clinical suitability as an RSA marker, which is the subject of further study at our institution.

When considering the model, it is apparent that this is not an in vivo situation. Exact reproduction and modeling of cyclic aortic motion remains difficult. Further testing is needed to evaluate the RSA technique and the endovascular clip before patient studies can be undertaken.

Conclusion

RSA is an accurate and feasible tool to measure stent-graft migration in a pulsatile environment. Migration measurement with RSA is more accurate than with 3D image reconstruction of CT scans. Because RSA has several other advantages over CT, it may be a valuable tool for EVAR surveillance. The nitinol clip tested in this study has the potential to be an aortic reference marker in patients.

Acknowledgements

References

1. van Marrewijk CJ, Fransen G, Laheij RJ, et al. Is a type II endoleak after EVAR a harbinger of risk? Causes and outcome of open conversion and aneurysm rupture during follow-up. *Eur J Vasc Endovasc Surg*. 2004;27:128-137.

2. Harris PL, Vallabhaneni SR, Desgranges P, et al. Incidence and risk factors of late rupture, conversion, and death after endovascular repair of infrarenal aortic aneurysms: the EUROSTAR experience. *J Vasc Surg*. 2000;32:739-749.

3. Sun Z. Three-dimensional visualization of suprarenal aortic stent-grafts: evaluation of migration in midterm follow-up. *J Endovasc Ther*. 2006;13:85-93.

4. Greenberg RK, Chuter TA, Sternbergh WC, et al. Zenith AAA endovascular graft: intermediate-term results of the US multicenter trial. *J Vasc Surg*. 2004;39:1209-1218.

5. Alric P, Hinchliffe RJ, Wenham PW, Whitaker SC, Chuter TA, Hopkinson BR Lessons learned from the long-term follow-up of a first-generation aortic stent graft. *J Vasc Surg*. 2003;37:367-373.

6. Wolf YG, Hill BR, Lee WA, et al. Eccentric stent graft compression: an indicator of insecure proximal fixation of aortic stent graft. *J Vasc Surg*. 2001;33:481-487.

7. Prinssen M, Buskens E, de Jong Seca et al. Cost-effectiveness of endovascular versus conventional abdominal aortic aneurysm repair at one year. Results of a randomized trial. In: Prinssen M, ed. DREAM. Oud-Beijerland, The Netherlands: As BV; 2005:89-103.

8. Verhoeven EL, Tielliu IF, Prins TR, et al. Frequency and outcome of re-interventions after endovascular repair for abdominal aortic aneurysm: a prospective cohort study. *Eur J Vasc Endovasc Surg*. 2004;28:357-364.

9. Koning OH, Oudegeest OR, Valstar ER, et al. Roentgen stereophotogrammetric analysis: an accurate tool to assess stent-graft migration. *J Endovasc Ther*. 2006;13:457-467.

10. Karrholm J. Roentgen stereophotogrammetry. Review of orthopedic applications. *Acta Orthop Scand*. 1989;60:491-503.

11. Valstar ER, Vrooman HA, Toksvig-Larsen S, et al. Digital automated RSA compared to manually operated RSA. *J Biomech*. 2000;33:1593-1599.

12. Vrooman HA, Valstar ER, Brand GJ, et al. Fast and accurate automated measurements in digitized stereophotogrammetric radiographs. *J Biomech*. 1998;31:491-498.

13. Valstar ER, de Jong FW, Vrooman HA, et al. Model-based Roentgen stereophotogrammetry of orthopaedic implants. *J Biomech*. 2001;34:715-722.

14. Hinnen JW, Visser MJ, van Bockel JH. Aneurysm sac pressure monitoring: effect of technique on interpretation of measurements. *Eur J Vasc Endovasc Surg* 2005;29:233-238.

15. Valstar ER. Digital roentgen stereophotogrammetry. Development, validation, and clinical application. Thesis, Leiden University. Den Haag, The Netherlands: Pasmans BV, 2001.

16. Stefanadis C, Dernellis J, Vlachopoulos C, et al. Aortic function in arterial hypertension determined by pressure-diameter relation: effects of diltiazem. *Circulation*. 1997;96:1853-1858.

17. Flora HS, Woodhouse N, Robson S, et al. Micromovements at the aortic aneurysm neck measured during open surgery with close-range photogrammetry: implications for aortic endografts. *J Endovasc Ther*. 2001;8:511-520.

18. Verhagen HJ, Teutelink A, Olree M, et al. Dynamic CTA for cutting edge AAA imaging: insights into aortic distensibility and movement with possible consequences for endograft sizing and stent design [Abstract]. *J Endovasc Ther*. 2005;12(suppl I):I-45.

19. Vos AW, Wisselink W, Marcus JT, et al. Cine MRI assessment of aortic aneurysm dynamics before and after endovascular repair. *J Endovasc Ther*. 2003;10:433-439.

20. Spoor CW, Veldpaus FE. Rigid body motion calculated from spatial co-ordinates of markers. *J Biomech*. 1980;13:391-393.

CHAPTER 5

Roentgen Stereophotogrammetric Analysis to detect and quantify stentgraft migration in an animal model

Olivier H.J. Koning

Jan-Willem Hinnen

Eric H. Garling

Lucia J.M. Kroft

Edwin van der Linden

Jaap F. Hamming

Edward R. Valstar

and J. Hajo van Bockel

Abstract

Objective: To study detection and quantify stentgraft migration with RSA in-vivo as compared with CT and to evaluate the application and detection of a nitinol endovascular clip as an aorta reference marker for RSA.

Design: experimental animal model.

Materials and Methods: A model of a stentgraft was positioned in the thoracic aorta of two pigs. Tantalum aortic reference markers were attached to the adventitia for CT and RSA analysis. Nitinol endovascular clips (NEC) were inserted in the aortic wall for RSA analysis. Stentgraft migrations were measured with CT and RSA. CT images acquired with 64×0.5-mm beam collimation were analyzed with Vitrea postprocessing software using a standard clinical protocol and central lumen line reconstruction. RSA images were analyzed using standard Medis RSA software.

Results: The standard deviation of the measurements by RSA using tantalum markers was 0.33mm**.** The standard deviation of the measurements by CT with 3D reconstruction was 0.47mm. Placement of the clips was performed without difficulty or adverse effects but radiopacity of the clips was insufficient to allow detection with the RSA software.

Conclusion: RSA to measure stent-graft migration in vivo is feasible and very precise. Precision of RSA was superior to CT with 3D image reconstruction if a well defined aortic reference marker was applied for CT analysis. Placement of an aortic reference marker may facilitate CT surveillance for migration after EVAR. RSA has several other advantages over CT. Therefore, it may be a valuable tool for EVAR surveillance. The nitinol clip tested in this study as an aortic reference marker needs to be modified to increase radiopacity to enable RSA analysis.

Introduction

Stentgraft migration is a potentially lethal failure after endovascular aneurysm repair (EVAR)[1]. Migration incidence increases over time and still occurs despite modifications of design in the latest generation of stentgrafts.[2-5] In a patient cohort study by Sun, comparing measurement in axial CTA images to 3D image reconstructions, stentgraft migration appeared to occur in all patients, even if supplied with strong hooks and barbs, proving that more accurate detection methods indeed show more stentgraft migration.[4] In case of aneurysm diameter reduction after EVAR, the main points of interest in surveillance are detection of stentgraft migration and stentgraft disintegration at the earliest stage.

In previous studies of experimental models, detection of stentgraft migration using Roentgen Stereophotogrammetric Analysis (RSA) has been described.[6-8] RSA proved to be very accurate and stentgraft migration could be detected with RSA with a mean error of 0.5mm.[7] RSA imaging also enables stentgraft structure evaluation.[6,7]

Compared to CT with 3D image reconstruction, advantages of RSA over CT are that RSA is a low cost test, with a radiation exposure that is only a fraction of that of CT, while intravascular contrast is not required.[6] Furthermore, RSA compared favorably to CT with 3D image reconstruction in detecting migration in experimental studies.[6,7] However, RSA has not been tested in vivo for evaluation of stentgraft migration. The influences of human size soft tissue surroundings and respiratory and cardiac action on the results of RSA have not been modeled and are an essential step in preclinical evaluation of the technique.

A disadvantage of RSA is that a reference marker is required in the aortic wall. Inserting this marker constitutes an additional procedure during the EVAR operation. A nitinol endovascular clip (NEC), designed as an endovascular stapler, has been proposed to serve this purpose, and this device has been tested successfully in an experimental model.[7]

The present study analyses the detection of stentgraft migration with RSA in in-vivo animal experiments. Furthermore, we tested the application and detection of a NEC as an aorta reference marker for RSA.

Materials and METHODS

Animal model with stentgraft

Two 100 Kg female pigs were used. The Institutional Review Board for animal experimentation approved the study and the animals were cared for in compliance with the national guidelines

for animal experiments. After general anesthesia, the pulse rate was kept at approximately 90 per minute. Thoraco-laparotomy was performed exposing the thoracic and infrarenal aorta. Heparine was continuously administered. A Dacron 8mm conduit (Gelsoft Plus, Vascutek, Inchinnan, UK) was attached to the infrarenal aorta as a conduit for vascular access.

A Gianturco stent (Cook, Bjaeverskov, Denmark) was placed inside the thoracic aorta (Figure 1) via endovascular technique. The thoracic aorta was chosen for placement as it has the largest available aortic diameter, resembling the human situation as much as possible. The stent could be displaced, "migrated" along the aorta by pulling on monofilament fishing wire (Spro, Vianen, The Netherlands), attached to each stent side. The cranial end of the wire was passed through the left carotid artery, the caudal end was passed through the conduit on the infrarenal aorta. For RSA analysis, markers had been added at the cranial and caudal corners of the stent prior to placement (stentgraft markers). In a clinical situation, markers used to position the EVAR device can be used for this purpose.

CT analysis of stentgraft migration requires a point of reference. There is no major vascular branch in the descending aorta available as a reference for measurement like the renal artery in human clinical practice. Therefore, a 1mm tantalum spherical marker was glued to the adventitia of the aorta with Histoacryl® (B.Braun Aesculap, Tuttlingen, Germany).
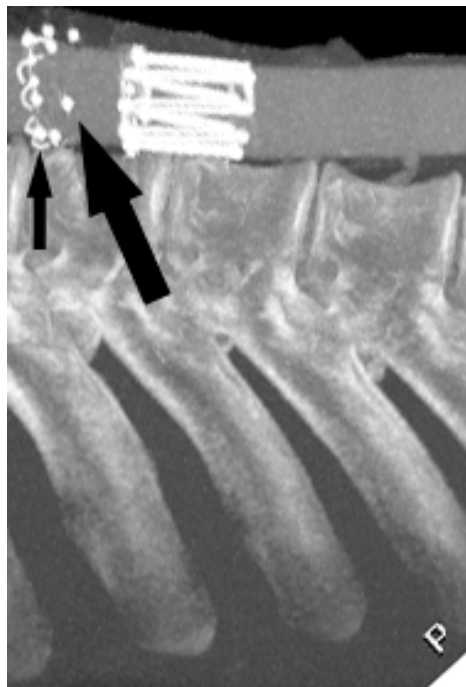

Figure 1. 3D maximum intensity projection of the CT image of the thoracic aorta. Small arrow lower left: nitinol clip; large arrow right: tantalum marker. Cranial side to the left.

Also for RSA analysis, reference markers were attached to the aorta, the aorta markers. We tested two sets of aorta markers: a cluster of 8 tantalum markers (with a diameter of 1 mm), glued to the adventitia with Histoacryl®, representing the standard clinical RSA situation as used to detect micromotion after joint replacement surgery (Figure 1); and three Anson Refix® Nitinol endovascular clips (Lombard Medical, Didcot, United Kingdom) (Figure 1 and 2) placed in the aortic wall by endovascular technique, to represent a clinical endovascular application. In the first animal, two stentgraft positions were analyzed: the initial or reference position and one migration. In the second animal, five stentgraft positions were analyzed: the initial or reference position and four migrations.

Figure 2. Nitinol endovascular clip.

For each stent-graft position CT and RSA imaging was performed. The stent-graft was migrated caudally under visual control with an image intensifier (Philips BV300 plus, Philips Medical Systems Europe, The Netherlands).
The animals were sacrificed after the experiments and autopsy was performed to study the position of the clips and local adverse effects of the clip placement.

RSA imaging technique

Roentgen Stereophotogrammetric Analysis (RSA) is comparable to stereo vision of human eye sight. By comparing two calibrated simultaneous images taken at a different angle, the position of an object in space can be determined. It is based on calculating 3-dimensional coordinates of radiopaque markers in the body using a stereo image of these markers. [6,9] A calibration box is positioned between the patient and the X-ray films, to define a 3-D laboratory coordinate system.[6] We used two manually synchronized standard mobile Roentgen tubes (Philips Practix 2000, Philips Medical Systems Europe, The Netherlands). The exposure settings used were: 125 kV/15mAs, resulting in an exposure time of 160msec for all RSA images.

The image postprocessing was done on a personal computer with the help of special RSA software[9-11] (Model Based RSA software, MEDIS Specials BV, Leiden, The Netherlands) after digitizing the films.[6] The RSA images were randomly numbered and the reviewer was blinded for the distance of migration induced.

Using RSA, it is possible to calculate the distance between two (groups of) markers inside the body. Migration is determined by comparing an initial, reference RSA image to the follow up RSA image. The technique was described in more detail in previous studies.[6,7]

In RSA analysis, the relative positions of markers do not change in absence of migration. Any change in relative position indicates movement between the markers. Positioning of the animal, or the patient in clinical practice, is not critical as the calibration box will facilitate the calculation of marker coordinates each time an RSA image is taken.

Pulsatile motion of the aorta may influence measurement, as each RSA image is acquired at a random point in the cardiac cycle. To study the in-vivo situation and the influence of pulsatile motion on migration measurement by RSA, 5 RSA images were acquired of the reference position and 9 images of each stentgraft position after migration. The RSA images were acquired at a random point in the cycle of pulsatile circulation. Migration was assessed using cross-table analysis, comparing each of the 5 reference images to all 9 follow-up images. This resulted in 45 measurements per migration, resembling the 45 possible clinical combinations of RSA images. The measurements were performed using tantalum markers as well as NEC-s. The Nitinol endovascular clips were evaluated for feasibility as an aorta reference marker and for applicability.

To summarize the RSA results, we pooled the data to determine the variance of the method. This was done by calculating the average migration per group of 45 measurements. Afterwards, this value was subtracted from every single measurement in the same group, thereby calculating a variance from the mean value. This enabled calculation of the standard deviation and range of deviation of all RSA measurements (n=225).

Computer Tomography (CT)

CT analysis of stentgraft migration was performed using the same technique for post-processing and analysis to measure stentgraft position is used for CT follow up in our clinical setting. Instead of using the orifice of the renal artery as a point of reference, we used a tantalum marker fixed to the adventitia of the thoracic aorta.

The CT images were acquired with a 64 detector row CT scanner, Toshiba Aquilion (Toshiba Medical Systems, Otawara, Japan). Scanning parameters were: 100 kV, 350 mA, 500-ms rotation,

pitch factor 0.83, 0.5-mm beam collimation. The images were reconstructed with a 0.5-mm thickness and 0.4-mm reconstruction interval.

The CT images were enhanced with Iomeprol 816.5 mg/ml intravascular contrast (Iomeron 400, Altana Pharma, Hoofddorp, The Netherlands) to obtain an enhancement level of 250 Hounsfield units in the aorta for each CT image acquisition.

A reference CT scan was made of the initial stentgraft position. After each stentgraft migration, imaging was repeated. The CT images were randomly numbered and the observers were blinded for the amount of migration induced.

Using Vitrea2 post-processing software (Vital Images Inc., Plymouth, MN, USA), stentgraft migration was measured on 3D curved multiplanar reconstructions along the aortic central lumen line to evaluate the aorta in 2 perpendicular longitudinal directions as well as the perpendicular axial direction. Using automatic calipers, the distance was measured between the tantalum aorta reference marker and the stent at the level where the first circumferential view of the stent was observed (in perpendicular axial direction). The stent struts were used for orientation.

CT requires interpretation by an observer, and subsequently involves possible human error and inter-observer variability. To correct for inter-observer variability, CT scans were evaluated by five medical specialists; four radiologists and a vascular surgeon, all experienced users of this technique. Migration was determined by comparing the distance between the aortic reference marker and the stentgraft in the follow up CT to the distance in the reference CT image, as measured by the same observer.

To summarize the CT results, we pooled the data to determine the variance of the modality. This was done by calculating the average migration per group of 5 measurements. Afterwards, this value was subtracted from every single measurement in the group of five, thereby calculating a variance from the mean value. This enabled calculation of the standard deviation and range of deviation of all CT measurements (n=25).

Results

Nitinol endovascular clip

The application of the NEC was performed without difficulty or complications in both animals. The clips could be positioned and repositioned without failure of device and introducer. Visibility of the NEC with the image intensifier was good. Autopsy revealed no local adverse effects,
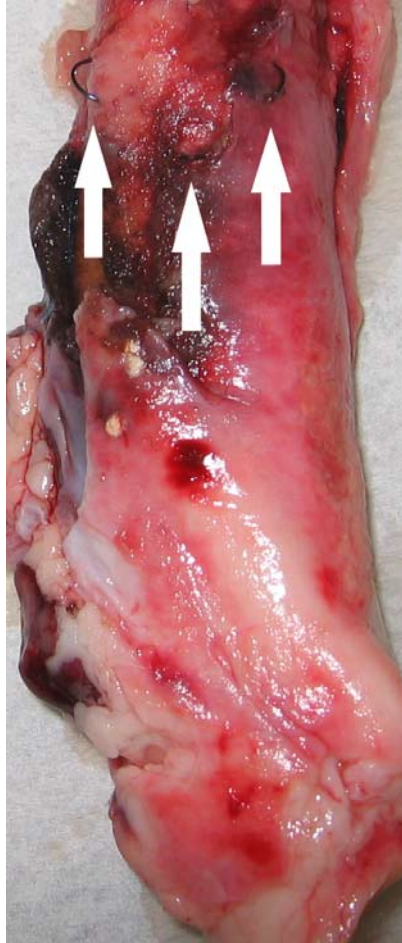
Figure 3. Specimen of the thoracic aorta. The wall of the aorta is (intentionally) perforated by the clip (arrows). No adverse effects were noted locally.

specifically no evidence of haematoma or perforation other than the intended perforation of the aortic wall by the anchors of the NEC (Figure 3).

However, the NEC had insufficient radiopacity to enable analysis of the stereo images with RSA in large animals of 100 kg. Therefore, the marker position could not be determined accurately using the software.

RSA measurements

RSA measurement of stentgraft migration with the tantalum aorta reference markers was possible in all cases. The results of the RSA measurements of stentgraft migration are shown in Figure 4. The standard deviation of the measurements by RSA was 0.33mm (range -1.35

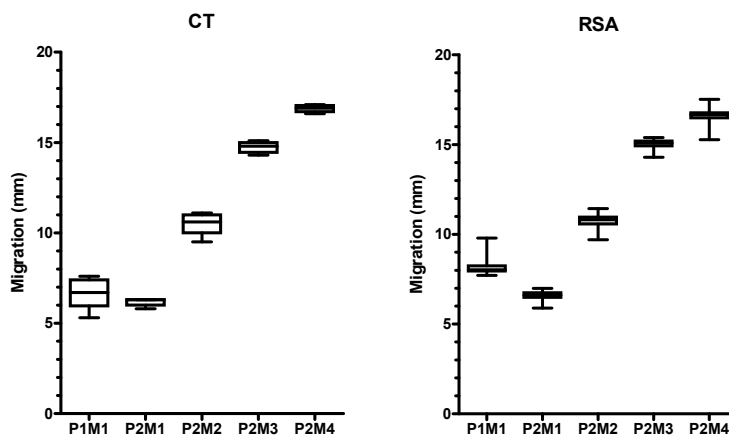**Figure 4.** Results of the measurements with RSA and CT with 3D image reconstructions using a tantalum marker as a reference point (see figure 1). X-axis: P1M1=Pig 1, Migration 1; P2M1=Pig 2, Migration1; etc. Y-axis :migration (mm) mean, 25th and 75th percentiles and range, including all outliers.

– 1.64mm) as compared to the mean value of the corresponding group of migrations (n=225). There were five outliers with a deviation from the mean of >1 mm (2.2%).

CT measurements

The results of the CT measurements of stentgraft migration using a tantalum aorta marker as a point of reference are shown in Figure 4. The standard deviation of the measurements by CT with 3D reconstruction was 0.47mm (-1.38 – 0.92mm) as compared to the mean value of the corresponding group of migrations (n=25). There were two outliers with a deviation from the mean >1 mm (8%).

Discussion

Roentgen stereophotogrammetric analysis of stentgraft migration is feasible and very precise in this in vivo animal model. This study confirms favorable results in previous in-vitro work. Despite soft tissue surroundings and the pulsatile change that occurred due to cardiac action, the variation in measurement is very low (SD = 0.36mm). Unfortunately, the nitinol endovascular clip did not have sufficient radiopacity to allow detection by RSA software.

Five outliers with a deviation of more than 1 mm from the mean were identified in 225 measurements (2%). We analyzed the outliers and found that these were due to the fact that the software had problems in identifying the markers on the cranial side of the stent due position symmetry of the markers. The circular position (see figure 1) diminishes the ability

of the software to recognize the 9 identical markers based on the stereo image, in which they projected in one row. An asymmetrical distribution of markers on the stent will solve this problem. The currently marketed stentgrafts either have this asymmetrical distribution (e.g. Zenith, Cook) or have less and therefore easier distinguishable markers (e.i. Excluder, Gore and Talent, Medtronic). Furthermore, automated pattern recognition of the stent could enable RSA data analysis regardless of marker position. This is subject to further study at our institution.

The reproducibility of CT with 3D image reconstruction (SD=0.47) was slightly less than RSA. This compared favorably to a previous study comparing 3D-CT to RSA in a pulsatile in vitro model.[7] In this model, a renal artery was used as a reference. As expected, it appears that the accuracy of the CT measurements increases by using a better defined reference point like a tantalum marker as compared with the less defined renal artery. Thus, adding a marker to the aortic wall as a reference point for CT analysis facilitates highly accurate migration detection with CT analysis using 3D image reconstruction, and this result is achieved without the use of intravascular contrast. 3D image reconstruction is a powerful tool to detect stentgraft migration and has shown better results in migration detection than reviewing axial images only, as is current practice in many centers world wide.[4] Furthermore, the cost of routine post-EVAR surveillance using CT will remain high, although radiation dose could possibly be diminished to that of a low dose CT image. Because of these considerations, we believe that RSA could be preferable over CT for routine surveillance in patients with a decreased aneurysm size after EVAR.

When considering our animal model, this experiment represents a step closer to clinical applicability. The study clearly shows feasibility of RSA under physiological in-vivo conditions. However, the consistency of the aorta of the pig is different from an atherosclerotic aneurysm neck. This may have impact on NEC placement in the bare aortic wall. During placement, the visibility of the marker using the image intensifier was good. As stated, the NEC could not be detected by the RSA software due to insufficient radiopacity of these markers in moderate low contrast resolution projection imaging techniques. Because a stereo image is produced for RSA, scatter

Figure 5. Platinum ring attached to the nitinol endovascular clip for enhanced radiopacity.

radiation may further decrease image contrast and visibility of the marker. In order to enable RSA analysis using the NEC as a reference marker, the radiopacity of the marker should be enhanced. This could be achieved by adding radiopaque metal to the clip, for instance a small gold or platinum ring (Figure 5). Recent preliminary studies at our institution into this issue are encouraging. Digital flat panel Roentgen detectors instead of analogue films will also enhance marker visibility. The design and safety of the marker are subject to further study at our institution.

Conclusion

RSA to measure stent-graft migration in vivo is feasible and very precise. Precision of RSA was superior to CT with 3D image reconstruction if a well defined aortic reference marker was applied for CT analysis. Placement of an aortic reference marker facilitates CT surveillance for migration after EVAR. Because RSA has several other advantages over CT, it may be a valuable tool for EVAR surveillance. The nitinol clip, tested in this study as an aortic reference marker, needs to be modified to increase radiopacity to enable RSA analysis.

Acknowledgements

References

1. Fransen GA, Vallabhaneni SR Sr, van Marrewijk CJ, Laheij RJ, Harris PL, Buth J; EUROSTAR Rupture of infra-renal aortic aneurysm after endovascular repair: a series from EUROSTAR registry. *Eur J Vasc Endovasc Surg*. 2003;26(5):487-93.

2. van Herwaarden, Joost A., van de Pavoordt, Eric D.W.M., Waasdorp, Evert J., Albert Vos, Jan, ThC. Overtoom, Tim, Kelder, Johannes C., Moll, Frans L., de Vries, Jean-Paul P.M. Long-Term Single-Center Results with Aneurx Endografts for Endovascular Abdominal Aortic Aneurysm Repair. *J Endovasc Ther*. 2007;14(3):307-317.

3. Greenberg RK, Chuter TA, Sternbergh WC 3rd, Fearnot NE; Zenith Investigators. Zenith AAA endovascular graft: intermediate-term results of the US multicenter trial. *J Vasc Surg*. 2004;39(6):1209-18.

4. Sun Z. Three-Dimensional Visualization of Suprarenal Aortic Stent-Grafts: Evaluation of Migration in Midterm Follow-up. *J Endovasc Ther*. 2006;13(1):85-93.

5. Torsello G, Posada N, Florek HJ, Horsch S, Kortmann H, Luska G, Scharrer-Pamler R, Schmiedt W, Umscheid T, Wozniak G; Talent AAA Retrospective Longterm Study Group Long-term outcome after Talent endograft implantation for aneurysms of the abdominal aorta: a multicenter retrospective study. *J Vasc Surg*. 2006;43(2):277-84)

6. Koning OH, Oudegeest OR, Valstar ER, Garling EH, van der Linden E, Hinnen JW, et al. Roentgen Stereophotogrammetric Analysis: an accurate tool to assess endovascular stentgraft migration. *J Endovasc Ther*. 2006;13:468-475

7. Koning OH, Garling EH, Hinnen JW, Kroft LJ, van der Linden E, Hamming JF, et al. Accurate detection of stentgraft migration in a pulsatile aorta using Roentgen Stereophotogrammetric Analysis. *J Endovasc Ther*. 2007;14(1):30-8.

8. Georg C, Welker V, Eidam H, et al. Aortic stent-graft movement detection using digital roentgen stereophotogrammetric analysis on plane film radiographs – initial results of a phantom study. Rofo. 2005;177:321-325.

9. Vrooman HA, Valstar ER, Brand GJ, Admiraal DR, Rozing PM, Reiber JH. Fast and accurate automated measurements in digitized stereophotogrammetric radiographs. *J Biomech*. 1998;31:491-498.

10. Valstar ER, Vrooman HA, Toksvig-Larsen S, Ryd L, Nelissen RG. Digital automated RSA compared to manually operated RSA. *J Biomech*. 2000;33:1593-1599.

11. Valstar ER, de Jong FW, Vrooman HA, Rozing PM, Reiber JH. Model-based Roentgen stereophotogrammetry of orthopaedic implants. *J Biomech*. 2001;34:715-722.

Accurate Roentgen Stereophotogrammetric Analysis of stent-graft migration using a single aortic reference marker

Olivier H.J. Koning

Eric H. Garling

Jan-Willem Hinnen

Martijn Holleman

Jaap F. Hamming

Edward R. Valstar

and J. Hajo van Bockel

Abstract

Purpose: To assess the accuracy of detection of stent-graft migration with RSA using one single aortic reference marker instead of a cluster of several markers, as is currently standard in clinical RSA.

Methods: A model of a stentgraft was positioned in an aortic model that was connected to an artificial circulation with a physiological flow and pressure profile. A similar model of a stent-graft was positioned in the thoracic aorta of two pigs. Stent-graft migration was simulated in these in-vitro and in-vivo models. The amount of migration was determined using standard RSA with multiple aortic reference markers as well as with RSA using only one aortic reference marker (1-ref-RSA). RSA measurements with the circulation switched off were used as the reference standard to determine stent-graft migration in the in-vitro model. The measurement error of 1-ref-RSA was determined during pulsatile circulation in the in-vitro model. In-vivo, the results of RSA stent-graft migration measurement using a single reference marker and a standard cluster of reference markers were compared.

Results: The mean measurement error ± SD of standard RSA during pulsatile circulation in-vitro was -0.5 ± 0.16mm. Using 1-ref-RSA, the mean measurement error in-vitro was -0.73 ± 0.12mm. In-vivo, the standard deviation of all measurements by standard RSA was 0.33mm as compared to the mean value of the corresponding group of migration measurements. 1-ref-RSA had a pooled mean error of 0.17 ± 0.65mm as compared to standard RSA in-vivo.

Conclusion: Roentgen Stereophotogrammetric analysis with a single aortic reference marker enables very accurate detection of stent-graft migration.

Introduction

Stentgraft migration still occurs in spite of major improvement in stentgraft design over the past decade. Migration constitutes a potentially lethal complication after endovascular aneurysm repair (EVAR).[1-5] The current gold standard for detection of this phenomenon is contrast enhanced CT imaging.[6] However, contrast enhanced CT has several disadvantages of which nephrotoxic contrast, high radiation dose and logistical burden are most important. Furthermore, the high cost of this investigation renders EVAR less cost effective.[7] If the aneurysm size decreases during follow-up with ultrasound, migration and stentgraft integrity are the key points of interest in EVAR surveillance.

Roentgen stereophotogrammetric analysis (RSA) is a method that measures prosthesis migration relative to reference markers in the body (Figure 1). [8-11] RSA has proven to be highly accurate in clinical detection of prosthesis micro-motion after joint replacement surgery.[12,13] It also demonstrated to be feasible and highly accurate in several stent-graft migration studies in-vitro and in-vivo.[8,9,14] Furthermore, RSA is cheap, relatively simple and can also be used to detect stent fractures. Consequently, it has the potential to become the new gold standard for stentgraft migration detection.

RSA requires markers to perform position measurements and detect migration during follow up.[8-11] The most important disadvantage of RSA is that a reference marker is required that is attached to the aortic wall.[8,9,14] This marker is used to determine position change, or migration, of the graft and will have to be inserted during the EVAR procedure. An enhanced version of the Anson Refix® Nitinol endovascular clip (Lombard Medical, Didcot, United Kingdom), an endovascular stapler device to secure a stent-graft to the aortic wall, might be used for this purpose.[9,14] The design of the marker is currently under investigation at our institution.[9,14]

An important question that has remained unanswered is how many markers are needed for accurate detection of axial stent-graft migration. At least three non linear placed markers are required in surveillance after joint replacement surgery.[10] Using only one marker minimizes the additional risk and cost of the procedure. However, reducing the number of reference markers may diminish the accuracy of RSA measurement of axial migration of a stent-graft.

To assess the accuracy of detection of stent-graft migration with RSA using one single aortic reference marker instead of a cluster of reference markers as is currently standard in clinical RSA, we performed in-vivo and in-vitro experiments comparing these different reference points.
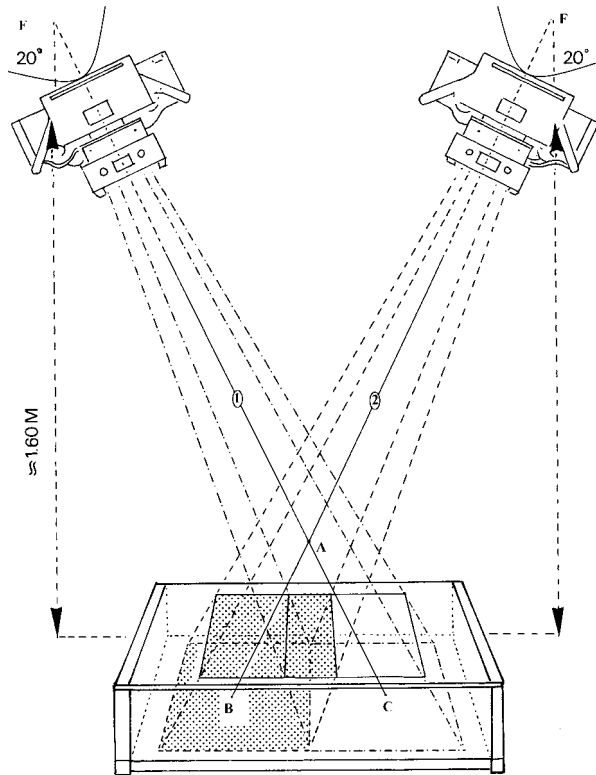
Figure 1. Schematic drawing of the RSA technique. Two standard hospital X-ray tubes (F) are used, in combination with two standard X-ray films or flat panel detectors placed directly under a calibration box that is positioned under the patient. The projection of the calibration box markers on the film is used to reconstruct the position of the Roentgen foci (F) and their relation to the two X-ray films. Graft marker A gives projections B and C on the films. With known focus position, projection lines 1 and 2 can be reconstructed; Calculating the intersection of lines 1 and 2 in space gives the position of A.

Methods

Pulsatile Aortic Model With Stent-Graft

A pulsatile flow model was developed to simulate migration of a stent-graft in the pulsating aorta.[9,15] A human cadaver spine was obtained from the anatomical department and used according to the standard consent procedures of our Institutional Review Board. A fresh specimen of a pig thoracic aorta was attached to the cadaver spine, replacing the cadaveric aorta. The spine, including the surrounding soft tissues, was conserved in a solution of formaldehyde, ethanol, glycerin, and phenol (Figure 2).[9] The model was placed in an Acrylic box, topped off with water to simulate soft tissue.

Figure 2. Model of the fresh pig aorta fixed to a human cadaver spine, complete with soft tissue. Three clusters of *aortic reference markers* are attached to the adventitia (arrows).

The perfusate of this artificial circulation was starch solution with the same viscosity as blood. To generate pulsatility, the model was connected to an artificial circulation set at 70 beats per minute with a 75 mL/s flow rate, which produced a physiological flow and pressure profile.[9,15] The pulsatility resulted in a luminal diameter change from 20.0 to 21.5 mm, as recorded in M-mode ultrasound with a 7.5-MHz linear array probe (ProSound SSD-5500; ALOKA, Tokyo, Japan). This diameter change was induced to simulate aortic diameter changes measured in vivo.[16-18]

A Gianturco stent (Cook, Bjaeverskov, Denmark) was placed inside the aorta by endovascular technique. A stent rather than a stent-graft was used to model migration since radiological imaging techniques use the stents of the stent-graft for analysis. Furthermore, deleting the fabric from the model facilitated the induction of migration. The stent could be "migrated" along the aorta by pulling on monofilament fishing wire (Spro, Vianen, The Netherlands), which was attached to each side of the stent. To prevent unintended migration, the fishing wire was fixed to the box during the measurements.

For RSA analysis, markers were added at the cranial and caudal corners of the stent (i.e., *stent-graft markers*), and reference markers were attached to the aorta (i.e., *aortic markers*). The *aortic markers* consisted of three clusters of 1mm diameter tantalum markers glued to the aortic adventitia with Histoacryl (B. Braun Aesculap, Tuttlingen, Germany). These markers are also used in standard clinical RSA in joint replacement surgery (Figure 2). The aortic marker closest to the stent in the initial position / image was used for RSA analysis with one single reference marker (1-ref-RSA).

Three stent-graft positions were analyzed with RSA: the initial or reference position and 2 migrations. The stent-graft was migrated caudally under visual control provided by an image intensifier (Philips BV300 plus; Philips Medical Systems Europe, The Netherlands).

Since RSA is proven to be highly accurate in a static environment, RSA of the model without pulsatile circulation was used as the reference standard to determine actual stent-graft migration. [8-11] Five RSA images of the reference position and 3 images of each stent-graft position after migration were acquired. These results could later be compared to standard RSA and 1-ref-RSA with pulsatile circulation in the model, to determine the measurement error of the 2 techniques. The migration was assessed using cross-table analysis, comparing each of the 5 reference images to all 3 follow-up images, producing 15 measurements per migration.[9]

To determine the influence of pulsatility on RSA and 1-ref-RSA migration measurement, 11 RSA images were acquired of each stent-graft position at a random point in the pulsatile cycle. Migration was determined by cross-table analysis, comparing each of the 11 reference images to all 11 follow-up images, resulting in 121 measurements per migration or 121 possible clinical combinations of RSA images per migration. These images were assessed using all aortic reference markers ("standard" RSA) as well as one single reference marker (1-ref-RSA).

Animal Model With Stent-Graft

Two 100 Kg female pigs were used. The Institutional Review Board for animal experimentation approved the study and the animals were cared for in compliance with the national guidelines for animal experiments. After general anesthesia, the pulse rate was kept at approximately 90 per minute. Thoraco-laparotomy was performed exposing the thoracic and infrarenal aorta. Heparine was continuously administered. A Dacron 8mm tube graft (Gelsoft Plus, Vascutek, Inchinnan, UK) was attached to the infrarenal aorta as a conduit for vascular access.[14]

A Gianturco stent as described above was placed inside the thoracic aorta via endovascular technique. The thoracic aorta was chosen for placement as it has the largest available aortic diameter, resembling the human situation as much as possible. Migration was induced under visual control as described above, the fishing wire was positioned as a "body floss" through the left carotid artery and the conduit. Eight tantalum reference markers (with a diameter of 1 mm) were glued to the adventitia of the thoracic aorta using Histoacryl® (B.Braun Aesculap, Tuttlingen, Germany), the *aortic markers*. The aortic marker closest to the stent in the initial position / image was used for 1-ref-RSA analysis.

In the first animal, two stentgraft positions were analyzed: the initial or reference position and one migration. In the second animal, five stentgraft positions were analyzed: the initial or reference position and four migrations.

For each stent-graft position RSA imaging was performed.[14] To simulate the in-vivo human situation and the influence of pulsatile motion on migration measurement by RSA and 1-ref-RSA, 5 RSA images were acquired of the reference position and 9 images of each stentgraft position after migration. The RSA images were acquired at a random point in the cycle of pulsatile circulation. Migration was assessed using cross-table analysis, comparing each of the 5 reference images to all 9 follow-up images. This resulted in 45 measurements per migration, resembling the 45 possible clinical combinations of RSA images. These images were assessed using all aortic reference markers ("standard" RSA) as well as only one reference marker (1-ref-RSA). To summarize the standard-RSA results, we pooled the data to determine the variance of the method. This was done by calculating the mean migration per group of 45 measurements. Afterwards, this value was subtracted from every single measurement in the same group, thereby calculating the variance of the standard-RSA measurement. This enabled calculation of the standard deviation and range of deviation of all standard-RSA measurements (n=225). The measurement error of 1-ref-RSA was determined by comparing each 1-ref-RSA observation to the corresponding mean value of migration measured by standard-RSA.

RSA imaging technique

We used two manually synchronized standard mobile Roentgen tubes to acquire the RSA images (Philips Practix 2000, Philips Medical Systems Europe, The Netherlands) (Figure 1). The exposure settings used were: 110 kV / 8.5 mAs, resulting in an exposure time of 78 ms for the in-vitro model and 125 kV / 15mAs, resulting in an exposure time of 160 ms for the animal studies.[9,14]

After digitizing the films, image postprocessing was done on a personal computer with the help of special RSA software (Model Based RSA software, MEDIS Specials BV, Leiden, The Netherlands). [8-11,14] The RSA images were randomly numbered and the reviewer was blinded for the distance of migration induced.

Using RSA, it is possible to calculate the distance between two (groups of) markers inside the body. Migration is determined by comparing an initial, reference RSA image to the follow up RSA image. The technique was previously described in more detail. [8-11]

In RSA analysis, the relative positions of markers do not change in absence of migration. Any change in relative position indicates movement between the markers. Positioning of the

model, animal, or the patient, is not critical as the calibration box will facilitate the calculation of marker coordinates each time an RSA image is taken.

Results

In-vitro

The actual migration of the stent in the model as determined by standard RSA in a non pulsatile situation was 7.00 ± 0.02mm (n=15) for the first migration; the second migration was 13.90 ± 0.03mm (n=15).[9]

In the pulsatile situation standard RSA registered a migration of 6.50 ± 0.08mm for the first, and 13.4 ± 0.21mm for the second migration (n=121), the pooled measurement error was -0.50 ± 0.16mm.[9]

According to 1-ref-RSA, the first migration in the pulsatile situation was 6.17 ± 0.08mm (n=121). For the second migration 1-ref-RSA determined a mean migration of 13.28 ± 0.08mm (n=121). The pooled measurement error of all migration measurements by 1-ref-RSA was -0.73 ± 0.12mm. A box plot of the measurements is shown in Figure 3.

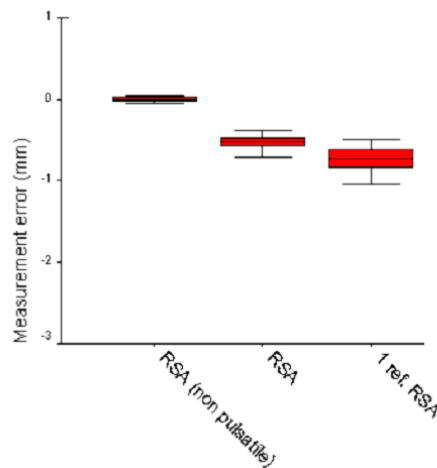**Figure 3.** Boxplot of RSA migration detection in an in-vitro pulsatile model. X-axis: Standard of reference is RSA in the model without pulsatile circulation (RSA (non pulsatile)). RSA represents measurement error with three clusters of aortic reference markers. 1-ref-RSA represents measurement error with a single aortic reference marker. Box plot represents mean, 25th and 75th percentile and range.

In-vivo

Standard RSA measured a migration of 8.15 ± 0.39mm for the migration in the first pig, migration 1-4 in the second pig were 6.59 ± 0.23mm, 10.74 ± 0.36mm, 15.03 ± 0.26mm and 16.62 ± 0.35mm, respectively. The standard deviation of all measurements by RSA was 0.33mm as compared to the mean value of the corresponding group of migrations (n=225).[14]

The results of 1-ref-RSA were 9.09 ± 0.68mm for the migration in the first pig and 6.42 ± 0.84mm, 9.95 ± 0.31mm, 14.73 ± 0.15mm and 16.51 ± 0.17mm for the migrations in the second pig, respectively. 1-ref-RSA had a pooled mean error of 0.17 ± 0.65mm as compared to standard RSA.

Discussion

For the detection of stentgraft migration, the accuracy of RSA using only one single reference marker is slightly less accurate compared to standard, multiple reference markers. The in-vitro and in-vivo measurement errors of standard RSA as well as of RSA using one single reference marker appear to be well below 1mm, a difference that is clinically very acceptable and compares favorably with other techniques to determination stentgraft migration.[8,9,14,20] Reduction of the number of reference markers to only one single aortic reference marker for RSA surveillance of stent-graft migration appears to be feasible.

RSA requires a reference marker to measure a change in position. This reference marker is best attached to the aortic wall, close to the stent-graft.[9,19] As discussed previously, a bony reference marker like the lumbar spine, or an artificial marker attached to the spine, is not useful because of the significant cyclic motion of the aorta-stent-graft complex relative to the lumbar spine.[8,17,18,21] This cyclic motion will induce a cyclic error in measurement when bony reference markers are used, adding to the measurement error of RSA itself. Furthermore, it is difficult to accurately reproduce bony reference markers in a clinical setting. The stentgraft markers that are used to position the graft during surgical placement can be used for RSA-detection of the graft. However, it is important to be able to identify the different markers either through asymmetric placement on the graft or by specific marker characteristics. If this is not the case, symmetrical marker configurations will result in measurement errors due to erroneous identification and consequent position calculation of the marker by the software.

In orthopedic surgery, a cluster of at least three non linear placed tantalum markers are used to detect prosthesis micro-motion. Using this configuration enables accurate quantification of micro-motion in three dimensions, including rotational micro-motion. Using less than three markers eliminates the possibility of rotational motion measurement. Other forms of

motion are detectible using only one reference marker. The issue of interest in surveillance after EVAR is to detect stentgraft migration along the vessel wall. Rotation inside the vessel is of less importance for long term follow-up, and migration outside the vessel has not been reported. Therefore, on theoretical grounds, one single marker to detect axial migration could be sufficient. Our data show that the accuracy of RSA using a single reference marker is not significantly hampered for clinical use. Therefore, it appears that one single aortic reference marker is sufficient for stent-graft migration surveillance after endovascular aneurysm repair. Design, safety and positioning of the aortic reference marker are subject to further study at our institution.[9,14]

Conclusion

Roentgen Stereophotogrammetric analysis with a single aortic reference marker enables very accurate detection of stent-graft migration.

Acknowledgement

References

1. Fransen GA, Vallabhaneni SR Sr, van Marrewijk CJ, Laheij RJ, Harris PL, Buth J; EUROSTAR Rupture of infra-renal aortic aneurysm after endovascular repair: a series from EUROSTAR registry. *Eur J Vasc Endovasc Surg*. 2003;26(5):487-93.

2. van Herwaarden, Joost A., van de Pavoordt, Eric D.W.M., Waasdorp, Evert J., Albert Vos, Jan, ThC. Overtoom, Tim, Kelder, Johannes C., Moll, Frans L., de Vries, Jean-Paul P.M. Long-Term Single-Center Results with Aneurx Endografts for Endovascular Abdominal Aortic Aneurysm Repair. *J Endovasc Ther*. 2007;14(3):307-317.

3. Greenberg RK, Chuter TA, Sternbergh WC 3rd, Fearnot NE; Zenith Investigators. Zenith AAA endovascular graft: intermediate-term results of the US multicenter trial. *J Vasc Surg*. 2004;39(6):1209-18.

4. Sun Z. Three-Dimensional Visualization of Suprarenal Aortic Stent-Grafts: Evaluation of Migration in Midterm Follow-up. *J Endovasc Ther*. 2006;13(1):85-93.

5. Torsello G, Posada N, Florek HJ, Horsch S, Kortmann H, Luska G, Scharrer-Pamler R, Schmiedt W, Umscheid T, Wozniak G; Talent AAA Retrospective Longterm Study Group Long-term outcome after Talent endograft implantation for aneurysms of the abdominal aorta: a multicenter retrospective study. *J Vasc Surg*. 2006;43(2):277-84)

6. Wolf YG, Hill BR, Lee WA, et al. Eccentric stent graft compression: an indicator of insecure proximal fixation of aortic stent graft. J Vasc Surg. 2001;33:481–487.

7. Prinssen M, Buskens E, de Jong Seca, et al. Cost-effectiveness of endovascular versus conventional abdominal aortic aneurysm repair at one year. Results of a randomized trial. In: Prinssen M, ed. DREAM. Oud-Beijerland, The Netherlands: As BV; 2005:89–103.

8. Koning OH, Oudegeest OR, Valstar ER, Garling EH, van der Linden E, Hinnen JW, et al. Roentgen Stereophotogrammetric Analysis: an accurate tool to assess endovascular stentgraft migration. *J Endovasc Ther*. 2006;13:468-475

9. Koning OH, Garling EH, Hinnen JW, Kroft LJ, van der Linden E, Hamming JF, et al. Accurate detection of stentgraft migration in a pulsatile aorta using Roentgen Stereophotogrammetric Analysis. *J Endovasc Ther*. 2007;14(1):30-8.

10. Valstar ER. Digital roentgen stereophotogrammetry. Development, validation, and clinical application. Thesis, Leiden University. Den Haag, The Netherlands: Pasmans BV, 2001.

11. Vrooman HA, Valstar ER, Brand GJ, Admiraal DR, Rozing PM, Reiber JH. Fast and accurate automated measurements in digitized stereophotogrammetric radiographs. J Biomech. 1998;31:491-498.

12. Ryd L, Albrektsson BE, Carlsson L. F. Dansgard F, Herberts P, Lindstrand A, Regner L, and S. Toksvig-Larsen. Roentgen stereophotogrammetric analysis as a predictor of mechanical loosening of knee prostheses. J Bone Joint Surg Br. 1995;77:377–383.

13. Kärrholm J, Gill RH, Valstar ER. The history and future of radiostereometric analysis. Clin Orthop Relat Res. 2006 Jul;448:10-21.

14. Koning OH, Hinnen JW, Garling EH, Kroft LJ, van der Linden E, Hamming JF, et al. Roentgen Stereophotogrammetric Analysis to detect stentgraft migration in an animal model. Submitted for publication.

15. Hinnen JW, Visser MJ, van Bockel JH. Aneurysm sac pressure monitoring: effect of technique on interpretation of measurements. Eur J Vasc Endovasc Surg. 2005;29:233–238.

16. Stefanadis C, Dernellis J, Vlachopoulos C, et al. Aortic function in arterial hypertension determined by pressure-diameter relation: effects of diltiazem. Circulation. 1997;96:1853–1858.

17. Flora HS, Woodhouse N, Robson S, et al. Micromovements at the aortic aneurysm neck measured during open surgery with closerange photogrammetry: implications for aortic endografts. J Endovasc Ther. 2001;8:511–520.

18. Verhagen HJ, Teutelink A, Olree M, et al. Dynamic CTA for cutting edge AAA imaging: insights into aortic distensibility and movement with possible consequences for endograft sizing and stent design [Abstract]. J Endovasc Ther. 2005;12(suppl l):l–45.

19. Spoor CW, Veldpaus FE. Rigid body motion calculated from spatial co-ordinates of markers. J Biomech. 1980;13:391–393.

20. Hodgson R, McWilliams RG, Simpson A, et al. Migration versus apparent migration: importance of errors due to positioning variation in plain radiographic follow-up of aortic stent-grafts. J Endovasc Ther. 2003;10:902-910.

21. Vos AW, Wisselink W, Marcus JT, et al. Cine MRI assessment of aortic aneurysm dynamics before and after endovascular repair. J Endovasc Ther. 2003;10:433–439.

CHAPTER 7

Plain radiographic images have insufficient accuracy and precision to detect stent-graft migration

Olivier H.J. Koning

Eric H. Garling

Jan Willem Hinnen

M.J.H. Holleman

Stephan F.G.C. Frerichs

Jaap F. Hamming

Edward R. Valstar

and J.Hajo van Bockel

ABSTRACT

Purpose: To determine the accuracy and precision of plain abdominal radiography (AXR) as a method to detect stent-graft migration and thereby define its clinical applicability.

Methods: Stent-graft migration was simulated in a static model of an aorta with stent-graft. Migration was measured by five different observers in AXR images with image acquisition and analysis according to a standardized protocol with correction for geometric distortion. The results were compared to Roentgen stereophotogrammetric analysis as the standard of reference. This way, accuracy and precision could be determined in-vitro. Next, the five observers determined stent-graft migration in two consecutive AXR images of four patients after endovascular aneurysm repair (EVAR). The results of the five observers were compared to determine the precision of the method in-vivo.

Results: In-vitro, migration as measured with RSA was 9.97 mm for the first and 27.75 mm for the second migration. The mean migration determined with AXR was 8.6 ± 2.5 mm (range 0.4 – 20.6 mm, n=57) and 23.7 ± 2.2 mm (range 14.7 – 27.4 mm, n=57), respectively. The mean pooled error of AXR as compared to RSA was 3.0 ± 2.4 mm (range 0.01-13.1 mm, n=114). Of all AXR measurements, 16% had an error larger than 5mm. In-vivo, the pooled mean variation was 3.0mm ± 4.5mm (n=76). The maximum difference between measurements in one patient was 33.0 mm. There was no significant inter-observer variability in the in-vitro and in-vivo groups.

Conclusion: The accuracy and precision of plain radiography for detection of stent-graft migration after EVAR is insufficient for clinical use, especially when early and accurate identification of minimal migration is required like in patients with short aneurysm necks. .

Introduction

P lain abdominal radiography (AXR) is widely used as a practical and reliable tool for routine surveillance after endovascular aneurysm repair (EVAR).[1-3] AXR is fast and requires only limited hospital resources in terms of personnel and equipment. Other advantages of AXR are that it does not require nephrotoxic contrast enhancement and has a low radiation dose per investigation. Therefore, it compares favorably to CT as a tool for surveillance after EVAR.

AXR reveals information about stent-graft position and integrity, enabling detection of stent-graft migration, kinking/deformity, limb dislocation, hook and stent fracture, anchor-stent separation, and progressive dilatation of the native vessels.[1] Hodgson et al. demonstrated that an accuracy of 2 mm could be achieved to detect stent-graft migration in a static model using standardized AXR and an algorithm to correct for geometrical distortion due to varying positioning of the Roentgen tube.[2] They did not describe the effect of inter-observer variation on the measurement, nor the precision of repeated measurements with AXR. These aspects of AXR remain unclear, even though AXR has found such widespread acceptance for an important aspect of surveillance after EVAR.

In AXR, the spine is used as the point of reference to detect stentgraft migration, by comparing the position of the stent-graft relative to the lumbar spine in sequential examinations.[2] However, the spine is not always a stable landmark over time. Moreover, cranio-caudal stent-graft motion during the cardiac cycle has been described up to 3 mm in a small number of patients, making a wider range of motion likely.[4-6] Because of this pulsatile motion of the graft, the use of bony points of reference seems to be hazardous in terms of measurement accuracy. Furthermore, the minimum acceptable aneurysm neck length continues to decrease with increased experience and new generation stent-grafts, approaching 5mm.[7] This requires increased accuracy of our tools for migration surveillance.

In this study, we determined the accuracy and precision of AXR as a method to detect in-vitro and in-vivo stent-graft migration to further define its clinical applicability.

METHODS

Plain Radiography (AXR) versus RSA in-vitro

For the in-vitro condition we used a static model to acquire AXR images according to a standard clinical protocol and compared the measurements to RSA, the standard of reference for

this experiment. Roentgen stereophotogrammetric analysis (RSA) is a method that uses stereo roentgen images to determine the 3D position of markers relative to each other. RSA has been used for many years to detect micro-motion of orthopedic prosthesis with sub-millimeter accuracy.[8-10] In recent literature, it has also been proposed as a highly accurate tool for migration surveillance after EVAR.[11-12] An accuracy of 0.002 ± 0.044 mm was demonstrated in a static model of stent-graft migration.[11] Because RSA acquires a calibrated stereo plain radiographic image, it has the same possibilities and advantages as AXR. RSA combines these advantages with a very high accuracy for micro-motion measurement.[11-12] RSA was regarded as the standard of reference in the static situation because of its proven high accuracy. This comparison of AXR to a highly accurate standard of reference is a measure for the accuracy of AXR, the measurement error.

A static model was developed to simulate stent-graft migration. The model consisted of a fresh thoracic pig aorta, fixed to a cadaver human spine complete with soft tissue. The spine was obtained from the anatomical department and used according to the standard consent procedures of our Institutional Review Board. It was conserved in a solution of formaldehyde, ethanol, glycerin, and phenol (Figure 1). The model was placed in an acrylic box, topped off with water to simulate soft tissue.

A Gianturco stent (Cook, Bjaeverskov, Denmark) was placed inside the aorta. A stent rather than a stent-graft was used to model migration since radiological imaging techniques use the stents of the stent-graft for analysis. Furthermore, deleting the fabric from the model facilitated the induction of migration. Three stent-graft positions were analyzed with RSA and AXR: the initial or reference position and 2 migrations, induced by pulling on a thin wire attached to the stent. For RSA analysis, markers were added at the cranial and caudal corners of the stent (i.e., *stent-graft markers*), and reference markers were attached to the aorta (i.e., *aortic markers*), as published previously.[12] RSA imaging and measurement was performed as published previously.[9,11-12]

For plain radiography, the same setup was used to determine migration as is current practice in our clinical setting for EVAR surveillance, as described by Murphy et al.[3] From every position one anterior- posterior and three left lateral radiographs were produced using a Bucky set-up by Oldelft (Triathlon DR, Oldelft Veenendaal, The Netherlands) with the tube positioned 1 meter above one 35 x 43 cm digital flat panel detector (CXDI-50G, Canon, Amstelveen, the Netherlands). As described by Hodgson et al.[2], the exact position of a stentgraft inside the body is impossible to determine from the outside of the patient in a clinical situation. Therefore, lateral photos cannot always be taken through the exact center of the top of the stentgraft. To

Figure 1. Model of an aorta with stent-graft. Fresh pig aorta fixed to a human spine complete with soft tissue. Spherical markers are attached to the adventitia as reference markers for RSA.

mimic a clinical setting, and reproducing the experiment performed by Hodgson et al [2], three different lateral radiographs were acquired, one with the center of the X-ray beam aimed at the center of the stent and one aimed 7.5 cm cranial and 7.5 cm caudal to this point.

The position of the stent was determined by measuring the distance between two reference points. We used the center of one end of the stent as the stent reference. Similarly, the vertebral reference was the center of the vertebral endplate closest to the stent reference point on the initial photo. It is preferable to choose the centers of the stent and vertebra as reference points instead of the edges, because the centers are less affected by variation in angulation, distortion or vertebral osteophytes at the border of the vertebra.[2]

The AXR images were randomly numbered and measured by 5 different observers. Two observers performed five measurements per image; three observers performed three measurements per image. All observers were blinded for the amount of migration. This way, a total of 19 measurements were performed on three images per position (cranial, center and caudal image). This lead to 57 measurements per migration, and therefore a total of 114 measurements of the two induced migrations. Geometric distortion was corrected according to the suggestions by Hodgson et al.[2] Migration was determined by calculating the difference in distance from the vertebral endplate to the stent, as measured in the reference radiographs and follow up images.[2]

Plain Radiography (AXR) in-vivo

Next, we measured the variability of AXR measurements of stent-graft migration in patients who had undergone EVAR. The standard deviation and the maximum variation between all observations per migration are a measure for the precision of the technique. To determine the precision of AXR in a clinical setting, migration was measured in four randomly chosen patients who underwent EVAR.

The AXR image pairs (AP and lateral) were acquired at two different points in time: one reference image directly post-operative and a randomly chosen follow-up image. The AXR image pairs were acquired according to the protocol as described by Murphy et al.[3], with a standard Bucky imaging set-up (Philips Medio 50 CP, Philips Medical Systems Europe, the Netherlands) positioned 1 meter above a 35 x 43 cm film (Kodak, Amsterdam, the Netherlands). The exposure was regulated automatically at approximately 75 kV. The AXR measurements of the stent-graft position were performed in the same way as described for the in-vitro experiment following the Hodgson protocol, determining the vertical distance between the vertebral endplate and the center of one end of the top stent of the stent-graft.[2] . As in the in-vitro experiments, two observers performed five measurements per image; three observers performed three measurements per image. This way, 19 measurements were performed in four patients, leading to a total of 76 measurements in-vivo. To determine the pooled mean deviation and standard deviation of AXR, we compared each AXR measurement to the mean of the AXR measurements of the same patient to determine the variation compared to the mean measurement. Subsequently, we pooled these data.

Statistics

Levene's test for variance was used to detect statistically significant interobserver variability between the measurement errors of the observers. $P<0.05$ represented a statistically significant difference. Standard deviation and maximum variation of the measurements were determined for each migration. The tests were performed in cooperation with the Medical Statistics department of the LUMC using SPSS for Windows (version 11.0; SPSS Inc., Chicago, IL, USA).

Results

Plain Radiography (AXR) versus RSA in-vitro

RSA analysis revealed a stent-graft migration of 9.97 mm for the first migration, and 27.75 mm for the second migration. The mean migration determined with AXR with correction for

geometric distortion was 8.6 ± 2.5 mm (range 0.4 – 20.6 mm, n=57) and 23.7 ± 2.2 mm (range 14.7 – 27.4 mm, n=57), respectively. No significant difference was found between the observers using Levene's test for variance (P=0.466). The pooled mean error of AXR as compared to RSA in a static in-vitro condition was 3.0 ± 2.4 mm (range 0.01-13.1 mm, n=114). Of all 114 AXR measurements, 16% had an error larger than 5mm in this model without pulsatile stent-graft motion (Figure 2).
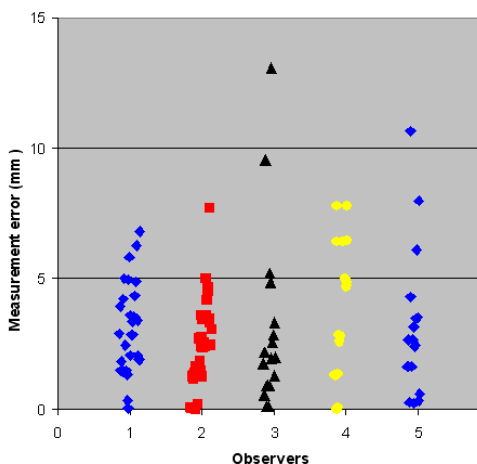

Figure 2. AXR measurement error of 5 different observers using a static model and RSA as standard of reference. In 16% the error was larger than 5mm. No significant difference was found between the observers.

Plain Radiography (AXR) in-vivo

Migration of the stent-graft as measured by AXR with correction for geometric distortion is shown in Figure 3. The pooled mean variation of AXR was 3.0mm ± 4.5mm (range 0.0 - 22.4 mm) (n=76). The maximum difference between measurements in one patient was 33.0 mm. No significant difference was found between the observers using Levene's test for variance (P=0.284).

Discussion

This study demonstrates that plain abdominal radiography has poor accuracy and precision to measure stent-graft migration despite adherence to a strict imaging and measurement protocol.

A mean error of 3.0 ± 2.4 mm was found in a model without pulsatile motion. This displays a low accuracy and precision. This is emphasized by the finding that 16% of the measurement errors were larger than 5mm. In the developments in design of stent-grafts and growing experience

of endovascular specialists, the accepted neck length of aneurysms is constantly decreasing, approaching 5mm.[7] Stent-graft migration of only several millimeters could already be very significant in these cases. The cyclic cranio-caudal motion of the stentgraft relative to the spine, the point of reference for AXR, has been reported to be up to 5,8mm. [4-6,11,13] Combining the measurement error found in this study with the understanding of this cyclic motion, an aneurysm neck length of 5-10 mm seems to be too short for surveillance of stent-graft migration by AXR alone.

In the in-vivo measurements, the accuracy and precision could have been reduced due to the pulsatile motion of the graft relative to the spine. This could possibly explain the disappointing precision of AXR found in-vivo. The variation of 3.0mm was large, especially when considering the very high standard deviation of this result: 4.5mm. This standard deviation would yield a 95% confidence interval of stentgraft migration measurement with AXR of 9mm. When stent-graft migration of 5mm is considered significant, AXR is simply not precise enough to reliably determine presence or absence of this complication.

The current gold standard to detect stent-graft migration after EVAR is contrast enhanced multi-detector CT with sub-millimeter beam collimation and 3D image reconstruction.[14] This method has the advantage of enabling detection of possible endoleaks and aneurysm sac growth or shrinkage, apart from measuring stent-graft position. However, these advantages come at a price in terms of cost and logistical burden. The contrast requirement and, to a lesser
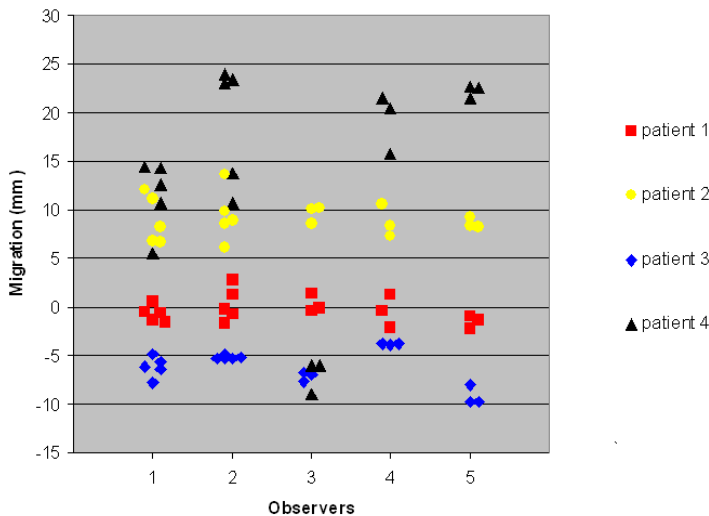

Figure 3. Results of migration measurements using AXR in patients after EVAR by 5 different observers, no significant difference was found between the observers.

extent, radiation dose can be a considerable disadvantage. Furthermore, 3D image reconstruction is not available in every hospital, nor is a multi-detector CT. CT without contrast enhancement, small acquisition slice thickness or 3D image reconstruction will undoubtedly produce less accurate results[14], however the accuracy of such measurements has not been quantified. Roentgen stereophotogrammetric analysis has been described as a possible tool to meet the requirements of high accuracy of stentgraft position measurement without the disadvantages of CT.[11,12] Unfortunately, RSA is still not suitable for widespread clinical introduction.

When considering the accuracy and precision of AXR, combined with a minimum length of the proximal neck zone to secure aneurysm exclusion, the results of our study imply that AXR is unreliable for surveillance of patients with an aneurysm neck of less than 15 – 20mm. For safety reasons, an aneurysm neck length of 30mm seems to be more appropriate when AXR is used for migration surveillance. In clinical practice, the vast majority of cases have an aneurysm neck length of less than 30mm, and the average length in reported series is deminishing.[15-17] Therefore, most of the patients after EVAR are unsuitable for this method of migration surveillance alone.

Limitations

This study is a combination of an in-vitro and an in-vivo study. The model is by nature of its design limited because of the absence of normal physiological behavior due to cardiac and respiratory motion. Furthermore, only a limited amount of soft tissue was simulated by means of water, an isodense substance. However, the accuracy and precision of AXR measurements will most likely further decrease if the above mentioned factors would have been present in the model.

We measured a limited number of four patients for the in-vivo part of the study. These results already show a considerable variation between measurements, without showing significant inter-observer variation. Considering the finding that the range of measurements as found in each patient was at least 5mm (Figure 2), a larger sample of patients and images will not contribute significantly to the data.

Conclusion

The accuracy and precision of plain radiography for detection of stent-graft migration after EVAR is insufficient for clinical use, especially when early and accurate identification of minimal migration is required like in patients with short aneurysm necks.

Acknowledgement

References

1. Fearn S, Lawrence-Brown MMD, Semmens JB, et al. Follow-up after endoluminal grafting: the plain radiograph has an essential role in surveillance. *J Endovasc Ther.* 2003;10:894–901.

2. Hodgson R, McWilliams RG, Simpson A, et al. Migration versus apparent migration: the importance of errors due to positioning variation in plain radiographic follow-up of aortic stentgrafts. *J Endovasc Ther.* 2003;10:902–910.

3. Murphy M, Hodgson R, Harris PL, et al. Plain radiographic surveillance of abdominal aortic stent-grafts: the Liverpool/Perth protocol. *J Endovasc Ther.* 2003;10:911–912.

4. Flora HS, Woodhouse N, Robson S, Adiseshiah M. Micromovements at the aortic aneurysm neck measured during open surgery with close-range photogrammetry: implications for aortic endografts. *J Endovasc Ther.* 2001;8:511-520.

5. Vos AW, Wisselink W, Marcus JT, Vahl AC, Manoliu RA, Rauwerda JA. Cine MRI assessment of aortic aneurysm dynamics before and after endovascular repair. *J Endovasc Ther* 2003;10:433-9.

6. Verhagen, HJ, Teutelink A, Olree M, et al. Dynamic CTA for cutting edge AAA imaging: Insights into aortic distensibility and movement with possible consequences for endograft sizing and stentdesign. *J Endovasc Ther.* 2005;12:l-45.

7. Kapma, MR, Groen, H, Oranen, BI, van der Hilst, CS, Tielliu, IF, Zeebrechts, CJ, Prins, TR, van den Dungen, J, Verhoeven EL. Emergency abdominal aortic aneurysm repair with a preferential endovascular strategy: mortality and cost-effectiveness analysis. *J Endovasc Ther* 2007;14:777-784.

8. Kärrholm J, Gill RH, Valstar ER. The history and future of radiostereometric analysis. Clin Orthop Relat Res. 2006;448:10-21.

9. Valstar ER. Digital roentgen stereophotogrammetry. Development, validation, and clinical application. Thesis, Leiden University. Den Haag, The Netherlands: Pasmans BV, 2001.

10. Vrooman HA, Valstar ER, Brand GJ, Admiraal DR, Rozing PM, Reiber JH. Fast and accurate automated measurements in digitized stereophotogrammetric radiographs. *J Biomech.* 1998;31:491-498.

11. Koning OH, Oudegeest OR, Valstar ER, Garling EH, Linden Evan der, Hinnen JW, et al. Roentgen Stereophotogrammetric Analysis: an accurate tool to assess endovascular stentgraft migration. *J Endovasc Ther.* 2006;13:468-75.

12. Koning OH, Garling EH, Hinnen JW, Kroft LJ, van der Linden E, Hamming JF, et al. Accurate detection of stentgraft migration in a pulsatile aortic model using Roentgen Stereophotogrammetric Analysis. *J Endovasc Ther.* 2007;14:30-8.

13. Koning OH, Kaptein BL, van der Vijver R, Dias, NV, Malina, M, Schalij, MJ, Valstar, ER, van Bockel, JH. Fluoroscopic roentgen stereophotogrammetric analysis (FRSA) to study 3-D stent-graft dynamics in patients: a pilot study. J Vasc Surg, in press.

14. Sun Z. Three-dimensional visualization of suprarenal aortic stent-grafts: evaluation of migration in midterm follow-up. J Endovasc Ther. 2006;13:85–93.

15. Marrewijk CJ, Leurs LJ, Vallabhaneni SR, Harris PL, Buth J, Laheij RJ. Risk-adjusted outcome analysis of endovascular abdominal aortic aneurysm repair in a large population: how do stent-grafts compare? *J Endovasc Ther* 2005;12:417-429.

16. Herwaarden JA, van de Pavoordt HD, Waasdorp EJ, Vos JA, Overtoom TT, Kelder JC, Moll FL, de Vries JP. Long-term single centre results with AneuRx endografts for endovascular abdominal aortic aneurysm repair. *J Endovasc Ther.* 2007;14:307-17.

17. Tanski W, Fillinger M. Outcomes of original and low-permeability Gore Excluder endoprosthesis for endovascular abdominal aortic aneurysm repair. *J Vasc Surg* 2007;45:243-249.

PART II

Quantification of 3-D stent-graft dynamics using Fluoroscopic Roentgen Stereophotogrammetric Analysis

CHAPTER

8

Assessment of 3-D stentgraft dynamics using fluoroscopic roentgen stereophotogrammetric analysis (FRSA)

Olivier H. J. Koning

Bart L. Kaptein

Eric H. Garling

Jan Willem Hinnen

Jaap F. Hamming

Edward R. Valstar

and J. H. van Bockel

Abstract

Objective: To validate the use of Fluoroscopic Roentgen Stereophotogrammetric Analysis (FRSA) for its feasibility and accuracy to measure 3-D dynamic motion of stentgrafts.

Methods: A digital bi-plane fluoroscopy set-up was calibrated (Siemens Axiom Artis dBc®). Stereo images were acquired of a static aortic model with a stentgraft in different axial positions, imposed by a micromanipulator. The 3-D measurement error of FRSA was determined by comparing FRSA measurements to the micromanipulator. An aortic model with stent-graft was constructed and connected to an artificial circulation with a physiological flow and pressure profile. Markers were added to the spine (tantalum spherical markers, diameter 1mm) and stent (welding tin, diameter 1mm). 3-D measurement precision was determined by measuring the position of a single (stable) spine marker during 2 pulsatile cycles. Finally, 3-D stent marker motion was analyzed with a frame rate of 30 images per second, including 3-D marker position (change), diameter change, and center of circle position change.

Results: The mean error of FRSA measurement of displacement was 0.003mm (SD=0.019mm, max. error 0.058mm). A very high precision of position measurement was found (SD=0.009-0.015mm). During pulsatile motion, the position (changes) of the markers could be assessed in X, Y and Z direction, as well as stent diameter change and center of circle position change.

Conclusion: FRSA has proven to be a method with very high accuracy and temporal resolution to measure three dimensional stentgraft motion in a pulsatile environment. This technique has the potential to contribute significantly to the knowledge of stentgraft behavior after endovascular aneurysm repair and improvements in stentgraft design. The technique is ready for clinical testing.

Introduction

Endovascular repair (EVAR) of an abdominal aortic aneurysm (AAA) is a widely used therapeutic alternative to open repair. A known problem with this technique is that the stentgraft can fail due to device defects caused by the continuous and significant forces of pulsatile blood flow. These failures have potential detrimental effects on patient health and safety.[1,2] An important problem of understanding failures is that it is difficult to study and measure aorta and stentgraft dynamics after EVAR, and clinical data are therefore limited. For the development, improvement and evaluation of new and current stentgrafts, it is of significant interest to understand aorta and stentgraft dynamics in vivo. Modeling of these blood flow related dynamics is very difficult. Subsequently, bench-testing of repetitive motion of stentgrafts is often inadequate and can lead to faulty stentgraft design.

Currently, cinegraphic CT and MRI can be used to measure aorta and stentgraft motion during the cardiac cycle.[3-5] An important limitation of these imaging modalities is that motion can only be measured in one plane. Three dimensional motion of specific points of a stentgraft cannot be quantified. Furthermore, the spatial resolution of these techniques is limited.[5]

Roentgen stereophotogrammetric analysis (RSA) is a tool to assess marker positions using stereo roentgen images.[6,7] This technique has proven to be highly accurate, and is used to measure prosthesis migration in the relative static environment of follow-up after joint replacement surgery.[8-11] Recently, RSA was introduced as an accurate tool to measure stentgraft migration during post-EVAR surveillance.[12,13] RSA can not be used to measure stentgraft motion during the cardiac cycle, since it uses one single stereo image acquired with two regular "single-shot" X-ray machines. It is therefore impossible to acquire a rapid sequence of calibrated images.

With the development of digital bi-plane fluoroscopic imaging systems, accurate measurement of three dimensional stentgraft motion during the cardiac cycle can become possible by combining stereo fluoroscopy with the RSA technique. This could enable in-vivo motion analysis of stentgrafts during the cardiac cycle. We validated the use of this combination of techniques: Fluoroscopic Roentgen Stereophotogrammetric Analysis, or FRSA, for its feasibility and accuracy to measure 3-D dynamic motion of stentgrafts.
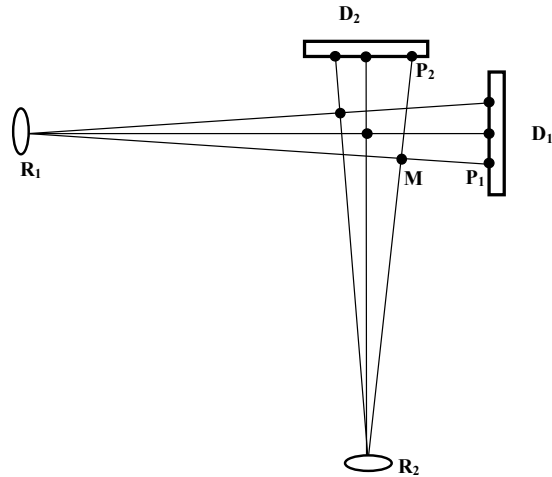
D₂

D_2

P_2

R_1

D_1

M P_1

R_2

Figure 1. Schematic drawing of FRSA technique. The positions of the Roentgen foci (R_1 and R_2), the detectors (D1 and D2) and their relative position are known by calibration of the set-up. Graft markers give projections P and P' on the detectors. With a calibrated set-up, projection lines can be reconstructed. Calculation of intersections M of these projection lines in space gives the positions of the markers.

Methods

The concept of FRSA

Roentgen stereophotogrammetric analysis (RSA) is performed by calculating the point of inter-section of two projection lines of a marker in space, using calibrated stereo Roentgen imaging (Figure 1).[6-13] FRSA uses high resolution digital stereo fluoroscopic images that are calibrated according to the same principles as RSA to calculate marker positions. Fast image acquisition and high frame rate theoretically enable accurate measurement of stentgraft motion in high spatial and temporal resolution.

FRSA set-up

We used a Siemens Axiom Artis dBc imaging system (Siemens Nederland NV Medical Solutions, The Hague, The Netherlands) (Figure 2), which consists of two C-arms with digital flat panel Roentgen detectors. The focus to detector distance was set at 95 cm. The two C-arms were positioned at a 90 degree angle, to produce a posterior-anterior image and a lateral image. The images were acquired and stored in 1024 x 1024 pixels, 14 bits grey scale resolution (Figure 3). The frame rate was 30 bi-directional images per second. Each stereo image is acquired as two
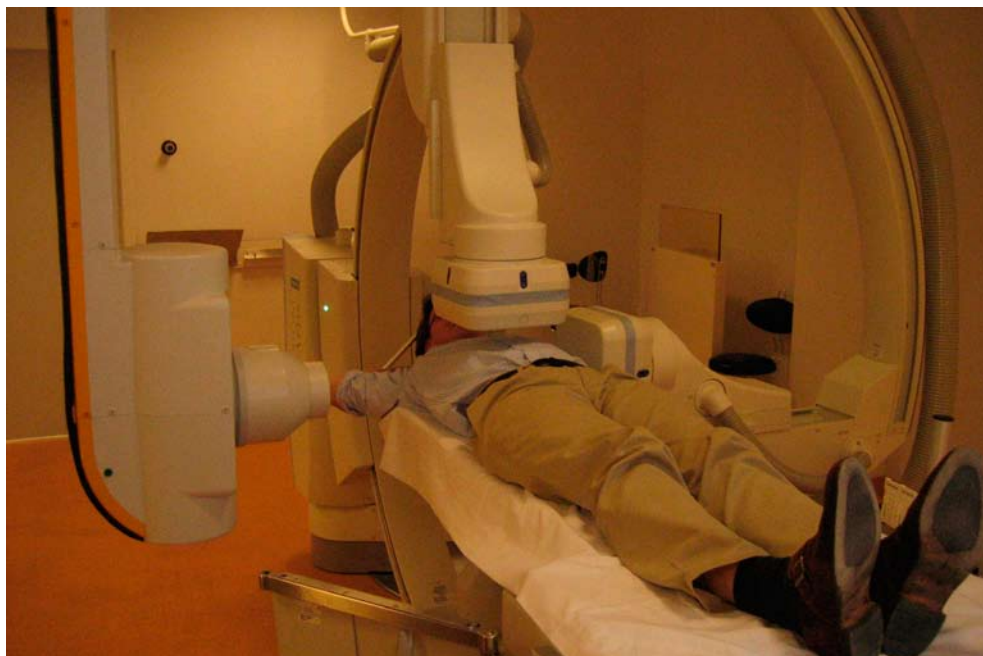
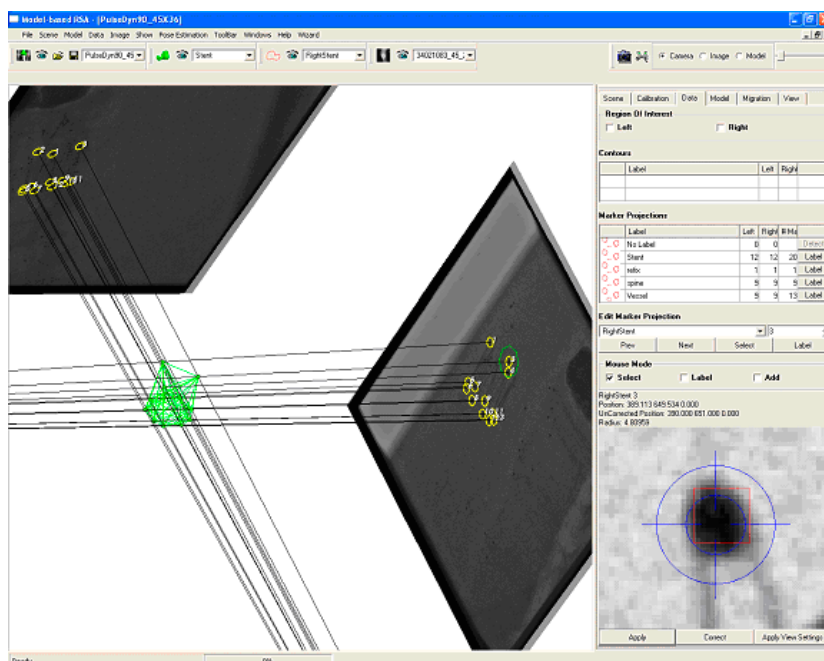**Figure 2.** Clinical set-up of the bi-plane fluoroscope

Figure 3. Image of the software with reconstruction of the stentgraft in space. The two images of a stereo image pair, a lateral and a postero-anterior image are visible. Right lower corner shows a detected stent marker.

separate alternating images, resulting in 60 alternating images per second. The exposure time of each image was 4 ms. The time between the posterior-anterior image and lateral image was 12.7 ms. For each analysis reported in this study, a 1.5 second run (45 stereo images) was acquired. The image pairs were analyzed using Model-based RSA software (MB-RSA, MEDIS specials, Leiden, The Netherlands) to calculate the relative 3-D marker positions.[8-11] No image reconstruction is required before analyzing the image pairs.

FRSA set-up calibration

To calibrate the set-up, a single focus run of a specially designed acrylic (PMMA, Vink Kunststoffen, Didam, The Netherlands) calibration box was acquired with each of the two C-arms.[14] From each run, a randomly chosen image was analyzed using the calibration algorithm as published previously.[14] This algorithm provides the calibration parameters to correct for image scale and geometric distortion, as well as the position of the Roentgen focus relative to the image for each C-arm. The relative position and orientation between the two C-arm images is necessary to calculate the 3-D marker positions using RSA analysis. This was achieved using a calibration object with 11 markers in known positions (Figure 4). The two images of the object were aligned to reconstruct the marker positions in space, reversing the calculation used to reconstruct an RSA image (Figure 1). This gave the position and orientation between the C-arms.

 Further analysis of the experimental images as described below could now be performed within this calibrated set-up.
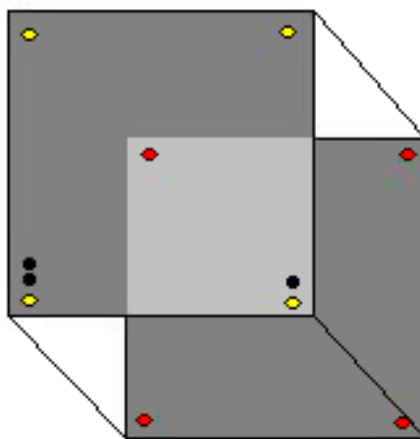

Figure 4. Calibration object. Plexiglas block, dimensions w x d x h: 8 x 8 x 5 cm. In every corner one tantalum marker, diameter 1mm (red and yellow). In the top layer three extra markers, diameter 2mm (black) for ease of identification of the different markers.

Static model experiments

A static model of an aorta with stentgraft, with markers in known positions, was placed in the set-up (Figure 5). The same model was used as described previously.[12] The stentgraft could be translated accurately in the aorta lumen with a micromanipulator. The stentgraft was moved in axial direction inside the aorta over a distance of 1, 1.5 and 3mm, using the micromanipulator. The increments of the micromanipulator were accurate up to 0.01 mm according to the manu-facturer, and confirmed by laboratory testing at our institution. The translation of the stent resulted in a 3D displacement of the markers. Three random stereo images were taken from an acquisition run of each position. Five marker positions were determined using FRSA. This was done to test for accuracy of measurement of the relative change in position of the markers by comparing the change in X, Y and Z coordinates and calculating the length of the resulting vec-tor of displacement. Mean, standard deviation, minimum and maximum of the translations of the markers were measured and the results were compared to the micromanipulator settings, used as the standard of reference. This way, the measurement error of FRSA was determined for all measurements (n=45). These data were pooled to describe the mean error, standard deviation and maximum measurement error of marker position change as measured by FRSA.

Figure 5. Static model of an aorta (tube) with stentgraft (visible inside tube). Micromanipulator is on the left side.

Pulsatile model experiments

For measurements under flow conditions, we developed a model to simulate a pulsating aorta with a stent-graft. To resemble human aorta characteristics, a fresh specimen of a porcine thoracic aorta was used, as published previously.[13] The porcine aorta was fixed to a human cadaver spine, replacing the cadaver aorta. The spine was complete with soft tissue (Figure 6). As an internal control for the experiments, the spine was marked with nine tantalum markers.

Figure 6. Pulsatile flow model. A fresh specimen of a porcine aorta was positioned ventral to a preserved human spine, complete with soft tissue. The porcine aorta replaced the human aorta. The aorta is connected to a pulsatile flow generator with physiologic flow and pressure profiles.

The aorta was filled with a starch solution with the same viscosity as blood. Inside the aorta, a Gianturco stent (Cook, Bjaeverskov, Denmark) was placed. The stent was marked with small drops of welding tin with a diameter of 1mm; the stent graft markers included nine at the cranial side and three at the caudal side. We used a stent rather than a stentgraft to study marker motion, since FRSA uses the stents of the stentgraft for analysis, identical to other radiological imaging techniques. The model was placed in a Plexiglas box, topped of with water to simulate soft tissue.

To test the feasibility to measure marker motion in a clinical situation, a study of a pulsating aorta was performed. The porcine – human aorta model was connected to an artificial circulation with a physiologic flow and pressure profile, as published previously.[13,15] This induced pulsatile marker motion of the aorta and stentgraft markers in X, Y and Z direction. With a pulse rate set at 80 per minute, a bi-plane fluoroscopy run of 1.5 sec resulted in imaging 2 pulsatile cycles. 3-D marker positions of the stent markers and the control markers in the spine were determined in every stereo image.

The tantalum spine markers were used to determine measurement precision. For each stereo image, the coordinates of a randomly chosen spine marker were determined (n=45). The X, Y and Z coordinates of the markers were compared to the average of the 45 measured positions and the standard deviation, minimum and maximum deviation were determined. This is a measure for the precision of the position estimation of a marker in consecutive stereo images using FRSA.

Finally, 3-dimensional stent marker motion was analyzed. The marker positions were determined for each sequential frame. The resulting series of marker positions was analyzed for

marker motion. Furthermore, a circle was estimated through the nine cranial markers in every stereo image. The resulting series of circles were analyzed for change of diameter (i.e. the stentgraft and inner vessel diameter) and motion of the circle center, as a measure for the three dimensional motion of the aorta – stentgraft complex. Analysis was performed with Matlab r2006B (The MathWorks, Natick, USA).

Results

Using the calibration box, the set-up was tested for image distortion. No image distortion was found.

Validation studies

The mean, standard deviation, minimum and maximum of the relative changes in position of the markers in the static stentgraft model are presented in Table 1. After pooling the measurement errors of FRSA, as compared to the micromanipulator, the mean error of 3D marker motion measurement by FRSA was 0.003mm, SD 0.019mm, maximum error 0.058mm (n=45). The precision of 3D marker position measurement by FRSA was determined by analysis of the position of one of the spine markers in 45 consecutive frames. The results are presented in Table 2. The precision is expressed by the standard deviation of the measured laboratory coordinates (0.009-0.015mm).

Table 1. 3D Changes in position (mm) of 5 markers measured by FRSA in 3 image frames (n=15 per displacement) compared to actual displacements as imposed by the micromanipulator which was applied as the "gold standard".

		Imposed Translation		
		1 mm	1.5 mm	3 mm
Measurements	Mean	1.007	1.497	3.004
	St Dev	0.015	0.022	0.023
	Min	0.979	1.442	2.967
	Max	1.025	1.513	3.030

Table 2. Precision of position measurement of one spine marker in the 45 image frames (n=45).

	X (mm)	Y (mm)	Z (mm)
St Dev	0.015	0.009	0.012
Min dev	-0.032	-0.020	-0.023
Max dev	0.027	0.017	0.027
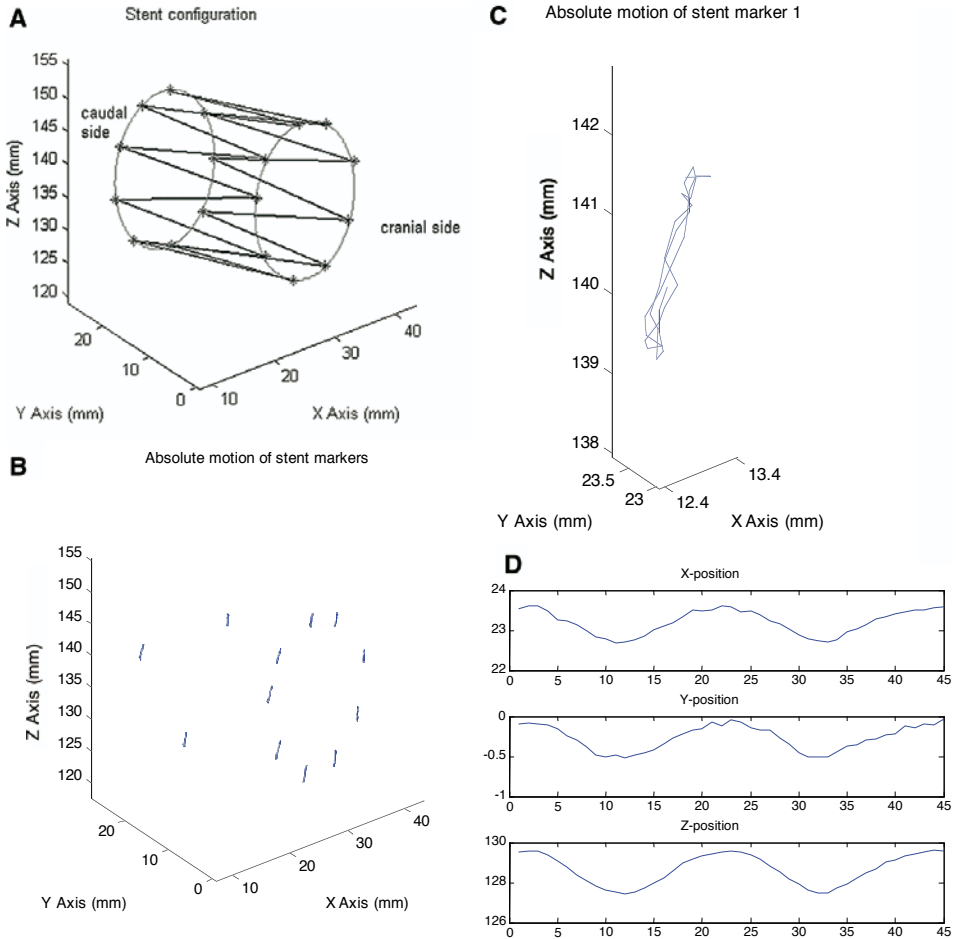
Figure 7. 3-D motion of the stentgraft markers. a) drawing of stent configuration. b) overview of the motion of twelve stentgraft markers, nine at the cranial side and three at the caudal side. c) 3D motion of a single stentgraft marker plotted in X, Y and Z direction. d) motion analysis of a stentgraft marker. break down in motion in X, Y and Z direction. X-axis depicts the images (1-45), Y-axis depicts the position relative to the laboratory coordinate system (in mm).

Measurement of stentgraft dynamics

Finally, the pulsatile dynamics of the stentgraft were analyzed using the calibrated and validated set-up.

There appeared to be a cyclic motion of the stentgraft. This motion occurred in all directions. Figure 7a shows a schematic drawing of the stent configuration. Figure 7b shows the position (changes) of the stentgraft markers during the 2 pulsatile cycles (1.5 second acquisition run, 45 images). Figure 7c shows the position (changes) of a single marker during the same period. Figure 7d shows a break down of this marker motion in X, Y and Z direction.

Figure 8 shows the circle that was estimated through the cranial markers of the stentgraft. The cyclic diameter change of the circle is shown in Figure 9. The circle center motion is displayed in Figure 10, showing cyclic motion of the stent in all directions.

Discussion

Fluoroscopic Roentgen Stereophotogrammetric Analysis (FRSA) enables highly accurate measurement of three dimensional motion of markers on a stentgraft in a pulsatile in-vitro model. Axial, lateral and rotational motion can be measured with a mean error of less than 0.01 millimeter, in every direction (error: 0.003mm, SD 0.019). The precision of 3D marker position measurement by FRSA is very high, expressed by the small standard deviation of the measurement of the X, Y and Z coordinates of the markers (0.009-0.015mm). This non-invasive technique enables quantifying clinical assessment of 3D-motion of a stentgraft in vivo at a high frame rate. This method is extremely important because the effects of pulsatile flow and stentgraft design on motion of the various stentgraft parts can be measured real time, in detail. Until now, this was impossible. FRSA may provide information that is crucial for further improvements in stentgraft design.

The use of CT and MRI for assessment of stentgraft motion has been reported, but these techniques are limited to the measurement of motion in a single plane.[3-5] Furthermore, the accuracy and reproducibility of these measurements have not been validated. This limitation to single plane analysis prevents analysis of complex motion patterns that occur differently in the various stentgrafts during the cardiac cycle, and include axial, transverse and rotational components.[3-5,16] This technical limitation of CT and MRI is caused by the fact that there currently is no technique available to follow a specific point (marker) of the graft in time through the 4D image data set. Moreover, application of MRI is limited by the fact that certain stentgrafts cause significant artifacts in MRI images.

Single focus fluoroscopic measurement of marker motion has been used to assess joint kinematics in orthopedic applications, using single plane images. This method is accurate parallel to the image plane (reported measurement error 0,1-0,17mm), but out of plane measurement error is relatively large (0,7-1,9mm).[14,17] Furthermore, this technique requires a fixed configuration of, at least 3, markers to enable reconstruction of the position of the implant. This fixed configuration cannot be achieved in the dynamic structure of current stentgrafts, making single focus fluoroscopy inappropriate for application in EVAR evaluation.
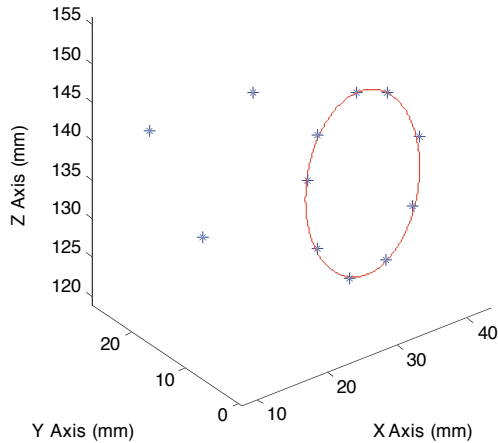
Figure 8. Circle fit through the nine cranial stent markers.

In this study, we used two sets of markers. One was the tantalum marker, a highly radiopaque, spherical marker, resulting in the best possible measurement in orthopedic RSA. This kind of marker could be added to the stentgraft by the manufacturer. The other marker we used was a drop of welding tin. These already occur in certain stentgrafts that are currently in wide clinical use. Markers that are used for positioning of the graft during EVAR can also be used for this procedure. Alternatively, automated pattern recognition of the stentgraft could be used to facilitate measurements without the need for markers. These aspects of FRSA are subject to further evaluation at our institution. In contrast to RSA, used to detect graft migration during follow-up [12,13], no additional markers are needed in the wall of the aorta to perform these dynamic measurements. The spine markers used in our study were solely used for this experiment to determine measurement precision and as an internal control. They were not used to determine the actual stent motion. The latter is done by independently reconstructing the position of each stent marker in space in the sequential images acquired by the calibrated set up, and calculating the marker displacement between these consecutive images.

Limitations

A model was used to study pulsatile change in an aorta with a stentgraft. Patient studies have to be undertaken to assess the quality of the images and visibility of the markers of a stentgraft in vivo, surrounded by soft tissue. However, when considering the image quality of clinical
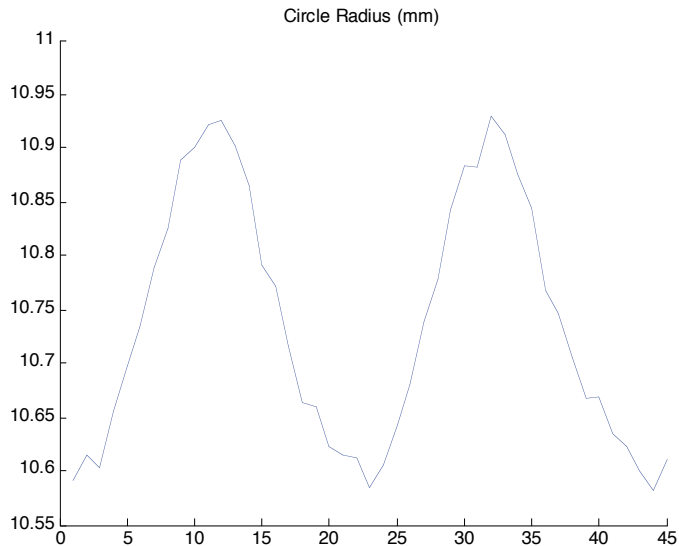
Figure 9. Change in radius of the circle in mm (Y-axis), as fitted through the 45 images (X-axis).

cardiovascular studies acquired by the Siemens set-up, and the validation of FRSA as demonstrated in this study, we are certain that analysis of patient images is feasible, and therefore analysis of stentgraft motion in-vivo can be performed.

Different commercially available stentgrafts bare different markers. In this study only one graft design was tested. Based of our experience with RSA, including pilot testing of imaging and detectability of markers on different commercially available stentgrafts, we believe that motion analysis of different commercially available grafts is feasible. This issue is subject to further study at our institution.

Practical applications

Further, detailed, knowledge of stentgraft motion during the cardiac cycle is required to better understand in-vivo behavior of stentgrafts after EVAR. New stentgrafts can be evaluated, as well as existing grafts. With this knowledge, virtual mechanical modeling becomes possible and assessment of the failure modus of the stentgraft, such as failure due to metal fatigue is facilitated. Based on clinically acquired, detailed knowledge of stentgraft motion, forces acting on the stentgraft during the cardiac cycle can be calculated more accurately. With this knowledge, it is possible to evaluate pre-clinical bench testing of stentgrafts and verify its adequacy. Bench testing itself will be improved according to in-vivo measured clinical data. Knowledge of in-vivo stentgraft motion should be an important adjunct in phase I clinical evaluation of
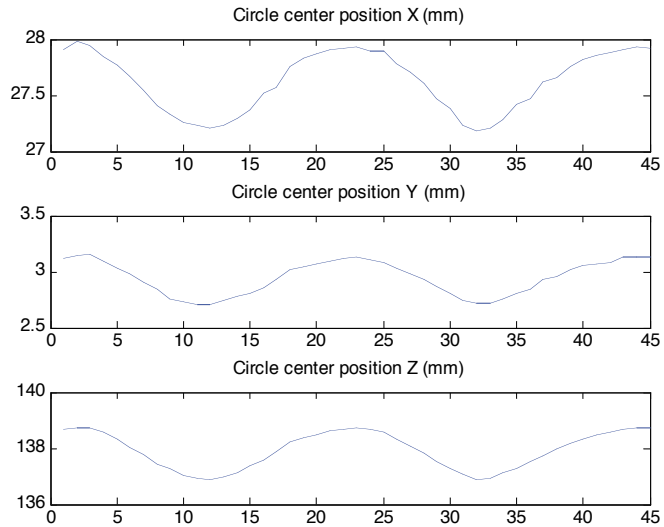
Figure 10. Change of position of the circle center. X-axis depicts the images (1-45), Y-axis depicts the position relative to the laboratory coordinate system (in mm).

stentgrafts. Withdrawal of a graft from the market due to mechanical defects that arise after widespread introduction could be prevented with better bench testing and early detection of unexpected graft motion.

The radiation dose of FRSA was determined in a separate, unpublished experiment by our clinical physicists. The radiation dose is approximately 0.1 mSv for a 3 second study, which corresponds to 4 cardiac cycles at a heart rate of 80 bpm. This compares very favorable to the 17 mSv dose of triple phase CT scan used for EVAR follow up.

Conclusion

In this study, FRSA has proven to be a method with very high accuracy and temporal resolution to measure three dimensional stentgraft motion in a pulsatile environment. This technique has the potential to contribute significantly to the knowledge of stentgraft behavior after endovascular aneurysm repair and improvements in stentgraft design. The technique is ready for clinical testing.

Acknowledgements

We would like to acknowledge the help of the following persons:

8

II Assessment of 3D S-G dynamics using FRSA

References

1. Bockler D, von Tengg-Kobligk H, Schumacher H, Ockert S, Schwarzbach M, Allenberg JR. Late surgical conversion after thoracic endograft failure due to fracture of the longitudinal support wire. J Endovasc Ther. 2005 Feb;12(1):98-102.

2. Jacobs TS, Won J, Gravereaux EC, Faries PL, Morrissey N, Teodorescu VJ, et al. Mechanical failure of prosthetic human implants: a 10-year experience with aortic stent graft devices. J Vasc Surg. 2003 Jan;37(1):16-26.

3. Verhagen, HJ, Teutelink A, Olree M, Rutten A, de Vos AM, Raaijmakers R, et al. Dynamic CTA for cutting edge AAA imaging: Insights into aortic distensibility and movement with possible consequences for endograft sizing and stentdesign *J Endovasc Ther*. 2005;12:I-45.

4. Teutelink A, Rutten A, Muhs BE, Olree M, van Herwaarden JA, de Vos AM, et al. Pilot study of dynamic cine CT angiography for the evaluation of abdominal aortic aneurysms: implications for endograft treatment. J Endovasc Ther. 2006 Apr;13(2):139-44.

5. Vos AW, Wisselink W, Marcus JT, Vahl AC, Manoliu RA, Rauwerda JA. Cine MRI assessment of aortic aneurysm dynamics before and after endovascular repair.*J Endovasc Ther* 2003;10:433-9.

6. Selvik G. Roentgen stereophotogrammetry. A method for the study of the kinematics of the skeletal system. *Acta Orthop Scand Suppl*. 1989;232:1-51.

7. Karrholm J. Roentgen stereophotogrammetry. Review of orthopedic applications. *Acta Orthop Scand*. 1989;60:491-503.

8. Valstar ER, Vrooman HA, Toksvig-Larsen S, Ryd L, Nelissen RG. Digital automated RSA compared to manually operated RSA. *J Biomech*. 2000;33:1593-1599.

9. Vrooman HA, Valstar ER, Brand GJ, Admiraal DR, Rozing PM, Reiber JH. Fast and accurate automated measurements in digitized stereophotogrammetric radiographs. *J Biomech*. 1998;31:491-498.

10. Valstar ER, de Jong FW, Vrooman HA, Rozing PM, Reiber JH. Model-based Roentgen stereophotogrammetry of orthopaedic implants. *J Biomech*. 2001;34:715-722.

11. Kaptein BL, Valstar ER, Stoel BC, Rozing PM, Reiber JAC. A new model-based RSA method validated using CAD models and models from reversed engineering. *J Biomech*. 2003;36:873-882.

12. Koning OH, Oudegeest OR, Valstar ER, Garling EH, van der Linden E, Hinnen JW, et al. Roentgen Stereophotogrammetric Analysis: an accurate tool to assess endovascular stentgraft migration. *J Endovasc Ther*. 2006;13:468-475

13. Koning OH, Garling EH, Hinnen JW, Kroft LJ, van der Linden E, Hamming JF, et al. Accurate detection of stentgraft migration in a pulsatile aorta using Roentgen Stereophotogrammetric Analysis. *J Endovasc Ther*. 2007;14(1):30-8.

14. Garling EH, Kaptein BL, Geleijns K, Nelissen RG, Valstar ER. Marker Configuration Model-Based Roentgen Fluoroscopic Analysis. J Biomech. 2005;38(4):893-901.

15. Hinnen, JW, Visser MJ, Van Bockel JH. Aneurysm sac pressure monitoring: effect of technique on interpretation of measurements. *Eur J Vasc Endovasc Surg* 2005; 29:233-8

16. Flora HS, Woodhouse N, Robson S, Adiseshiah M. Micromovements at the aortic aneurysm neck measured during open surgery with close-range photogrammetry: implications for aortic endografts. *J Endovasc Ther*. 2001;8:511-520.

17. Ioppolo J, Borlin N, Bragdon C, Li M, Price R, Wood D, et al. Validation of a low-dose hybrid RSA and fluoroscopy technique: Determination of accuracy, bias and precision. *J Biomech*. 2007;40(3):686-92.

CHAPTER

9

Fluoroscopic roentgen stereophotogrammetric analysis (FRSA) to study 3-D stent-graft dynamics in patients: a pilot study

Olivier H. J. Koning
Bart L. Kaptein
Rozemarijn van der Vijver
Nuno V. Dias
Martin Malina
Martin J. Schalij
Edward R. Valstar
and J. Hajo van Bockel

Abstract

Objective: To study the feasibility and analyze the first results of Fluoroscopic Roentgen Stereophotogrammetric Analysis (FRSA) quantifing real time three-dimensional dynamic motion of stent-grafts (SG) in patients after endovascular aortic aneurysm repair (EVAR).

Methods: A digital bi-plane fluoroscopy set-up was calibrated (Siemens Axiom Artis dBc®). Stereo images were acquired of a patient after thoracic EVAR and of a patient after abdominal EVAR. Images were analyzed using a customized version of commercially available software for Roentgen stereophotogrammetric analysis (MB-RSA, MEDIS specials BV). SG motion was measured during the cardiac cycle with respiratory arrest. In addition, SG motion due to respiratory action was measured in the patient after abdominal EVAR.

Results: SG motion could be quantified in all 3 dimensions at 30 (stereo) frames per second in both patients without difficulty. For the thoracic SG, the maximum translational motions of the center of mass of the top stent in X-, Y-, and Z- direction (TM XYZ) were 2.3mm, 2.5mm, 1.9mm respectively. The diameter changed (DC) between 27.9mm and 28.7mm. Motion in axial direction (AX) was 2.9mm. Rotational motion around the longitudinal axis of the top stent (RM) was 3.5°. For the abdominal SG, the TM XYZ were 1.2mm, 1.0mm, 1.5mm respectively. DC: 22.8mm-23.5mm. AX: 1.6mm. RM: 1.1°. During respiratory action TM XYZ were 5.8mm, 1.5mm, 2.4mm respectively.

Conclusion: FRSA is the first validated clinically feasible tool to quantify real time three-dimensional stent-graft dynamics after EVAR. Because quantification of three-dimensional motion was not available until now, FRSA can provide crucial information of the continuous forces that are exerted in all directions on stent-grafts. Thus, it will provide essential information for further improvements in stent-graft design.

Introduction

Endovascular repair (EVAR) is widely accepted as a reliable technique for treatment of selected abdominal and thoracic aortic aneurysms. Stent-graft failure can occur due to the physically demanding environment in which the device is placed. The repetitive strain that is induced by the cardiac and respiratory cycle can result in device failure such as stent fractures, fabric perforation and migration. These failures are a threat to patient health and safety.[1-3] Detailed knowledge of stent-graft dynamics after EVAR is indispensable to minimize the risk of graft failure by continuously improving stent-graft design and testing.

Stent-graft dynamics appear to be complex and three-dimensional. Axial, transverse and rotational motion of the aorta, as well as dilatation have been reported to occur during the cardiac cycle.[4-8]

Currently, it is impossible to precisely quantify stent-graft dynamics with current clinically used imaging techniques. The two main modalities used to study stent-graft dynamics during the cardiac cycle are cinematographic (cine-) CT and MRI.[4-6] These techniques have several disadvantages and technical limitations. The most important of these is the fact that the reconstructions are limited to a single, two-dimensional plane.[9]

Recently, an experimental study was published on the use of fluoroscopic roentgen stereophotogrammetric analysis (FRSA) to quantify real time three-dimensional dynamics of stentgrafts during the cardiac cycle.[10] FRSA is a combination of a commercially available digital bi-plane fluoroscopic imaging system and the well known and validated method of roentgen stereophotogrammetric analysis, used to measure micromotion in-vivo.[11-18] FRSA uses calibrated, high resolution digital stereo images to assess the position of (metallic) markers using specialized software. The images are acquired at 30 stereo frames per second. The technique is completely non-invasive, does not require intravascular contrast and has a radiation exposure of approximately only 0.1 mSv for a 3 second study, which corresponds to 4 cardiac cycles at a heart rate of 80 bpm.[10]

In this study, we have evaluated the feasibility and obtained the first results of Fluoroscopic Roentgen Stereophotogrammetric Analysis (FRSA) to quantify real time three-dimensional dynamic motion of stent-grafts in patients after EVAR.

Methods

FRSA set-up

We used a Siemens Axiom Artis dBc imaging system (Siemens AG, Erlangen, Germany) (Figure 1), which consists of two C-arms with digital flat panel Roentgen detectors. The focus to detector distance was set at 95 cm. The two C-arms were positioned at a 90 degree angle, to produce a posterior-anterior image and a lateral image. The images were acquired and stored in 1024 x 1024 pixels, 14 bits grey scale resolution (Figure 2 and 3). The frame rate was 30 bi-directional images per second. Each stereo image was acquired as two separate alternating images, resulting in 60 alternating images per second. The set-up was calibrated to determine the exact relative position of the two Roentgen foci and the two detectors. The procedure was performed as described previously, using a calibration box with markers in known postions.[10] For each analysis reported in this study, a 1.5 second run (45 stereo images) was analyzed.

Figure 1. FRSA set-up consisting of two C-arms with digital flat panal Roentgen detectors (Siemens Axiom Artis dBc imaging system, Siemens AG, Erlangen, Germany).
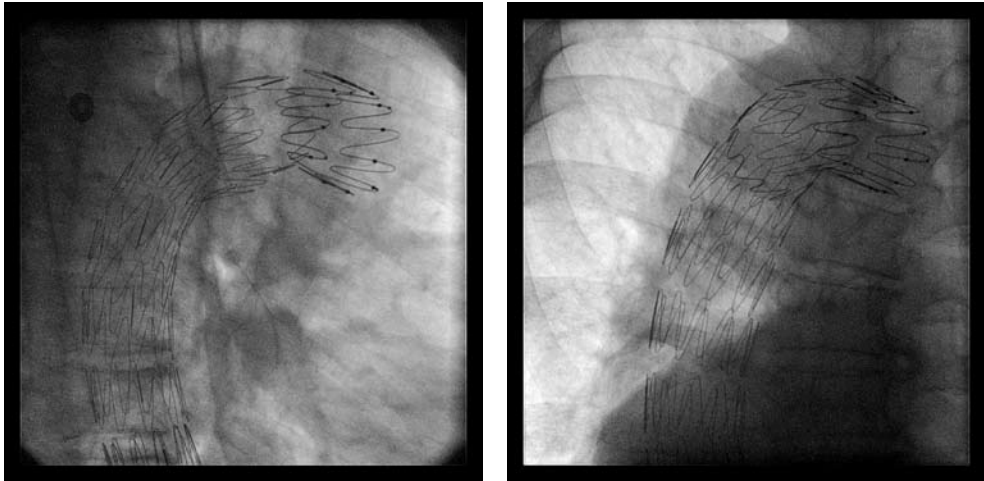
Figure 2. Lateral and Posterior-Anterior fluoroscopic images of the thoracic stent. The spherical shaped welding points and fabric markers are visible on the top stent.
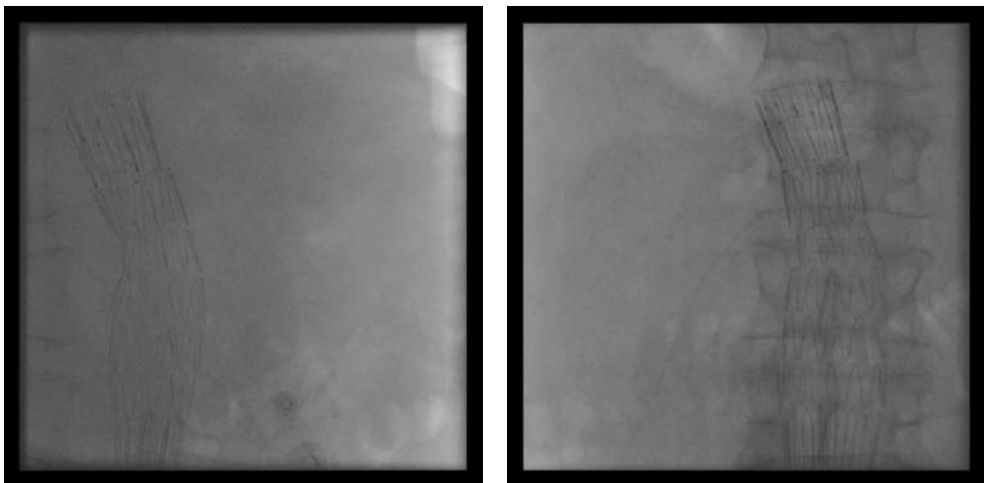
Figure 3. Lateral and Posterior-Anterior fluoroscopic images of the abdominal stent. The spherical shaped welding points and fabric markers are visible on the top stent.

The image pairs were analyzed using Model-based RSA software (ModelBased-RSA, version 3.2, MEDIS specials, Leiden, The Netherlands) to calculate the relative 3-D marker positions.[10-16] No image reconstruction is required before analyzing the image pairs.

Patients

Two patients were randomly selected for this pilot study. Both had undergone EVAR within a week before evaluation. The first patient was a 57 year old male with a symptomatic type-B

aortic dissection.. A proximal component of a Zenith TX2® thoracic stent-graft device (Cook, Bjaeverskov, Denmark) was implanted, intentionally covering the ostium of the left subclavian artery. The graft had a diameter of 34mm. The blood pressure during imaging was 160/97 mmHg with a pulse rate of 100 per minute, which corresponds to 2.5 cardiac cycles during the 1.5 second image acquisition run. The imaging of the stent-graft dynamics during the cardiac cycle was performed during respiratory arrest.

The second patient was a 75 year old male with an abdominal aortic aneurysm. He was treated with a Zenith® stent-graft (Cook, Bjaeverskov, Denmark). The proximal graft diameter was 28mm. The patient had a blood pressure during imaging of 129/69 mmHg and a pulse rate of 80 per minute, which corresponds to 2 cardiac cycles during the 1.5 second image acquisition run. The imaging of the stent-graft dynamics during the cardiac cycle was performed during respiratory arrest. As an additional study, stent-graft displacement as a result of respiratory action was measured in a separate image run.

The study was approved by our institution's ethics review committee.

Analysis of stent-graft dynamics

The welding points of the hooks to the top stent of the stent-graft were used as markers for 3D motion analysis, as well as the gold markers designating the upper edge of the fabric of the graft (Figure 4). The marker positions were determined in each sequential frame. The resulting series of marker positions was analyzed for marker motion. The changing position of the center of mass of the stent markers was used to quantify three-dimensional motion of the aorta – stent-graft complex during the cardiac cycle. Furthermore, a cylindrical shape was fitted through the cranial markers in every stereo image (12 markers for the thoracic stent and 11 markers for the abdominal stent). The changing diameter of the cylinders was used as a measure for the pulsatility of the stent. Finally, rotation and translation of the stent around and along the longitudinal stent axis were assessed. Analysis was performed using routines that were implemented in Matlab r2006B (The MathWorks, Natick, USA).

The origin of the coordinate system was placed in the center of the markers in the first image frame. The positive X-axis was oriented in caudal direction, the positive Y-axis in lateral direction towards the right side of the patient, and the Z-axis in dorsal direction.
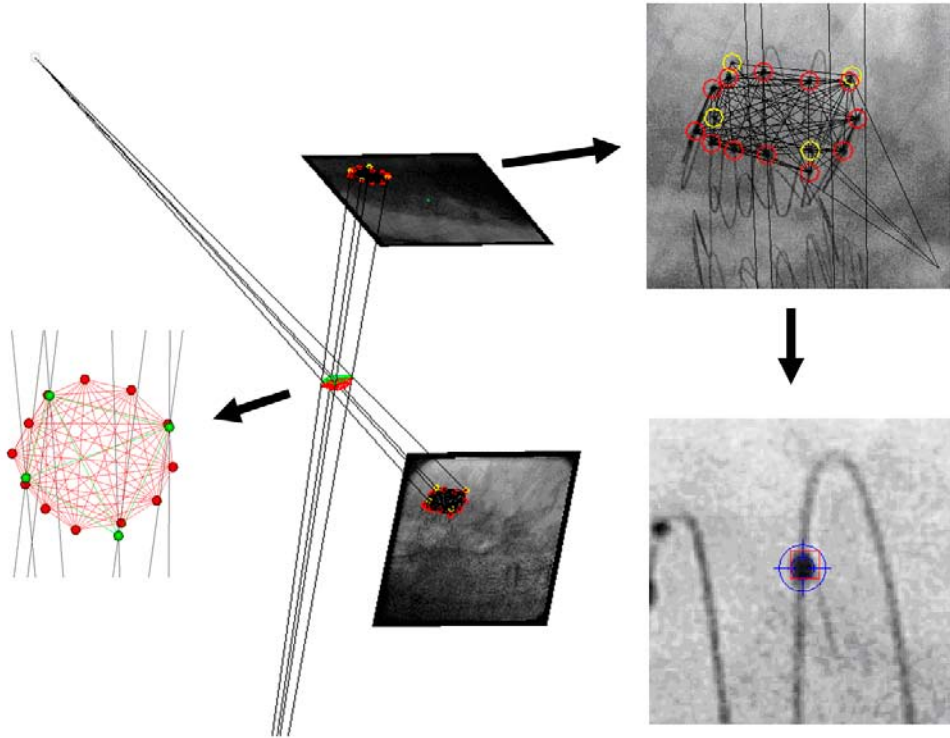
Figure 4. Overview of the stereo reconstruction of the thoracic stent-graft device.
Center: 3D reconstruction of the stereo image and the Roentgen foci of the bi-plane set-up. The crossing lines reflect the position of the stent-graft markers.
Left: Close-up of the 3D reconstructed markers, the red markers are reconstructed from the welding points of the hooks to the top-stent, and the green markers represent the gold markers at the upper edge of the fabric.
Upper right: Close-up of the image with the detected markers, the red markers designate the welding points; the yellow markers designate the gold markers.
Lower right: Close-up of a single welding point of the hook to the stent-graft. These welding points are used as markers to generate the 3D stent-graft image.

Results

Analysis of stent-graft dynamics

Thoracic stent-graft
Three-dimensional cyclic motion of the stent-graft was observed. Figure 2 shows the lateral and posterior-anterior images of a stereo image of the graft. Figure 4 shows a three-dimensional
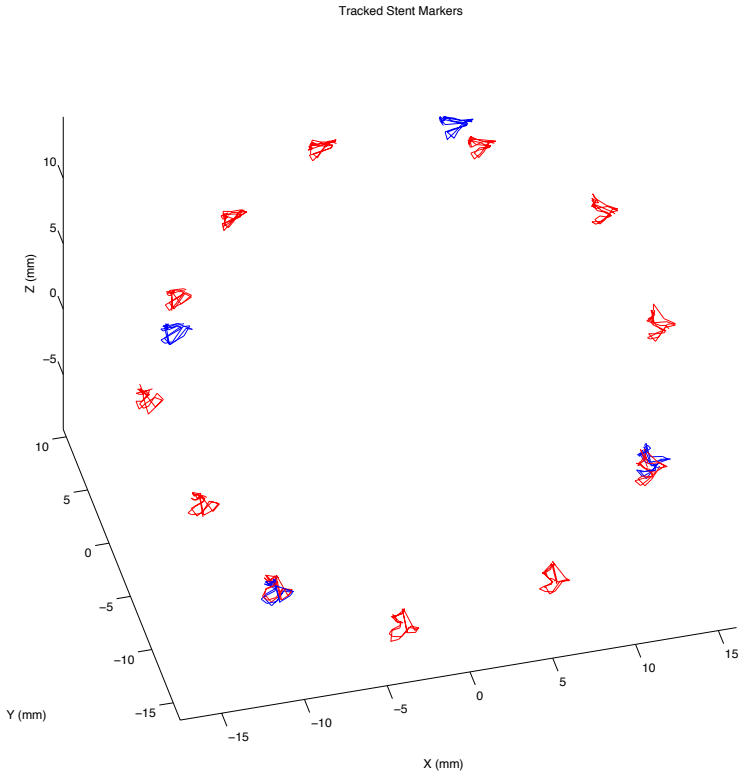
Figure 5. The tracked thoracic stent markers (welding points) (red) and gold fabric markers (blue).
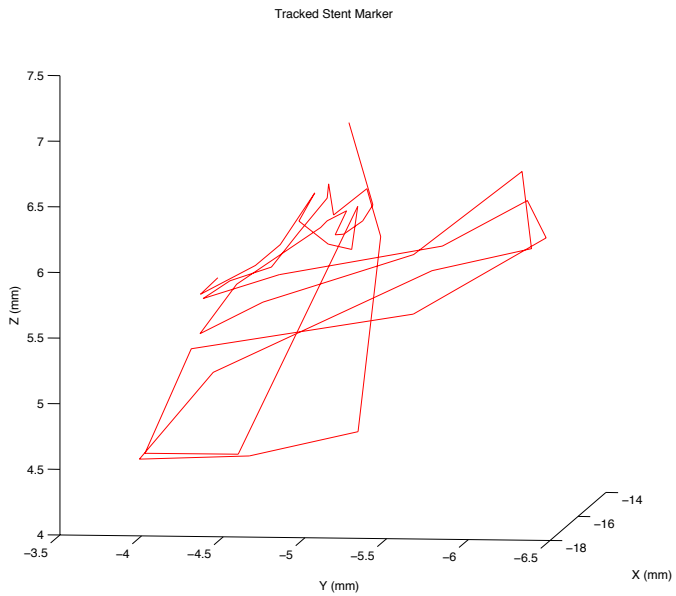
Figure 6. Detail of the typical track of a thoracic stent marker.

representation of the stent markers as reconstructed by the FRSA software. Figure 5 shows the position change of the stent markers and the gold fabric markers during the image acquisition run. Figure 6 shows the dynamics of a single, randomly chosen, marker during the cardiac cycle. Figure 7 shows a break down of all marker motions in X, Y and Z direction, relative to their positions at t=0.3, which is the start of the systole.

The dynamics of the center of mass of all markers are displayed in Figure 8, showing cyclic motion of the stent in all directions. The thoracic stent-graft showed a motion pattern of stent dilatation and a center of mass motion of the top stent in caudal-ventral-right hand side direction relative to the patient, followed by an over-compensation in opposite lateral and cranial direction and a gradual return to the starting position with reduction of diameter of the graft. This means that, at the start of the systole, the stent-graft moves toward the heart. This is probably due to contraction of the left ventricle. The maximum translational motions of the center of mass of the stent in X-, Y-, and Z- direction were 2.3mm, 2.5mm and 1.9mm respectively. A cylinder was fitted through the cranial markers of the stent-graft. The average distance from the markers to this cylinder was 0.14mm. The cyclic diameter change of the cylinder, between 27.9mm and 28.7mm, is also shown in Figure 8. The rotational motion of the top stent was 3.5° around its longitudinal axis. The stent motion along its long axis was 2.9mm per cycle.
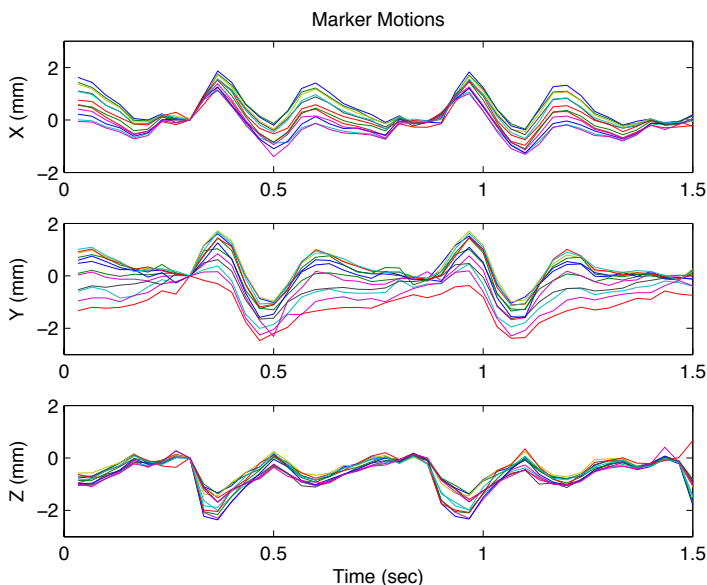
Figure 7. Motion of all thoracic stent markers relative to their first positions; break down in X, Y and Z direction. Note that the markers have different motion patterns as a result of the deformation of the stent.
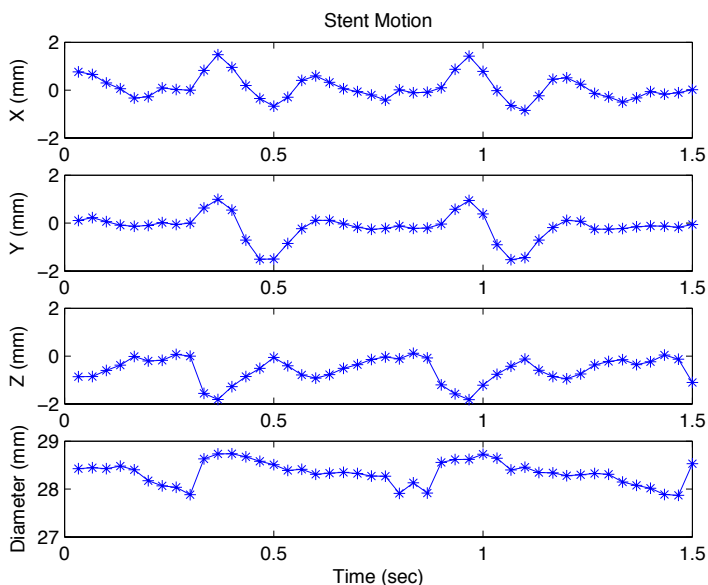
Figure 8. Thoracic stent motion (X, Y, Z motion of the center of mass of the top-stent and the change in diameter of the cylinder fitted through the stent markers).

Abdominal stent-graft

Three-dimensional cyclic motion of the stent-graft was observed. Figure 3 shows the lateral and posterior-anterior images of a stereo image of the graft. Figure 9 shows the cyclic change of position of the center of mass of the top-stent. The maximum translational motions of the center of mass of the stent in X-, Y-, and Z-direction were 1.2mm, 1.0mm and 1.5mm respectively. The average distance from the markers to the cylinder that was fitted through the markers was 0.26mm. The diameter change of the cylinder was between 22.8mm and 23.5mm (Figure 9). The rotational motion of the top stent was 1.1° around its longitudinal axis. The stent motion along its long axis was 1.6mm per cycle.

As a result of respiratory action, the maximum translational motions of the top stent in X-, Y-, and Z-direction were 5.8mm, 1.5mm and 2.4mm respectively.

Discussion

This study clearly demonstrates that fluoroscopic Roentgen stereophotogrammetric analysis (FRSA) is a clinically feasible, non-invasive tool to quantify real time 3-D stent-graft dynamics after EVAR in detail. For the first time, quantification of 3-D motion including rotational dynamics is possible.
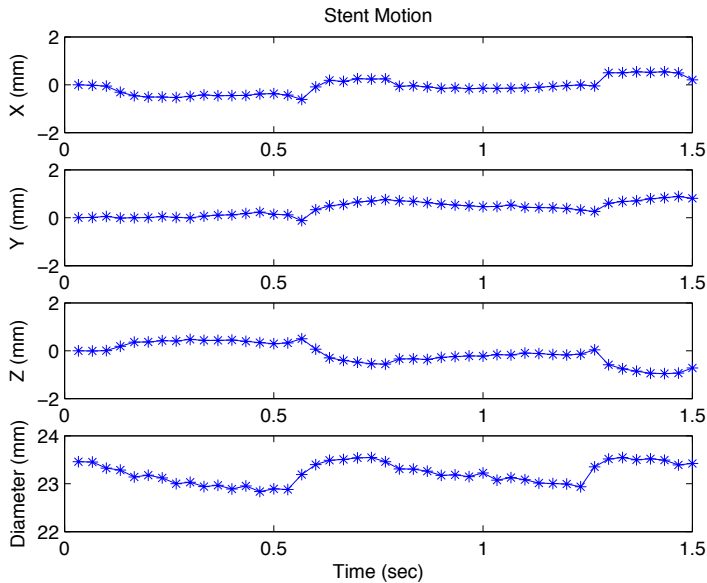
Figure 9. Abdominal stent motion (X, Y, Z motion of the center of mass of the top-stent and the change in diameter of the cylinder fitted through the stent markers).

Previous experimental validation studies have shown that the fast stereo image acquisition and high frame rate of FRSA enable accurate and precise quantification of stent-graft motion in high spatial and temporal resolution, with a mean measurement error of 0.003 ± 0.019 millimeter.[10]

Image acquisition itself is painless, of short duration, does not require intravascular contrast and with a radiation exposure of 0.1mSv the patient burden is very low.

The clinical data found in this study are limited in size. Therefore, it is of little interest to extensively discuss the nature and implications of the stent-graft motion found in these two patients. However, to point out the possible implications of our findings, it is interesting to review part of the presented data. The thoracic stent-graft showed a three-dimensional motion pattern of stent dilatation and a center of mass motion. If the dynamics of this thoracic stent-graft are assessed in a single reconstruction plane, as is the case with cine-CT or cine-MRI, the initial segment of the aorta as viewed in the first reconstructed image would be out of the reconstruction plane almost all the time. Only at the end of the diastole will it return to the initial position in the image reconstruction plane. As a result of this out of plane motion, dynamics of conically shaped stent-grafts or change of stent-graft angulation during cyclic motion can result in false measurements of shape or diameter change Therefore, FRSA is much more powerful than

current cinematographic imaging using cine-CT and cine-MRI as it enables quantification of the true changes of three-dimensional stent-graft position and configuration.

We found a significant motion of the abdominal stent-graft due to respiratory action of almost 6mm in caudal direction. When using plain abdominal radiography to detect long-term stent-graft migration, the dynamics due to respiratory action could result in under- or over-reporting of migration in individual cases. This is due to the change of position of the stent-graft as compared to the reference point, the vertebral column.

The results demonstrate that standard markers used for positioning of the graft during EVAR can easily be used for FRSA, as well as welding points of the hooks to the top stent. As an alternative to marker detection, automated pattern recognition of the stent-graft could be used to facilitate measurements without the need for markers. These aspects of FRSA are subject to further evaluation at our institutions. In contrast to standard Roentgen stereophotogram-metric analysis used to detect graft migration during long term follow-up with comparison of multiple investigations over time [12,17,18], additional markers in the wall of the aorta are not required to perform these dynamic measurements.

Contrary to cine-CT and cine-MRI, there are no limitations to FRSA in terms of direction of motion, type of motion or type of metal of the stent-graft, duration of image acquisition or ECG changes. Furthermore, no intravascular contrast is required. Motion analysis with cine-CT and cine-MRI is limited to a single (2-Dimensional) plane due to the reconstruction of the images.[9] Out-of-plane motion can not be quantified and complex three-dimensional motion can only be interpreted semi-quantitatively by analyzing different image planes. Moreover, rotational motion can not be quantified at all. In addition, the spatial resolution of these techniques is limited [6] and their accuracy and reproducibility have not been validated. Because FRSA uses direct three-dimensional reconstruction of the images, the listed limitations do not apply to this technique. Another disadvantage of cine- CT and -MRI is that both require intravascular contrast. Difficulties with ECG reconstruction, as is required with these techniques, can occur in patients without sinus rhythm. The resulting CT or MRI image is a compilation of several cardiac cycles, resulting in a "time average" dynamic image, rather than an actual "real time" view of the stent-graft motion. Contrary to cine-CT and -MRI, FRSA does not require ECG reconstruction because it uses real time images to quantify three-dimensional motion. Therefore, there are no technical time constraints or difficulties with ECG abnormalities with this technique. Finally, there are inherent technique specific disadvantages such as a high radiation dose in cine-CT and the limitations in imaging stainless steel stent-grafts in cine-MRI.

There are still many unknown aspects of stent-graft motion in-vivo. The cardiac and respiratory cycle, in conjunction with tissue properties of the aortic wall and surrounding tissues, result in repetitive strain on the stent-graft. This strain has lead to stent-graft failure resulting in devastating complications, despite intensive testing before clinical introduction. [1,2] The main reason for this kind of device failure is that preclinical testing depends on modeling of motion and forces acting on the stent-graft. Unexpected types of stent-graft motion, including stent-graft torsion, have revealed unanticipated forces acting on the stent-graft. These forces could obviously not have been modeled beforehand and therefore device failure was not anticipated.

Detailed knowledge of stent-graft motion after EVAR is vital to stent-graft development and improvement. Only with this knowledge it is possible to optimize modeling of graft safety testing and improve design e.g. by improved biocompatibility and (computer aided) fatigue modeling and bench testing. FRSA enables this kind of detailed real time imaging. Furthermore, modeling can be adjusted with the information obtained with FRSA after implantation in patients.

One could argue that assessment of the dynamics of a new stent-graft should be mandatory in the period of first clinical introduction to possibly detect unexpected motion in an early phase to determine if adequate bench testing has been performed and predict possible failure by fatigue modeling according to clinical motion data.

Currently, the only limitations of FRSA are that the field of view is limited by the detector size and that specifically identifiable markers are required to detect stent-graft position in consecutive images. We could visualize up to 8 stents of the thoracic or abdominal graft in one view (Figure 2 and 3) with the standard size digital detectors used for cardiac imaging. Larger detectors are commercially available and could enable imaging of the full length of longer grafts.

We plan to expand FRSA imaging and motion analysis to different stent-grafts and larger cohorts, as well as repeated imaging over time to study changes in motion pattern. The relative position change of the different stents of the stent-graft can also be measured. This way, angulation change and stent-graft torsion can be determined.

Conclusion

FRSA is the first clinically feasible tool to quantify real time three-dimensional stent-graft dynamics after EVAR. Because quantification of three-dimensional motion was not available until now, FRSA can provide crucial information of the continuous forces that are exerted in all directions on stent-grafts. Thus, it will provide essential information for further improvements in stent-graft design.

Acknowledgements

References

1. Bockler D, von Tengg-Kobligk H, Schumacher H, Ockert S, Schwarzbach M, Allenberg JR. Late surgical conversion after thoracic endograft failure due to fracture of the longitudinal support wire. J Endovasc Ther. 2005 Feb;12(1):98-102.

2. Jacobs TS, Won J, Gravereaux EC, Faries PL, Morrissey N, Teodorescu VJ, et al. Mechanical failure of prosthetic human implants: a 10-year experience with aortic stent graft devices. J Vasc Surg. 2003 Jan;37(1):16-26.

3. Tiesenhausen K, Hessinger M, Konstantiniuk P, Tomka M, Baumann A, Thalhammer M, Portugaller H. Surgical conversion of abdominal aortic stent-grafts--outcome and technical considerations. Eur J Vasc Endovasc Surg. 2006 Jan;31(1):36-41.

4. Verhagen, HJ, Teutelink A, Olree M, Rutten A, de Vos AM, Raaijmakers R, et al. Dynamic CTA for cutting edge AAA imaging: Insights into aortic distensibility and movement with possible consequences for endograft sizing and stentdesign *J Endovasc Ther*. 2005;12:I-45.

5. Teutelink A, Rutten A, Muhs BE, Olree M, van Herwaarden JA, de Vos AM, et al. Pilot study of dynamic cine CT angiography for the evaluation of abdominal aortic aneurysms: implications for endograft treatment. J Endovasc Ther. 2006 Apr;13(2):139-44.

6. Vos AW, Wisselink W, Marcus JT, Vahl AC, Manoliu RA, Rauwerda JA. Cine MRI assessment of aortic aneurysm dynamics before and after endovascular repair.*J Endovasc Ther* 2003;10:433-9.

7. Teutelink A, Muhs BE, Vincken KL, Bartels LW, Cornelissen SA, van Herwaarden JA, Prokop M, Moll FL, Verhagen HJ. Use of dynamic computed tomography to evaluate pre- and postoperative aortic changes in AAA patients undergoing endovascular aneurysm repair. J Endovasc Ther. 2007 Feb;14(1):44-9.

8. Flora HS, Woodhouse N, Robson S, Adiseshiah M. Micromovements at the aortic aneurysm neck measured during open surgery with close-range photogrammetry: implications for aortic endografts. *J Endovasc Ther*. 2001;8:511-520.

9. Muhs BE, Vincken KL, Teutelink A, Verhoeven EL, Prokop M, Moll FL, Verhagen HJ.Dynamic cine-computed tomography angiography imaging of standard and fenestrated endografts: differing effects on renal artery motion. Vasc Endovascular Surg. 2008 Feb-Mar;42(1):25-31.

10. Koning OH, Kaptein BL, Garling EH, Hinnen JW, Hamming JF, Valstar ER, Bockel JH. Assessment of three-dimensional stent-graft dynamics by using fluoroscopic roentgenographic stereophotogrammetric analysis. *J Vasc Surg*. 2007 Oct;46(4):773-779.

11. Selvik G. Roentgen stereophotogrammetry. A method for the study of the kinematics of the skeletal system. *Acta Orthop Scand Suppl*. 1989;232:1-51.

12. Karrholm J. Roentgen stereophotogrammetry. Review of orthopedic applications. *Acta Orthop Scand*. 1989;60:491-503.

13. Valstar ER, Vrooman HA, Toksvig-Larsen S, Ryd L, Nelissen RG. Digital automated RSA compared to manually operated RSA. *J Biomech*. 2000;33:1593-1599.

14. Vrooman HA, Valstar ER, Brand GJ, Admiraal DR, Rozing PM, Reiber JH. Fast and accurate automated measurements in digitized stereophotogrammetric radiographs. *J Biomech*. 1998;31:491-498.

15. Valstar ER, de Jong FW, Vrooman HA, Rozing PM, Reiber JH. Model-based Roentgen stereophotogrammetry of orthopaedic implants. *J Biomech*. 2001;34:715-722.

16. Kaptein BL, Valstar ER, Stoel BC, Rozing PM, Reiber JAC. A new model-based RSA method validated using CAD models and models from reversed engineering. *J Biomech*. 2003;36:873-882.

17. Koning OH, Oudegeest OR, Valstar ER, Garling EH, van der Linden E, Hinnen JW, et al. Roentgen Stereophotogrammetric Analysis: an accurate tool to assess endovascular stentgraft migration. *J Endovasc Ther*. 2006;13:468-475

18. Koning OH, Garling EH, Hinnen JW, Kroft LJ, van der Linden E, Hamming JF, et al. Accurate detection of stentgraft migration in a pulsatile aorta using Roentgen Stereophotogrammetric Analysis. *J Endovasc Ther*. 2007;14(1):30-8.

ADDENDUM

EVAR and radiation risks

C H A P T E R

10

Endovascular abdominal aortic aneurysm repair: patient dose and radiation risks

---

Koos Geleijns

Olivier H. J. Koning

and J. Hajo van Bockel

Abstract

Objective: To assess cumulative patient dose and to calculate associated radiation risks for patients undergoing abdominal endovascular aortic aneurysm repair (EVAR).

Design of study: A traditional protocol and a reduced dose scenario for medical imaging in EVAR planning, repair and surveillance was assumed and patient dose was assessed. The excess relative radiation risk was calculated using a model for age-, gender- and site-specific solid cancer mortality. Life tables were used to calculate risk related parameters for patients that underwent EVAR at 55, 65, 75 and 85 years of age. In addition to radiation risk, mortality rates that are typical for the EVAR population were taken into account, knowingly the probability of 30-day mortality and the mortality rate from AAA-related causes in general during follow-up.

Results: Effective dose for EVAR planning was 18 (8) mSv; for EVAR repair 10 (10) mSv; and during the first, second and subsequent years of surveillance 87.5 (35) mSv/y, 35 (17.5) mSv/y and 17.5 (17.5) mSv/y. The number of radiation induced deaths per 1000 EVAR patients was 12 (10), 8 (6), 4 (3) and 1 (1) for patients treated at ages 55, 65, 75 and 85 years (respectively traditional protocol and between brackets reduced dose scenario). The corresponding number of abdominal aortic aneurysm (AAA) related deaths per 1000 EVAR patients was: 126, 91, 67 and 47, respectively (for both the traditional protocol and the reduced dose scenario). The average radiation induced reduction of life expectancy was 40 (30), 21 (15), 8 (5) and 2 (1) days for patients treated at ages 55, 65, 75 and 85 years; corresponding AAA related reduction of life expectancy was 739 (740), 387 (387), 197 (197) and 82 (82) days (respectively traditional protocol and between brackets reduced dose scenario).

Conclusion: Radiation exposure accumulates rapidly for patients undergoing surveillance after abdominal EVAR. However, associated radiation risks are modest, even for the traditional surveillance protocol that is associated with a relatively high patient dose. Radiation risks are much smaller compared to AAA-related risks.

Introduction

X-ray imaging for image guided treatment, preoperative planning and postoperative surveillance is frequently used in vascular surgery. It is well known that X-ray imaging is associated with a certain risk for induction of malignant lesions, particularly if the radiation dose becomes relatively high. Proper radiation protection is required for such practices. Justification and optimization of practices are the two main principles in radiation protection. Specific guidance for proper radiation protection in medical applications is provided in a publication of the International Commission on Radiological Protection (ICRP) 'Radiological Protection In Medicine' [1]. Justification of radiation exposure for patients undergoing abdominal endovascular aortic aneurysm repair (EVAR) implies that EVAR, and its associated preoperative planning and postoperative surveillance, should as a rule improve patient care and that radiation induced side effects are minimized. In other words, radiation exposure for patients undergoing EVAR should do more good than harm to the individual patient. Optimization implies that the level of radiation protection is the best achievable under the prevailing circumstances, maximizing the margin of benefit over radiation induced harm.

Pre- and peroperative radiation exposure for patients undergoing EVAR is already relatively high and may accumulate further during postoperative surveillance depending on the type and frequency of postoperative testing, particularly when complications occur which are endovascularly treated. This raised concern about radiation doses and particularly about the potential radiation induced carcinogenic effect in the long term [2].

The x-ray imaging modalities that are used for patients undergoing EVAR are radiography, fluoroscopy and computed tomography (CT). For these imaging techniques, assessment of radiation exposure of patients is rather straightforward, and can be based on the output of x-ray imaging equipment. An adequate measure of the output is generally provided on the operator console after the examination, either as a dose-area product (fluoroscopy, radiography) or computed tomography dose index (CT scanner). Radiation risk assessment is required for balancing benefits against harm. In addition to the late mortality risk resulting from exposure to ionizing radiation, other acute and late mortality risks have to be taken into account for proper risk assessment of the complete EVAR procedure. These include the procedure related mortality risk and risks of death from aneurysm, other cardiovascular and non-vascular causes [3].

In this study two imaging strategies for EVAR were taken as a starting point, one strategy corresponding with traditional practices (traditional protocol) and one with more recent practices

(reduced dose protocol). The associated radiation exposures was assessed for both practices. Next, comprehensive radiation risk assessment was performed taking into account mortality rates that are typical for the EVAR population. To achieve this, a demographic methodology based on life tables was developed. These data were used to quantify the cumulative patient radiation dose and associated mortality risk for patients after abdominal endovascular aortic aneurysm repair (EVAR) in relation to all cause mortality risk for these patients.

Methods

Clinical practice

A traditional protocol for x-ray imaging of patients undergoing EVAR was defined based on a guideline of the European Collaborators on Stent-graft Techniques for Abdominal Aortic Aneurysm Repair (EUROSTAR) protocol [4;5]. A reduced dose protocol was derived from observed clinical practices. Surveillance with duplex ultrasound may be performed in EVAR patients but was not considered in this study since it does not add to the radiation exposure and radiation risk evaluation.

Radiation exposure

Radiation exposure from pre-operative and peroperative angiography depends strongly on the used equipment, local practices, experience of the operator and complexity of the procedure. For this study the exposure was estimated as 10 mSv effective dose per procedure [6]. Organ doses resulting from fluoroscopy corresponding to an effective dose of 10 mSv were assessed using PCXMC Monte Carlo software (STUK, Radiation and Nuclear Safety Authority, Finland). Assessment of radiation exposure from CT scans, i.e. organ doses and effective dose, was estimated from the clinical CT acquisition protocols as implemented in one hospital (ImPACT CT Patient Dose Calculator; [7]). Radiation exposure resulting from four radiographs of the abdomen was calculated from measurements of the dose area product using an anthropomorphic phantom representing a standard adult (Rando Male Phantom, The Phantom Laboratory, Salem, NY, USA) followed by organ dose and effective dose calculations with PCXMC Monte Carlo software. Doses were assessed for organs for which information on age and gender dependent excess relative radiation risk is provided in BEIR VII [8], i.e. bone marrow, stomach, colon, liver, lung, breast, prostate, uterus, ovary, bladder, thyroid, and finally, as one group, all other organs.

Risk assessment

Risk assessment was performed for males and females at four clinically relevant ages, i.e. patients undergoing abdominal EVAR at the ages of 55, 65, 75 and 85 years old; the age of 75 is approximately the average age of patients treated for abdominal aortic aneurysms [9]. The BEIR VII excess relative risk (ERR) model was used for radiation risk assessment [8]. In the BEIR VII model, organ specific solid cancer mortality is expressed relative to the background risk of solid tumor mortality; taking into account both gender and age. Data on the background risk of solid tumor mortality depending on organ, gender and attained age were derived from ICRP Publication 103 (Euro-American cancer mortality rates by age and site) [10]. Next, according to the BEIR VII model, an overall ERR function depending on organ dose, gender, age at exposure, and attained age was calculated for male and female patients with EVAR at the ages of 55, 65, 75 and 85 years old. Incurred organ dose was also incorporated in the risk model as a function of attained age, this was required because patients who undergo EVAR are exposed at different ages. In addition to radiation risk, mortality rates that are typical for the EVAR population were taken into account, i.e. the probability of 30-day mortality (0.007 at the ages 55 and 65; 0.016 at the age of 75; and 0.022 at the age of 85) and the mortality rate from AAA-related causes in general during follow-up (6 per 15 000 patient months) [3].

Life tables are used in demography for measuring and modeling population processes and they allow for calculation of death rate, life expectancy and reduction of life expectancy. The radiation induced, age, gender, and dose dependent overall mortality for the European population (Eurostat database [11]), was incorporated in life tables together with EVAR related mortality rates that are typical for the patient population and the gender and age specific probability of dying.

Results

Clinical practices

Traditional clinical practice included one pre-operative contrast enhanced CT scan in the arterial phase and a pre-operative angiogram, followed by fluoroscopy guided EVAR. Post operative evaluation after EVAR was performed directly after the procedure, and followed by surveillance 1, 3, 6, 12, 18, 24, and 36 months after EVAR; after 36 months surveillance was performed yearly. Common clinical practice is currently associated with reduced application of medical imaging, it includes one pre-operative contrast enhanced CT scan in the arterial phase, followed by fluoroscopy guided EVAR. Post operative evaluation after EVAR is performed directly after

the procedure, and followed by yearly surveillance. The post operative evaluation and surveil-
lance sessions included radiography (four projections (AP, LAT, 30°LPO, 30°RPO)) and CT (two
contrast enhanced scans, one arterial phase and one delayed phase scan).

Radiation exposure

Radiation exposure per procedure is presented in Table 1. Organ doses and effective dose are
listed for pre-operative CT, pre-operative fluoroscopy, operative fluoroscopy, post operative
and surveillance CT, and post operative and surveillance abdominal radiographs. Relatively
high organ doses were assessed for bone marrow, stomach, colon, liver, uterus, ovaries, and
bladder. From the radiation exposure per procedure and the observed practices, appropriate
organ doses and effective dose were assigned to the year before EVAR; to the year in which
EVAR was performed, and the years of post operative evaluation and surveillance (Table 2).
Due to the intensive use of x-ray imaging the effective dose accumulates rapidly to hundreds
of millisieverts for patients treated with EVAR; this is illustrated in Figure 1 by the cumulative
effective dose.

Table 1. Radiation exposure per procedure, expressed as organ dose (mGy) and effective dose
(mSv)

	Pre-operative CT 1 year before EVAR (mGy)	Pre-operative Fluoroscopy 1 year before EVAR (mGy)	Operative Fluoroscopy year at EVAR (mGy)	Post operative evaluation and Surveillance	
				CT (mGy)	Abdominal radiography (mGy)
Bone marrow (mGy)	6.1	16.7	16.7	12.2	0.7
Stomach (mGy)	17.0	5.6	5.6	34.0	2.3
Colon (mGy)	11.0	21.8	21.8	22.0	4.7
Liver (mGy)	15.0	3.1	3.1	30.0	1.8
Lung (mGy)	2.0	0.2	0.2	4.0	0.0
Breast (mGy)	0.5	0.0	0.0	1.0	0.0
Prostate (mGy)	1.0	0.6	0.6	2.0	0.2
Uterus (mGy)	16.0	27.6	27.6	32.0	3.2
Ovary (mGy)	14.4	31.7	31.7	28.8	3.2
Bladder (mGy)	14.0	9.2	9.2	28.0	3.2
Other solid cancers (mGy)	8.0	10.0	10.0	16.0	1.5
Thyroid (mGy)	0.0	0.0	0.0	0.1	0.0
Effective dose (mSv)	8.0 mSv	10.0 mSv	10.0 mSv	16.0 mSv	1.5 mSv

Table 2. Radiation exposure before, during and after EVAR, expressed as organ doses (mGy) and effective dose (mSv). Columns correspond with a traditional protocol (relatively high dose); or with a reduced protocol (reduced frequency for imaging during surveillance (relatively low dose))

	Preoperative (mGy)		EVAR and the first year of postoperative EVAR surveillance (mGy)		The second year of postoperative EVAR surveillance (mGy)		The third and following years of postoperative EVAR surveillance	
	Traditional [a]	Reduced [b]	Traditional [a]	Reduced [b]	Traditional [a]	Reduced [b]	Traditional [a]	Reduced [b]
Bone marrow, mGy	22.8	6.1	81.3	42.5	25.8	12.9	12.9	12.9
Stomach, mGy	22.6	17.0	186.9	78.1	72.5	36.3	36.3	36.3
Colon, mGy	32.8	11.0	155.5	75.3	53.5	26.7	26.7	26.7
Liver, mGy	18.1	15.0	162.0	66.6	63.6	31.8	31.8	31.8
Lung, mGy	2.2	2.0	20.4	8.3	8.1	4.0	4.0	4.0
Breast, mGy	0.6	0.5	5.3	2.1	2.1	1.0	1.0	1.0
Prostate, mGy	1.6	1.0	11.3	4.9	4.3	2.2	2.2	2.2
Uterus, mGy	43.6	16.0	203.5	98.0	70.4	35.2	35.2	35.2
Ovary, mGy	46.1	14.4	191.5	95.6	63.9	32.0	32.0	32.0
Bladder, mGy	23.2	14.0	165.1	71.6	62.4	31.2	31.2	31.2
Other solid cancers, mGy	18.0	8.0	97.5	45.0	35.0	17.5	17.5	17.5
Thyroid, mGy	0.0	0.0	0.4	0.2	0.2	0.1	0.1	0.1
Effective dose, mSv	18.0 mSv	8.0 mSv	97.5 mSv	45.0 mSv	35.0 mSv	17.5 mSv	17.5 mSv	17.5 mSv

[a] Pre-operative CT and fluoroscopy; operative fluoroscopy; post operative evaluation after EVAR, post operative surveillance at 1, 3, 6, 12, 18, 24 and 36 months after EVAR and next yearly after EVAR

[b] Pre-operative CT; operative fluoroscopy; post operative evaluation after EVAR, post operative surveillance at 6 and 12 months after EVAR and next yearly after EVAR
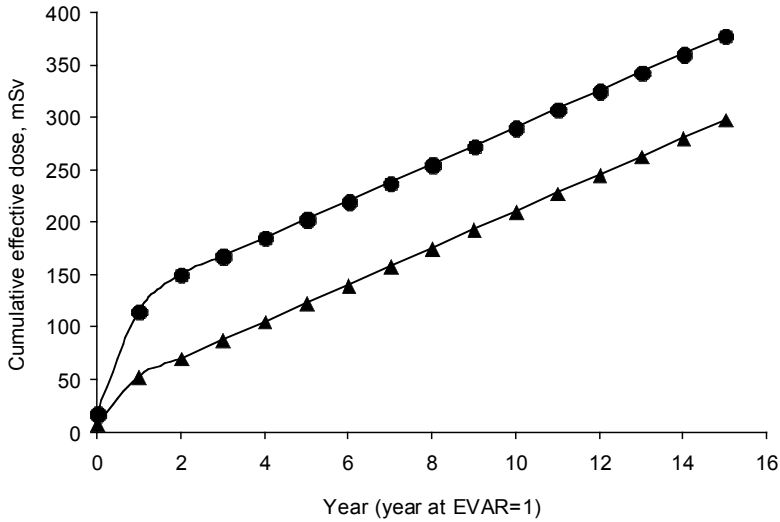
Figure 1. Cumulative effective dose (mSv) resulting from abdominal endovascular aortic aneurysm repair (EVAR) planning, repair and surveillance relative to the year of abdominal EVAR. Dots represent a traditional protocol (relatively high dose); triangles represent a protocol with a reduced frequency for imaging during surveillance (relatively low dose)

Risk assessment

Demographic and risk related parameters were derived from the life tables for patients aged 55, 65, 75 and 85 years at EVAR. This information is presented in Table 3. The number of natural deaths (per 1000 EVAR patients) increases with increasing age. The reason is that at higher ages the overall (natural) mortality increases rapidly, and both radiation induced deaths and AAA related deaths decrease with increasing age; this decrease is more prominent for radiation induced deaths. The number of radiation induced deaths is much smaller than the number of AAA related deaths.

The reduction of life expectancy associated with radiation exposure was for the traditional and reduced dose protocols (between brackets) respectively 40 (30), 21 (15), 8 (5) and 2 (1) days for patients treated with EVAR at 55, 65, 75 and 85 years of age. These figures are much smaller compared to the AAA related reduction of life expectancy of 739 (740), 387 (387), 197 (197) and 82 (82) days respectively. Reason for this is that compared to the more acute, disease related, risks that are typical for the EVAR population, radiation induced mortality requires a relatively long time to come to expression.

Table III. Calculated demographic and risk related parameters for patients (male and female) that underwent EVAR at the age of respectively 55, 65, 75 and 85 years of age.

	EVAR at 55 years of age						EVAR at 65 years of age					
	♂		♀		Avg (♂&♀)		♂		♀		Avg (♂&♀)	
	Tra	Red	Tra	Red	Tra	Red	Tra	Red	Tra	Red	Tra	Red
Number of natural deaths, per 1000 EVAR patients	872	874	853	856	862	864	909	911	895	897	901	903
Number of radiation induced deaths, per 1000 EVAR patients	12	9	13	10	12	10	8	6	8	6	8	6
Number of AAA related deaths, per 1000 EVAR patients	117	117	134	134	126	126	84	84	97	97	91	91
Life expectancy at age of EVAR, years	23.8	23.8	27.4	27.5	25.6	25.6	16.7	16.8	19.7	19.7	18.2	18.2
Overall reduction of life expectancy, days	689	682	868	860	779	771	359	353	456	450	407	402
Radiation induced reduction of life expectancy, days	37	28	43	33	40	30	20	14	21	15	21	15
EVAR induced reduction of life expectancy, days	653	654	825	827	739	740	339	339	435	435	387	387

	EVAR at 75 years of age						EVAR at 85 years of age					
	♂		♀		Avg (♂&♀)		♂		♀		Avg (♂&♀)	
	Tra	Red	Tra	Red	Tra	Red	Tra	Red	Tra	Red	Tra	Red
Number of natural deaths, per 1000 EVAR patients	933	934	926	927	929	930	951	951	952	953	952	952
Number of radiation induced deaths, per 1000 EVAR patients	4	3	4	2	4	3	2	1	1	1	1	1
Number of AAA related deaths, per 1000 EVAR patients	63	63	71	71	67	67	47	47	47	47	47	47
Life expectancy at age of EVAR, years	10.5	10.5	12.2	12.2	11.3	11.4	6.1	6.1	6.1	6.1	6.1	6.1
Overall reduction of life expectancy, days	186	183	223	221	205	202	86	85	81	81	83	83
Radiation induced reduction of life expectancy, days	8	5	7	5	8	5	2	1	1	1	2	1
EVAR induced reduction of life expectancy, days	178	178	216	216	197	197	83	83	80	80	82	82

Avg = Average; Tra = traditional protocol; Red = reduced dose protocol

Discussion

Only a few studies report on radiation exposure for patients that undergo EVAR. In one dosimetric study, 96 patients were included; an effective dose of 27 mSv (median value; range 16-117 mSv) was reported for EVAR (fluoroscopy time 21 minutes); and for both preoperative and surveillance CT scans an effective dose of 13 mSv was reported [2]. Cumulative effective dose in the first year following EVAR was 79 mSv. In another study a median effective dose of 8.7 mSv was reported for EVAR (n=24; average dose 10.5 mSv; range 2.5-28.1 mSv; fluoroscopy time 21 min), and for computed tomography 14.3 mSv (pre-operative CT), 10.8 mSv (first postoperative CT); and 5.4 mSv (surveillance CT) [6]. Under these latter conditions, the cumulative effective dose would be 115 mSv over a 10-year period. It is well known that considerable inter-hospital variations occur in radiation exposure for patients in both diagnostic- and interventional radiology. This is well illustrated by the large difference in the above reported median effective dose for EVAR, respectively 27 mSv and 8.7 mSv, whereas the reported fluoroscopy time is about the same. Reasons for such differences in patient dose may be technical (configuration and commissioning of the x-ray equipment), or operator dependent (choice for a certain fluoroscopy mode, proper use of collimation, positioning of the detector). The effective dose of 27 mSv seems to be rather high. In our calculations we used an estimated effective dose for fluoroscopy of 10 mSv. The patient dose of 16 mSv for computed tomography used in our calculations is close to the reported value of 13 mSv [2], and substantially higher compared to the value of 5.4 mSv reported by Geijer et al. [6]. Thus, patient dose from CT resulting from the EVAR surveillance regimen that was assumed for this study may be relatively high but is certainly well within the range of doses that occur in clinical practice.

We did not consider additional image guided interventions in our dose calculations. The number and intensity of these interventions varies to a great degree and can therefore not be standardized. With additional procedures the cumulative dose will rise accordingly, adding to the risk of radiation induced mortality.

Epidemiological and experimental studies provide evidence of radiation induced cancer risk, albeit with uncertainties at doses of about 100 mSv or less [10]. This suggests that radiation risks should be taken seriously, particularly for EVAR patients for whom cumulative effective dose during intensive surveillance protocols may exceed 100 mSv considerably. It has been recommended that epidemiologic studies should be performed on cohorts of patients that receive repeated CT scans during follow-up studies [8]. Results from such epidemiologic studies on patient cohorts are not yet available. Therefore, methodologies for assessing the potential risks associated with high-dose radiological examination based on effective dose and generic

fatal cancer estimates are proposed as a crude estimate of the number of fatal cancers [12]. Knowledge on radiation induced cancer risk is mainly derived from studies on radiation carcinogenesis at low doses in the atomic bomb survivors in Japan. Such a methodology was for example applied for estimating the risk of cancer from diagnostic X-ray imaging for the UK and 14 other countries [13]. Inevitably, inaccuracies of such methodologies occur due to the well known uncertainties in current quantitative radiation risk estimates. A major source of uncertainty and a fundamental shortcoming of such approaches is that specific demographic characteristics of patient cohorts are neglected. Published risk estimates are commonly based on the assumption that radiation induced carcinogenesis in patients is equal to that in the general population. Such an approach is inappropriate, particularly in EVAR patients, since EVAR procedure related risks and an increased risk of death from aneurysm, other cardiovascular and non-vascular causes, strongly determine life expectancy and the probability to develop a fatal (late) radiation induced cancer. Radiation carcinogenesis is a late effect that will be less prominent if additional competing mortality risks are taken into account. This study shows that radiation risk estimates can be calculated taking into account other relevant mortality risks. This was achieved by the application of life tables that integrate mortality from natural causes, radiation induced cancers, and EVAR and health status related mortality risks.

The probability of long term survival of patients after EVAR, stratified according to age, was reported in a study by Schermerhorn et al. For the 67-74 year age interval the 48 month probability of survival after EVAR was 0.78; for the 75-84 year age interval the probability was 0.69; and for the ≥85 year age interval the probability was 0.52 [9]. For the demographic model used in this study the 48 month probability of survival after EVAR was 0.95 for patients undergoing EVAR at the age of 55; and 0.92, 0.68 and 0.56 for patients undergoing EVAR at the age of 65, 75 an 85 years, respectively. Although comparison of the published data for the age intervals cannot be compared straightforwardly to the age specific results of this study, we concluded that the demographic model compares well with the observed survival of patients that underwent EVAR.

The results of this study show that a methodology based on life tables and a well accepted model for radiation carcinogenesis can be used to calculate radiation induced deaths and an associated radiation induced reduction of life expectancy for patients that undergo EVAR. The calculations show that for patients that are prone to exposure to a high cumulative effective dose, the risk of radiation induced carcinogenesis still remains rather small, both in quantitative terms as well as compared to procedure and health status related mortality risks. For a typical 75 year old EVAR patient, the number of radiation induced deaths per 1000 EVAR patients is 4 (3),

whereas the procedure and AAA related deaths is 67 (67) per 1000 EVAR patients. Correspond-
ing average radiation induced reduction of life expectancy is 8 (5) days, and procedure and AAA
related reduction of life expectancy is 197 (197) days (figures corresponding respectively to the
traditional and reduced dose (between brackets) protocol). It is concluded that cumulative
radiation exposure in EVAR patients, although relatively high, should not be associated with a
major concern with regard to radiation carcinogenesis. Still, any opportunity for optimization
and reduction of radiation exposure of EVAR patients should of course be pursued.

The two main study limitations are inaccuracies in BEIR VII model for radiation risk assessment
and uncertainties in patient dose assessment. Inherent inaccuracies of the BEIR VII committee's
preferred ERR model for estimating site-specific solid cancer mortality are the estimated errors
for the fit parameters for the model; and the uncertainty of the most appropriate dose and
dose-rate reduction factor (DDREF). Uncertainties in patient dose assessment originate from
the well know phenomenon of large variations in patient dose for one and the same proce-
dure; and from the lack of reliable information on typical exposures for patients undergoing
EVAR. However in this study we choose commonly accepted values, both with regard to the
ERR, DDREF and organ doses. Furthermore the effect that was observed was large enough
to reliably conclude that radiation risks associated with EVAR are modest and much smaller
compared to AAA related risks.

Although radiation risks are of minor concern in EVAR patients, there are still good reasons
for reconsidering current practices. First, it is a legal and ethical requirement that exposure to
radiation is always kept as low as possible, secondly the increasing number of EVAR patients
that now undergo intensive follow up place a growing burden on imaging capacity (equip-
ment, radiologists) and associated financial resources. Considering the increase of radiation
associated mortality risk with the decrease of age at EVAR procedure, the urge for reduction
of radiation exposure is especially strong for endovascular procedures in younger patients, for
instance after traumatic vascular injury. The most promising option for dose reduction and
health care cost saving in the EVAR population is optimization of the surveillance protocols.
Recent practices already indicate less frequent application of x-ray imaging. Other suggested
changes in EVAR surveillance are the use of color duplex ultrasonography [14]; introduction of
roentgen stereophotogrammetric analysis which provides (compared to CT) lower dose and
more cost effective surveillance [15]; and introduction of a reduced surveillance regimen [16].
Therefore further efforts are still needed to achieve optimized surveillance of patients that
underwent EVAR but it should be taken into account that optimization of surveillance should
also take into account detection of nonaneurysmal-related findings, particularly with CT [17].

Conclusion

Based on the results of this study, we conclude that radiation exposure accumulates rapidly for patients undergoing abdominal EVAR. However, associated radiation risks are modest and much smaller compared to AAA related risks.

References

1. ICRP. Radiological protection in Medicine, International Commission on Radiological Protection. ICRP Publication 105 2008.

2. Weerakkody RA, Walsh SR, Cousins C, Goldstone KE, Tang TY, Gaunt ME. Radiation exposure during endovascular aneurysm repair. Br J Surg 2008;95(6):699-702.

3. Epstein DM, Sculpher MJ, Manca A, Michaels J, Thompson SG, Brown LC et al. Modelling the long-term cost-effectiveness of endovascular or open repair for abdominal aortic aneurysm. Br J Surg 2008;95(2):183-90.

4. Leurs LJ, Laheij RJ, Buth J. What determines and are the consequences of surveillance intensity after endovascular abdominal aortic aneurysm repair? Ann Vasc Surg 2005;19(6):868-75.

5. Harris PL, Buth J, Mialhe C, Myhre HO, Norgren L. The need for clinical trials of endovascular abdominal aortic aneurysm stent-graft repair: The EUROSTAR Project. EUROpean collaborators on Stent-graft Techniques for abdominal aortic Aneurysm Repair. J Endovasc Surg 1997;4(1):72-7.

6. Geijer H, Larzon T, Popek R, Beckman KW. Radiation exposure in stent-grafting of abdominal aortic aneurysms. Br J Radiol 2005;78(934):906-12.

7. Shrimpton PC, Edyvean S. CT scanner dosimetry. Br J Radiol 1998;71(841):1-3.

8. NAS/NRC. Health risks from exposure to low levels of ionising radiation: BEIR VII phase 2. Board on Radiation Effects Research National Research Council of the national Academies, Washinton, D C 2006.

9. Schermerhorn ML, O'Malley AJ, Jhaveri A, Cotterill P, Pomposelli F, Landon BE. Endovascular vs. open repair of abdominal aortic aneurysms in the Medicare population. N Engl J Med 2008;358(5):464-74.

10. ICRP. The 2007 Recommendations of the International Commission on Radiological Protection. ICRP Publication 103 2007.

11. http://epp.eurostat.ec.europa.eu/. Eurostat 2007.

12. Hall EJ, Brenner DJ. Cancer risks from diagnostic radiology. Br J Radiol 2008;81(965):362-78.

13. Berrington A, Darby SC, Weiss HA, Doll R. 100 years of observation on British radiologists: mortality from cancer and other causes 1897-1997. Br J Radiol 2001;74(882):507-19.

14. Sun Z. Diagnostic value of color duplex ultrasonography in the follow-up of endovascular repair of abdominal aortic aneurysm. J Vasc Interv Radiol 2006;17(5):759-64.

15. Koning OH, Oudegeest OR, Valstar ER, Garling EH, van der LE, Hinnen JW et al. Roentgen stereophotogrammetric analysis: an accurate tool to assess stent-graft migration. 2006;13(4):468-75.

16. Sternbergh WC, III, Greenberg RK, Chuter TA, Tonnessen BH. Redefining postoperative surveillance after endovascular aneurysm repair: recommendations based on 5-year follow-up in the US Zenith multicenter trial. J Vasc Surg 2008;48(2):278-84.

17. Indes JE, Lipsitz EC, Veith FJ, Gargiulo NJ, III, Privrat AI, Eisdorfer J et al. Incidence and significance of nonaneurysmal-related computed tomography scan findings in patients undergoing endovascular aortic aneurysm repair. J Vasc Surg 2008;48(2):286-90.

CHAPTER

11

Summary, future aspects and conclusions

Part 1: Surveillance of stent-graft migration after EVAR

Chapter 1 describes the relevance of aortic aneurysmal disease, its treatment and the long term risks of endovascular aneurysm repair (EVAR). One of the major risks of EVAR is stent-graft migration. Migration can lead to repressurization of the aneurysm sac and consequent rupture of the aneurysm. Migration and other forms of device failure are caused by the repetitive strain on the stent-graft caused by the cardiac and respiratory cycle. These device failures can result in aneurysm related death of the patient despite previous EVAR.

Surveillance of EVAR patients is performed regularly to enable early detection of adverse events such as migration and stent fracture. CT Angiography is the current clinical gold standard to determine stent-graft position. However, CT has several disadvantages of which intravascular contrast requirement, cost and logistical burden are the most relevant. Furthermore, CT requires a significant radiation dose.

As an alternative to CT, plain abdominal radiography (AXR) is currently used to determine stent-graft position. Both CT and AXR are methods in which the observer determines the position of the stent-graft relative to a point of reference. Contrast enhanced CT enables the use of side branches as a point of reference. AXR images are analyzed with the vertebral end plate as point of reference. The points of reference are assigned by an observer; the measurements are consequently sensitive to human variance. Both methods have specific disadvantages, which are further discussed in Chapter 1. Furthermore, the accuracy of CT and AXR to detect stent-graft migration has not been described previously.

As a possible alternative to CT and AXR, Roentgen Stereophotogrammetric Analysis (RSA) could be considered as a method to detect stent-graft migration and detect possible stent fracture. RSA is a highly accurate technique to determine marker positions inside the body using calibrated, stereo plain radiography. RSA has a long and successful history in orthopedic surgery in surveillance of joint prosthesis micro-motion. The technical aspects of RSA are discussed in Chapter 2. In short, RSA is based on comparing the two (2-dimensional) images of a stereo roentgen projection to calculate a three dimensional image of the positions of markers in space, i.e. inside the human body. For use in endovascular surgery, RSA requires markers on the graft and in the aortic wall to determine the position of the stent-graft relative to a point of reference. These markers need to be positioned in the patient during surgery. These and several other technical and validation issues concerning RSA as a tool for surveillance after

EVAR were addressed in the first part of this thesis. Furthermore, we assessed the accuracy of CT and plain radiography to measure stent-graft migration.

Validation of RSA to determine stent-graft migration

Static model

In Chapter 3 RSA was validated as a technique to measure stent-graft migration in a static model. In this study, RSA was compared to CT with 3D image reconstruction. The model was constructed from a Plexiglas tube and a Gianturco stent cast in Plexiglas. Markers were added to the stent and the tube for RSA analysis. PTFE inlays in the tube were used to simulate the renal arteries for CT analysis. The stent was "migrated" in axial direction with a micromanipulator, which was used as the standard of reference for the experiment. The initial position and the position after stent-graft migration were imaged with RSA and CT. CT images were acquired with the highest available resolution and 3D image reconstruction was performed using advanced post-processing software with central lumen line reconstruction. This set-up is also used in the current clinical stent-graft surveillance protocol at the Leiden University Medical Center. To correct for inter-observer variability, CT measurements were performed by 3 different, experienced observers.

The results showed that RSA is a feasible method to detect stent-graft migration in a static model, and that it was highly accurate, with a mean error of 0.002mm, SD=0.044mm, maximum error=0.10mm. This was significantly more accurate than CT which had a mean error of 0.14mm, SD=0.29mm, maximum error=1.0mm (p < 0.0001). No significant inter-observer variation was found between the CT observers (p=0.17).

One of the questions that remained was what the influence of pulsatile motion would be on the accuracy of migration measurement. Theoretically, pulsatile motion of markers can produce errors in RSA measurement. These errors can occur due to marker motion during imaging.

RSA in a pulsatile environment

The question of the influence of pulsatile marker motion on RSA is discussed in Chapter 4. A model was constructed with a fresh thoracic pig aorta fixed to a human cadaver spine. A side branch was attached to resemble the renal artery for CT analysis. The model was connected to an artificial circulation with physiological flow and pressure profiles. A stent was placed inside the aorta. Markers were added to the stent and aortic wall for RSA analysis, including a potential endovascular marker for clinical use. RSA of the stent position without pulsatile

flow was used as the standard of reference for stent-graft migration. RSA and CT imaging were performed of every position of the stent.

Using standard tantalum markers, RSA had a mean error of -0.5mm, SD=0.16mm, maximum error= 0.7mm. Using the experimental endovascular marker, RSA had with a mean error of -0.4mm, SD=0.25mm, maximum error= 1.1mm. The marginally lower precision and higher maximum error are probably due to the fact that the endovascular marker is not spherical like the tantalum marker used in standard orthopedic practice. However, both RSA measurements with the different aortic reference markers compared favorably to CT with 3D image reconstruction which had a mean error of -1.1mm, SD=1.17mm, maximum error= 2.8mm.

These results demonstrated that RSA is a feasible and accurate method to detect stent-graft migration in this model despite pulsatile stent-graft motion. Migration measurements using RSA were more accurate than CT. Furthermore, the experimental endovascular marker proved promising with good measurement results.

Further studies were required to test the feasibility of RSA as well as the performance of the endovascular marker in-vivo, before clinical introduction of the technique can be considered. For these reasons, an animal study was undertaken.

RSA in-vivo

In Chapter 5, we describe an experimental study with two large, 100 Kg pigs. A model of a stent-graft was introduced into the thoracic aorta via thoracolaparotomy. Tantalum markers were attached to the adventitia of the aorta as points of reference for RSA. The tantalum marker closest to the stent-graft model was also used as a point of reference for the CT measurements. For RSA analysis, additional Nitinol endovascular clips were inserted in the aortic wall via endovascular technique as aortic reference markers. Stent-graft migrations were measured with CT and RSA.

The standard deviation of the measurements by RSA using tantalum markers was 0.36mm**.** The standard deviation of the measurements by CT with 3D reconstruction was 0.47mm. Radiopacity of the clips was insufficient to allow detection with the RSA software.

The study showed that RSA stent-graft migration measurement in vivo was feasible and very precise despite the physiological motion due to the cardiac and respiratory cycle and the large amount of soft tissue surrounding the markers. Precision of RSA was superior to CT with 3D image reconstruction if a well defined aortic reference marker was applied for CT analysis. It is likely that the precision of migration measurement with CT will decrease if a less well defined point of reference is used, for instance the renal or mesenteric artery, as is current practice. This

assumption seems to be supported by the fact that the variation of CT in the pulsatile model was already larger than the variation of measurement using a well defined reference marker. Therefore, we concluded that placement of an aortic reference marker may facilitate accurate stent-graft migration detection without the need for contrast enhancement. Although this would eliminate a significant disadvantage of CT surveillance, several other disadvantages such as the burden on logistics and cost, and to a lesser extent radiation burden, would remain.

As an aortic reference marker, the nitinol clip needs to be modified to increase radiopacity to enable RSA analysis. Enhancement of the endovascular marker with a gold or platinum ring could fulfill this purpose. Design testing needs to be performed before the marker can be introduced into practice.

Regarding aortic reference markers required for RSA

Apart from the issue of radiopacity, there are several other issues that need to be addressed regarding aortic reference markers. One of these issues is the question which is the appropriate position of the marker relative to the graft.

In the study described in Chapter 4, we found that an increasing distance between the aortic and stent-graft markers due to migration caused a slight increase in the error of measurement in our study, which corroborates with findings as reported in the orthopedic RSA literature. This implies that for the most accurate RSA measurement of stent-graft migration, the aortic markers need to be positioned as close to the stent-graft as possible.

Safety of the nitinol endovascular clip was also studied in the animal study described in Chapter 5. In both pigs the endovascular markers were replaced several times for evaluation purposes without difficulty. At post mortem investigation, the clips had (purposefully) penetrated the aortic wall. No adverse effects were found. It has to be remarked that this is, by nature of the experiment, a limited number of animals with a healthy aorta. Further studies are needed to evaluate the safety of a modified endovascular clip.

Another important question that remained was how many aortic reference markers are needed for accurate stent-graft migration detection with RSA. In orthopedic RSA multiple reference markers are used. As a rule, more markers will result in more accurate measurement with RSA. In endovascular surgery, a reference marker needs to be attached to the aortic wall. This implies that an extra procedure is needed during EVAR. Reducing the number of reference markers to only one would minimize additional risk.

One single reference marker will enable quantification of migration in every direction, except rotational displacement. In contrast to axial, cranio-caudal migration or angulation of the graft

relative to the aortic neck, rotation of an infrarenal stent-graft around its long axis is not a crucial problem since this type of displacement does not affect the sealing zone and should therefore not lead to complications. Furthermore, axial stent-graft rotation as a single phenomenon is not very likely to occur. The impact of reducing the amount of reference markers on the accuracy and precision of RSA migration measurement were unknown.

Accuracy of RSA using one aortic reference marker
In Chapter 6, we described the renewed analysis of the images of the model with pulsatile circulation and the animal experiments. Instead of using a cluster of reference markers for RSA analysis, we now only used one single aortic reference marker.

In the in-vitro model, the measurement error of RSA using multiple markers was -0.5 ± 0.16mm. Using only one single reference marker, the error of RSA was -0.73 ± 0.12mm. In-vivo, RSA using one reference marker had a pooled mean error of 0.17 ± 0.65mm as compared to standard RSA.

Our data showed a very accurate detection of stent-graft migration with RSA using a single reference marker. Therefore, it appears that one single aortic reference marker is sufficient for stent-graft migration surveillance after EVAR.

Clinical applicability of AXR for migration surveillance
Currently, plain abdominal radiography (AXR) is advocated by some to determine stent-graft position and detect migration. AXR has several advantages over CT. Because of these advantages, AXR is an attractive and readily available alternative to CT surveillance of stent-graft migration. The accuracy of AXR to measure position change has been reported to be 2mm in an experiment by Hodgson et al. with a static model using a standard protocol for image acquisition and analysis. Inter-observer variability and clinical precision have not been studied.

In AXR, the spine is used as the point of reference to detect stentgraft migration in sequential examinations. Cranio-caudal stent-graft motion during the cardiac cycle has been described up to 3 mm in a small number of patients, making a wider range of motion likely. Further more, in the clinical pilot study described in Chapter 9, we found cranio-caudal stent-graft motion of up to 5,8mm. Because of this motion of the graft, the use of bony points of reference seems to be hazardous in terms of measurement accuracy. Furthermore, with increased experience and new generation stent-grafts, the minimum acceptable aneurysm neck length continues to decrease, approaching 5mm. This requires increased accuracy of our tools for migration surveillance.

In Chapter 7, we report on a study that compared migration measurement using AXR to that of RSA. We performed in-vitro and in-vivo studies. Stent-graft migration was simulated in a static model of an aorta with stent-graft. Migration was measured by five different observers in AXR images with image acquisition and analysis according to standardized protocols. The results were compared to RSA as the standard of reference. This way, accuracy and precision could be determined in-vitro. Next, to determine the precision of AXR in-vivo, the observers measured stent-graft migration in two consecutive AXR images of four patients after EVAR.

The mean pooled error of AXR as compared to RSA was 3.0 ± 2.4 mm (range 0.01-13.1 mm, n=114). Of all AXR measurements, 16% had an error larger than 5mm. In-vivo, the pooled mean variation was 3.0 ± 4.5mm (n=76). The maximum difference between measurements in one patient was 33.0 mm. There was no significant inter-observer variability in the in-vitro and in-vivo groups.

The fact that a large portion of the measurements had an error or variation that was larger than 5mm is worrisome, especially in view of the ever diminishing accepted aneurysm neck length for endografting. In-vivo, the standard deviation of 4.5mm would yield a 95% confidence interval of 9mm in measuring stent-graft migration. It might be safe to use AXR in patients with an aneurysm neck length of more than 3cm. However, this is only a very small portion of the patient population.

Apart from the issue of accuracy and precision of measurement, there is the problem with the bony point of reference used in AXR. Changes in the vertebral column, e.g. due to osteoporosis or fractures, and possibly changes in neck angulation due to AAA shrinkage can influence (the relation to) this point of reference.

These results showed that the accuracy and precision of plain radiography for detection of stent-graft migration after EVAR is insufficient for clinical use, especially when early and accurate identification of minimal migration is required like in patients with short aneurysm necks.

Future aspects of RSA in endovascular surgery

RSA has several advantages over CT for its use in stent-graft migration surveillance: no nephrotoxic contrast requirement, ease of use for physicians and patients, low cost, low burden on hospital logistics, and low radiation dose. Furthermore, RSA seems to be more accurate than CT in measurement of stent-graft migration. This is an aspect that will be increasingly important in the near future since there is a strong tendency towards shorter accepted aneurysm neck length in EVAR and therefore increasing risk of complications due to slight stent-graft migrations.

There are still a lot of unanswered questions in the field of stent-graft migration that might be answered if accurate migration detection is routinely introduced. With more rigorous surveillance, more migration seems to be found. One of the questions concerns the pattern of migration. Does migration continue to occur once it takes place? If this is the case, early detection is even more crucial and could reveal a high risk subgroup of patients. Alternatively, migration may occur at first and stabilize thereafter. Is there a graft specific pattern of migration?

Part 2: Stent-graft dynamics

The second topic of this thesis is development of a method to study 3-Dimensional stent-graft motion after EVAR. The cardiac and respiratory cycle, in conjunction with tissue properties, result in repetitive stent-graft dynamics. Knowledge of cyclic stent-graft motion after EVAR is limited due to the limitations of current imaging modalities. This limited knowledge results in unintended stent-graft construction errors and, unavoidable, insufficient pre-clinical testing. These forms of device failure can lead to death of the patient. Detailed knowledge of stent-graft motion after EVAR is mandatory to further improve stent-graft durability.

Currently, dynamic studies of stent-graft motion can be performed with cinematographic (or cine-) CT and MRI. These methods have specific disadvantages to the patient in terms of intravascular contrast requirement, radiation dose (for CT) and limitation in analysis of stainless steel stent-grafts (MRI). Furthermore, there are technical difficulties in ECG gated analysis. The images that are produced represent a temporal reconstruction of an average stent-graft motion over several cardiac cycles.

The main disadvantage of cine-CT and cine MRI is that reconstruction of images is limited to one single plane. Therefore, quantification of out-of-plane motion is impossible with the current techniques. This thesis describes the development, validation and clinical introduction of Fluoroscopic Roentgen Stereophotogrammetric Analysis, FRSA. FRSA is a combination of existing RSA software and technique, and new digital imaging hardware.

In Chapter 2 we describe the technical aspects of FRSA. Contrary to RSA to detect long term stent-graft migration, FRSA does not require additional aortic reference markers to enable analysis of stent-graft dynamics. Stereo images are acquired with a Siemens digital bi-plane imaging system used for percutaneous cardiac intervention. The images are analyzed with a re-programmed version of Model-based RSA software by Medis Specials BV. The re-programming mainly consisted of enabling the calibration of the set-up without a calibration box being present in the image with the stent-graft, as is the case in standard RSA. The calculation of marker positions was unchanged.

In contrast to cine-CT and cine-MRI, there are no limitations in terms of direction of motion, type of graft, length of time of image acquisition or ECG changes.

Validation of FRSA

In Chapter 8 we describe a validation study of FRSA. The accuracy and precision of the set-up were validated with the use of a static and a pulsatile model of an aorta with stent-graft. Afterwards, three-dimensional stent marker motion was analyzed with a frame rate of 30 images per second, including three-dimensional marker position (change), diameter change and motion of the center of circle (center of the top end of the stent).

The results showed that the flat panel detectors did not distort the images, contrary to image intensifier images. The mean error of FRSA measurement of displacement was 0.003 mm (SD: 0.019 mm; maximum error: 0.058 mm). A very high precision of position measurement was found in the pulsatile model (SD: 0.009-0.015 mm). During pulsatile motion, the position (changes) of the markers could be assessed in the x, y, and z directions, as well as the stent diameter change and center of circle position change.

The radiation dose of FRSA was determined in a separate experiment by our clinical physicists. The radiation dose is approximately 0.1 mSv for a 3 second study, which corresponds to 4 cardiac cycles at a heart rate of 80 bpm. This compares very favorably to the 17 mSv dose of triple phase CT scan used for EVAR follow up.

Specifically distinguishable markers on commercially available stent-grafts, like welding points and positioning markers, can be used for stent-graft dynamics analysis with FRSA. Because there is no need for additional markers, FRSA could be introduced in a clinical pilot study.

FRSA in clinical stent-graft dynamics analysis

In Chapter 9 we describe the first results of a pilot study in two patients. Stent-graft motion was studied in a patient after thoracic EVAR and in one after abdominal EVAR. The motion of the grafts was calculated by quantification of the motion of the standard (commercially applied) markers used to position the stent-graft during EVAR, as well as welding points of the hooks to the top stent of the device. Stent-graft motion was measured during the cardiac cycle with respiratory arrest. In addition, stent-graft motion due to respiratory action was measured in the patient after abdominal EVAR.

Three dimensional stent-graft dynamics could be quantified at 30 (stereo) frames per second in both patients without difficulty. The thoracic stent-graft showed a motion pattern of stent dilatation and a center of mass motion of the top stent in caudal-ventral-right hand side

direction relative to the patient, followed by an over-compensation in opposite lateral and cranial direction and a gradual return to the starting position with reduction of diameter of the graft. In other words, at the start of the systole, the graft moves toward the heart. If this motion is assessed in a single plain as is the case with cine-CT or cine-MRI, the initial segment of the aorta as viewed in the first image would be out of the reconstruction plane almost all the time. Only at the end of the diastole will it return to the initial position in the image reconstruction plane. Therefore, FRSA is much more powerful than current cinematographic imaging using CT and MRI as it enables quantification of the true changes of three-dimensional stent-graft position and configuration.

We found a significant motion of the abdominal stent-graft due to respiratory action of almost 6mm in caudal direction. When using plain abdominal radiography to detect stent-graft migration as discussed in part 1 of this thesis, these dynamics due to respiratory action could result in under- or over-reporting of migration in individual cases due to the change of position of the stent-graft as compared to the reference point, the vertebral column.

These studies clearly demonstrate that fluoroscopic Roentgen stereophotogrammetric analysis (FRSA) is a clinically feasible, non-invasive tool to quantify real time 3-D stent-graft dynamics after EVAR in detail. The results of this pilot are very promising in the fact that quantification of 3D motion including rotational dynamics is now possible for the first time.

Future aspects of FRSA in endovascular surgery

The images of this non-invasive technique were of very high quality in terms of spatial and temporal resolution and measurement accuracy. Currently, the only limits are that specific markers are required to detect their position in consecutive images and that the field of view is limited by the detector size. As an alternative to marker detection, automated pattern recognition of the stent-graft could be used to facilitate measurements without the need for markers. These aspects of FRSA are subject to further evaluation at our institution.

Further, detailed, knowledge of stent-graft motion during the cardiac cycle is required to better understand in-vivo behavior of stent-grafts after EVAR. New stent-grafts can be evaluated, as well as existing grafts. With this knowledge, virtual mechanical modeling becomes possible and assessment of the failure modus of the stent-graft, such as failure due to metal fatigue is facilitated. Based on clinically acquired, detailed knowledge of stent-graft motion, forces acting on the stent-graft during the cardiac cycle can be calculated more accurately. Pre-clinical bench testing can be verified for adequacy. Bench testing itself will be improved according to in-vivo measured clinical data. One could argue that assessment of the dynamics

of a new stent-graft should be mandatory in the period of first clinical introduction to possibly detect unexpected motion in an early phase to determine if adequate bench testing has been performed and predict possible failure by fatigue modeling according to clinical motion data. Devastating complications and withdrawal of a graft from the market due to mechanical defects that arise after widespread introduction could be prevented with better bench testing and early detection of unexpected graft motion.

The medical ethics committee of the LUMC approved an initial pilot study for further research into the specifics of motion of different grafts in the thoracic and abdominal aorta.

Addendum
Risk of radiation exposure due to imaging in EVAR

Medical imaging with ionizing radiation is performed during endovascular abdominal aortic aneurysm repair (EVAR), preoperative planning and postoperative surveillance. Cumulative patient dose is relatively high and causes concern about radiation induced malignancies. In Chapter 10, the patient dose and excessive relative risk of cancer mortality is calculated for typical patients aged 55 to 85, using the BEIR VII model for age-, gender- and site-specific solid cancer mortality. The results showed that the number of radiation induced deaths per 1000 EVAR patients was 12, 8, 4 and 1 for patients treated at ages 55, 65, 75 and 85 years, respectively. The number of AAA related deaths per 1000 EVAR patients was: 126, 91, 67 and 47, respectively. The average radiation induced reduction of life expectancy was 40, 21, 8 and 2 days for patients treated with EVAR at 55, 65, 75 and 85 years of age respectively. Corresponding AAA related reduction of life expectancy was respectively 739, 387, 197 and 82 days. Therefore, we conclude that the impact of the considerable dose of ionizing radiation on patients after EVAR is small, especially when compared to the reduction of life expectancy related to vascular disease.

Final Conclusions

- Roentgen stereophotogrammetric analysis is a feasible and accurate method to detect stent-graft migration in-vivo.
- One single aortic reference marker is sufficient for accurate stent-graft migration detection with RSA and should be placed as close to the stent-graft as possible to ensure maximum measurement accuracy.

- Plain abdominal radiography has insufficient accuracy and precision to detect stent-graft migration, this is especially dangerous in patients with a shorter aneurysm neck (shorter than 2-3cm).
- Application of a reference marker to the aortic wall will facilitate more accurate detection of stent-graft migration with CT, without requiring intravascular contrast enhancement.

- FRSA has proven to be a method with very high accuracy and temporal resolution to measure real time three-dimensional stent-graft dynamics in a pulsatile environment. Measurement of 3-D stent-graft motion has become feasible in patients after EVAR.

- Radiation exposure accumulates rapidly for patients undergoing EVAR. However, associated radiation risks are modest and much smaller compared to AAA related risks.

C H A P T E R

12

Samenvatting, toekomst perspectieven en conclusies

Verklarende woordenlijst:

AAA abdominaal aorta aneurysma, verwijde buikslagader

EVAR endovasculaire aorta reparatie, behandeling van een aneurysma met een endoprothese

Endoprothese (eng: stent-graft) kunststof vaatprothese met een metalen (stent) geraamte voor bevestiging aan / in de vaatwand

Fluoroscopie filmtechniek met röntgen beelden

In-vivo in een levend wezen

Nauwkeurigheid grootte van de meetfout ten opzicht van een gouden standaard

Precisie maat voor de afwijking in uitkomst bij een herhaalde meting

RSA röntgen stereofotogrammetrische analyse, plaatsbepaling met stereo röntgenbeelden

Temporele resolutie het aantal metingen per tijdseenheid

Het aneurysma van de aorta is een plaatselijke toename van anderhalf maal de normale diameter van de hoofdlichaamsslagader. In de praktijk betekent dit dat we spreken van een abdominaal aorta (buikslagader) aneurysma, ofwel AAA, bij een diameter van meer dan 3-3,5 cm. Er is een langzame toename van de diameter. Klachten in dit stadium zijn meestal afwezig of zeer gering. Het AAA komt in Nederland bij 2,1% van de mensen ouder dan 55 jaar voor. Dit percentage stijgt met toename van de leeftijd en verschillende risicofactoren. Bij mannen boven de 60 jaar werd in 11,4% een AAA gevonden. Over de afgelopen decennia wordt een toename van het vóórkomen van AAA gezien.

Het belangrijkste risico van een aneurysma is dat het scheurt, een ruptuur. Bij een ruptuur is een sterfte risico beschreven tot 75-90%. Het doel van de behandeling is dan ook om het aneurysma uit te schakelen voordat het scheurt. Daarnaast wordt, vooralsnog experimenteel, onderzoek gedaan naar medicamenteuze groeiremming.

Het AAA wordt in principe behandeld als de diameter 5,5 cm of groter is. Boven 5,5 cm stijgt het risico op ruptuur snel. Sinds 1991 is, naast de gebruikelijke "open" operatieve behandeling, een nieuwe behandeling ontwikkeld: de endovasculaire aneurysmareparatie of EVAR. Met deze behandeling wordt het AAA uitgeschakeld via de binnenkant van de slagader. Dit gebeurt door een endoprothese (stent-graft) via de lies in te brengen en zodoende het AAA te overbruggen. Hierdoor herstelt de patiënt sneller dan na een "open" operatie via een buikincisie. Het belangrijkste voordeel van EVAR ten opzichte van de "open" operatie is dat het complicatie- en operatie-sterfterisico van EVAR lager is door het minder invasieve karakter van de ingreep.

EVAR heeft sinds de eerste introductie een stormachtige ontwikkeling doorgemaakt. De prothese kwaliteit en duurzaamheid zijn enorm toegenomen en EVAR is onderdeel geworden van de standaardbehandeling van aneurysmata. Jaarlijks worden vele duizenden patiënten over de wereld behandeld via EVAR. Naast het zeer aantrekkelijke korte termijn voordeel van een minimaal invasieve behandeling met EVAR, zijn er echter lange termijn risico's. De lange termijn complicaties zijn onder andere afknikken, trombose (verstoppen) en endolekkage (druk op het AAA door bloeddruk of –stroom via zijtakken of langs de prothese). Daarnaast zijn migratie en materiaalfalen / -desintegratie belangrijke risico's. De lange termijn aneurysma gerelateerde sterfte van 1-2% per jaar na EVAR is grotendeels te verklaren door deze complicaties. Om de complicaties in een vroeg stadium op te sporen wordt intensieve controle van patiënten na EVAR verricht. Dit onderzoek gebeurt met CT, echo en standaard buikoverzichts(röntgen) foto's. De verschillende methoden hebben specifieke nadelen en zijn kostbaar, waardoor de kosteneffectiviteit van EVAR wordt verminderd.

Migratie van de endoprothese is het verschuiven van de endoprothese binnen het bloedvat waardoor het aneurysma weer onder druk komt te staan met als gevolg opnieuw risico op ruptuur. Met de verdere ontwikkeling van de endoprotheses en het versterken van de fixatie aan de wand door bijvoorbeeld haakjes, is het risico op migratie afgenomen. Desondanks wordt migratie nog steeds in 1% - 66% van de patiënten gevonden, afhankelijk van de gebruikte opsporingsmethode en onderzoeksserie.

Materiaalfalen kan eveneens ruptuur tot gevolg hebben. Het materiaalfalen ontstaat als gevolg van de continue repeterende krachten en bewegingen door de hart- en ademhalingscyclus en kan ontstaan ondanks de uitgebreide preklinische testen van nieuwe endoprotheses. De complicaties na EVAR ten gevolge van deze dynamica zijn geanalyseerd en hebben geleid tot verdwijnen, aanpassen of volledig vernieuwen van endoprotheses en hun testmethoden.

Met de huidige beschikbare beeldvormende technieken is het onmogelijk om de 3 dimensionale dynamica van een endoprothese in het lichaam exact te kwantificeren. Om die reden is ook in het verleden gebleken dat preklinische testen (achteraf) onvoldoende bleken waardoor materiaalfalen kon optreden. Bewegingen als torsie en rotatie werden pas duidelijk nadat endoprotheses faalden en dit falen in het laboratorium werd gereconstrueerd.

Vergaren van kennis over de krachten en bewegingen waaraan een endoprothese wordt blootgesteld na plaatsing zijn van groot belang om de kwaliteit en duurzaamheid van de behandeling en de preklinische tests te vergroten.

Dit proefschrift bestudeert nieuwe methoden om endoprothesemigratie en -dynamica op te sporen en te kwantificeren.

Deel 1: Controle van endoprothese migratie na EVAR

Hoofdstuk 1 gaat verder in op aneurysmatische aandoeningen, EVAR en de lange termijn risico's. Eén van die risico's is zoals gezegd endoprothesemigratie. De klinische gouden standaard voor controle op endoprothesemigratie is CT-angiografie (CTA). CTA heeft als belangrijkste nadelen dat hiervoor contrastmiddelen worden gebruikt die schadelijk zijn voor de nieren, CTA hoge kosten heeft en een logistieke belasting is voor de ziekenhuisorganisatie. Daarnaast geeft CTA een redelijk forse stralenbelasting. Als alternatief kunnen standaard röntgen buikoverzichts-foto's (X-BOZ, Eng: AXR) worden gebruikt. Zowel bij CTA als X-BOZ wordt de positie van een endoprothese bepaald door een persoon die de afstand meet tussen de endoprothese en een referentiepunt. Het referentiepunt bij CTA is een zijtak van de aorta, bij X-BOZ is dit een wervel-lichaam. Doordat een persoon deze afstand meet is er een risico op meetvariatie tussen twee metingen door dezelfde of verschillende personen (resp. intra- en inter-observervariatie). De klinische nauwkeurigheid van beide methoden is niet gevalideerd. Daarnaast zijn er specifieke nadelen van beide methoden die in Hoofdstuk 1 worden besproken.

Als alternatief voor CTA en X-BOZ zou Röntgen Stereofotogrammetrische Analyse (RSA) kun-nen dienen. RSA heeft een lange en succesvolle geschiedenis binnen de orthopedie voor de detectie en kwantificering van microbewegingen van gewrichtsprotheses. Met behulp van gekalibreerde stereo röntgenfoto's wordt de plaats van de prothese bepaald ten opzichte van referentiemarkers die tijdens de operatie worden ingebracht. Voor EVAR betekent dit dat tijdens de EVAR procedure referentiemarkers in de aortawand moeten worden geplaatst. In Hoofdstuk 2 wordt de techniek van RSA in detail besproken. Voor het gebruik van RSA als controle op migratie na EVAR zijn verschillende technische- en validatievragen die beantwoord dienen te worden. Deze worden, samen met het onderzoek naar de nauwkeurigheid van detectie van migratie door CTA en X-BOZ, besproken in Deel 1 van dit proefschrift.

Validatie van RSA als methode om migratie vast te stellen

Statisch model

In Hoofdstuk 3 wordt beschreven hoe RSA is gevalideerd en de nauwkeurigheid voor de detectie van endoprothesemigratie is vergeleken met CT. Een plastic model werd gemaakt van een aorta met endoprothese. Met een micrometer kon de endoprothese worden "gemigreerd". De migratie meetresultaten van CT en RSA werden met elkaar en de micrometer, de gouden standaard, vergeleken.

CT analyse werd verricht met de best beschikbare resolutie en meetmethode, met 3D beeld-reconstructie. Om te corrigeren voor inter-observervariabiliteit in de metingen werden 3 personen gevraagd CT metingen te verrichten.

De resultaten toonden aan dat migratiemeting met RSA mogelijk was en zeer nauwkeurig in dit statische model. De gemiddelde fout van RSA was 0,002 mm (SD=0.044, max. fout 0.10 mm). Dit was significant nauwkeuriger dan CT (P<0.0001), dat een gemiddelde meetfout had van 0.14 mm (SD=0.29 mm, max. fout 1.0 mm). Er was geen significante inter-observervariabiliteit. (p=0.17).

Omdat (cyclische, pulserende) beweging de nauwkeurigheid van de meting nadelig zou kun-nen beïnvloeden, werd een volgend onderzoek verricht.

RSA in een pulsatiele omgeving

In Hoofdstuk 4 wordt een experiment beschreven met pulserende veranderingen, net als tijdens de hartslag. Een varkensaorta werd verbonden aan een humane wervelkolom. Een pul-serende circulatie werd ingesteld door de aorta. In de aorta werd een model van een endopro-these gepositioneerd, compleet met markers voor RSA analyse. Een zijtak werd geconstrueerd om een nierslagader na te bootsen. Aan de aortawand werden referentiemarkers geplaatst waaronder een potentiële endovasculaire referentiemarker voor toekomstig klinisch gebruik. Opnieuw werden RSA en CTA gebruikt om migratie te meten.

Dit onderzoek toonde aan dat migratiemeting met RSA mogelijk en nauwkeurig was in dit model, ondanks pulserende bewegingen. RSA metingen waren nauwkeuriger dan die met CT. De gebruikte endovasculaire marker bleek veelbelovend door goede meetresultaten.

Voordat klinische introductie mogelijk zou kunnen worden moest eerst de haalbaarheid van RSA en de endovasculaire marker worden getest in een levend model (*in-vivo*). Om die reden werd een dierproef verricht.

RSA in-vivo

In Hoofdstuk 5 wordt een studie met twee grote, 100 kg zware varkens beschreven. Een model van een endoprothese werd in de aorta gebracht. Standaard RSA markers werden op de aorta gefixeerd en endovasculaire referentiemarkers werden aan de binnenzijde van de aorta beves-tigd. De standaard referentiemarker die het dichtst bij de endoprothese lag werd gebruikt als referentiepunt voor CT meting.

De studie toonde aan dat migratiemeting met RSA (zeer precies) mogelijk was in-vivo, ondanks omgevende weefsels en hart- en ademhalingsactie. De precisie van RSA was groter dan die

van CT. Bij CT meting werd in dit onderzoek een zeer duidelijk gedefinieerd referentiepunt gebruikt, in tegenstelling tot de praktijk, waarbij een (minder duidelijk gedefinieerde) zijtak van de aorta wordt gebruikt. Wij concludeerden dat gebruik van een externe referentiemarker de nauwkeurigheid van CT meting kan vergroten, zonder de noodzaak van gebruik van (schadelijk) contrastmiddel.

De endovasculaire marker zoals deze werd gebruikt in dit diermodel was onvoldoende zichtbaar om te gebruiken als referentiemarker voor RSA. Om dit wel mogelijk te maken dient de marker te worden aangepast, bv. met een gouden of een platina ringetje. Verder onderzoek naar ontwerp en veiligheid dient te worden verricht.

Aorta referentiemarkers en RSA

Behalve zichtbaarheid van de marker zijn er andere belangrijke aspecten die verder moeten worden uitgezocht. Een daarvan is wat de beste positie is van de marker ten opzichte van de endoprothese. In Hoofdstuk 4 wordt beschreven dat een toenemende afstand tussen de referentiemarker en de endoprothese, conform resultaten in de orthopedische literatuur, een onnauwkeurigheid veroorzaakt. De referentie marker dient dus zo dicht mogelijk bij de endoprothese te worden geplaatst. In Hoofdstuk 5 wordt de diermodelstudie beschreven. Hier vonden we dat de endovasculaire markers zonder problemen konden worden geplaatst en gerepositioneerd. Bij postmortaal onderzoek van de varkens werden geen complicaties gevonden.

Een andere vraag is hoeveel referentie markers nodig zijn om de endoprothese positie nauwkeurig te meten. In de orthopedie worden meerdere markers geplaatst, omdat dit tot nauwkeuriger metingen leidt. In endovasculaire chirurgie betekent het plaatsen van een referentie marker een extra procedure en daardoor een (mogelijk gering) extra risico. Reduceren van het aantal referentiemarkers is dus wenselijk.

Nauwkeurigheid van RSA met één referentie marker

In Hoofdstuk 6 wordt beschreven hoe de beelden van het pulserende model en de diermodelstudie opnieuw werden geanalyseerd met RSA waarbij één aorta referentiemarker werd gebruikt in plaats van het eerder gebruikte cluster van referentiemarkers.

De resultaten toonden opnieuw een zeer nauwkeurige bepaling van migratie, ondanks geringe afname van nauwkeurigheid door reductie van de referentie markers tot het minimum. Eén aorta referentiemarker lijkt dus voldoende om migratie na EVAR te controleren.

Klinische toepasbaarheid x-boz voor migratie detectie

Standaard buikoverzichtsfoto's (X-BOZ) worden in sommige klinieken gebruikt om endoprothe-sepositie en eventuele -migratie te meten. X-BOZ heeft verschillende voordelen in vergelijking tot CT. Door deze voordelen is het een gemakkelijk en voor de hand liggend klinisch alternatief voor CT. De nauwkeurigheid / meetfout van X-BOZ is in een statische modelstudie beschreven als 2 mm. Klinische precisie en inter-observervariatie zijn niet beschreven. Bij het meten van endoprothesepositie met X-BOZ wordt een wervellichaam als referentie punt gebruikt. Er bestaat een risico dat de nauwkeurigheid van de meetmethode wordt verminderd doordat de aorta met de endoprothese als gevolg van de hartcyclus en ademhaling beweegt ten opzichte van de wervelkolom. Hierdoor kunnen niet bestaande endoprothesemigraties worden geme-ten (vals-positieve uitslag) of opgetreden migraties worden gemist (vals-negatieve uitslag). Deze bewegingen kunnen oplopen tot 5,8 mm, zoals gemeten in een patiënt beschreven in Hoofdstuk 9.

Door toename in ervaring van endovasculaire specialisten wordt de acceptabele minimale lengte van de normale aorta (de "aneurysmahals") waaraan de endoprothese wordt bevestigd steeds kleiner. Op dit moment wordt in sommige gevallen een aneurysmahals van slechts 5 mm geaccepteerd, waardoor klinisch relevante migratie al bij enkele millimeters kan optreden. Hierdoor is toenemende nauwkeurigheid van detectie methoden noodzakelijk.

In Hoofdstuk 7 wordt een studie beschreven waarin X-BOZ wordt vergeleken met RSA. In een model werden endoprothese migraties nagebootst en gemeten met RSA en X-BOZ. De X-BOZ metingen werden verricht door vijf personen. Hierdoor kon de meetfout van X-BOZ ten opzichte van RSA worden bepaald. Daarnaast werd endoprothesemigratie gemeten door vijf personen aan de hand van X-BOZ opnames van vier patiënten. Hierdoor kon de klinische precisie van X-BOZ worden bepaald.

De gemiddelde meetfout van X-BOZ ten opzichte van RSA was 3.0 mm. 16% van de metingen had een fout groter dan 5 mm. Bij de klinische metingen was de variatie 3.0 ± 4.5 mm. De maximale meetvariatie tussen twee personen was 33 mm.

Deze resultaten zijn verontrustend omdat een dergelijke variatie en meetfout het risico op vals-positieve en vals-negatieve uitslagen zeer groot maakt. Om die reden concluderen wij dat X-BOZ onvoldoende nauwkeurig en precies is om klinische endoprothesemigratie te meten, met name bij patiënten met een zeer korte aneurysmahals.

RSA in endovasculaire chirurgie: toekomstperspectief

RSA heeft verschillende voordelen in vergelijking met CTA voor endoprothesecontrole. Het is patiënt- en doktervriendelijk, er is geen schadelijk contrastmiddel nodig, het is weinig belastend voor het logistieke systeem van het ziekenhuis, goedkoop en geeft weinig stralen-belasting. Daarnaast is RSA nauwkeuriger dan CT voor het meten van endoprothesemigratie. Met nauwkeurige endoprothese positiemeting wordt meer migratie gevonden. Als meer gedetailleerde informatie beschikbaar is kunnen diverse vragen worden beantwoord, bijvoor-beeld over migratie patronen: Blijft migratie optreden als het eenmaal begint? Stabiliseert het na enige tijd? Zijn er endoprothese type-specifieke patronen herkenbaar?

Deel 2: Endoprothese-dynamica

Deel 2 van dit proefschrift gaat over 3-dimensionale endoprothese beweging na EVAR. Deze herhaalde endoprothesebewegingen ontstaan door een interactie tussen krachten van de hart- en ademhalingscyclus en de aortawand. Kennis van deze bewegingen is beperkt door de beperkingen van de beschikbare meetmethoden. Door deze beperkte kennis ontstaan onbedoelde fouten in endoprotheseconstructie en preklinische testmethodes. Hierdoor kan een endoprothese kapot gaan en dit kan de dood van de patiënt tot gevolg hebben. Op dit moment zijn cine-CT en –MRI de twee klinisch beschikbare methoden van onderzoek. Deze hebben beide echter beperkingen en specifieke nadelen. De reconstructies van de beelden naar een bewegend beeld ontstaan door combinaties van verschillende opnames en zijn dus niet "real-time".

Belangrijkste nadeel is dat cine-CT en –MRI alleen kunnen meten in één plat vlak. Hierdoor kunnen de complexe, 3-dimensionale bewegingen van een endoprothese niet in zijn geheel worden bestudeerd. Het gaat hier namelijk om bewegingen buiten het in beeld gebrachte, platte vlak ("out-of-plane motion"). In het bijzonder is het meten van rotatiebeweging onmo-gelijk. Deel 2 van dit proefschrift beschrijft de ontwikkeling, validatie en klinische introductie van Fluoroscopische Röntgen Stereofotogrammetrische Analyse (FRSA). FRSA is een combina-tie van conventionele RSA en nieuwe digitale beeldvorming.

In Hoofdstuk 2 worden de technische aspecten van FRSA beschreven. In tegenstelling tot RSA voor lange termijn migratiemeting, heeft FRSA geen extra toegevoegde aorta referentiemar-kers nodig om metingen mogelijk te maken. De beelden worden verkregen met een bi-plane röntgenapparaat dat gebruikt wordt in de interventie cardiologie. De RSA software werd opnieuw geprogrammeerd om kalibratie van de beelden mogelijk te maken. Verder werd de software onveranderd gebruikt.

In tegenstelling tot cine-CT en –MRI zijn er geen beperkingen met betrekking tot bewegings-richting, type endoprothese, duur van de opnamereeks of ECG afwijkingen.

Validatie van FRSA

In Hoofdstuk 8 wordt een validatie studie beschreven van FRSA. De nauwkeurigheid en precisie werden aan de hand van een model bepaald. Vervolgens werd met 30 beelden per seconde de 3-dimensionale positieverandering gemeten van de stent-markers, het centrum van de top van de stent, het zwaartepunt van de stent en de diameterverandering van de stent. De positieverandering van de markers kon in alle richtingen worden gemeten met een minimale meetfout en een zeer hoge precisie.

De röntgenstralenbelasting van FRSA werd in een apart experiment bepaald. Voor drie secon-den onderzoek werd een belasting gemeten van 0,1 mSv. Dit is minimaal vergeleken bij een CT-scan met een stralenbelasting van 17 mSv, een onderzoek dat de EVAR patiëntengroep diverse malen moet ondergaan voor de behandeling.

Het is voor FRSA niet nodig om extra markers op de stent aan te brengen. De markeerpunten die worden gebruikt voor het plaatsen van de stent tijdens de EVAR procedure, en enkele stent laspunten volstaan voor deze analyse. Om die reden kon de volgende stap, een patiëntenon-derzoek, worden gezet.

FRSA in klinische endoprothese-dynamica analyse

In Hoofdstuk 9 worden de eerste resultaten beschreven van een studie van twee patiënten. Een patiënt werd met EVAR behandeld in de thoracale (borstkas) aorta, en een patiënt in de abdominale (buik) aorta. Endoprothesebeweging ten gevolge van de hartcyclus werd gemeten tijdens ademstilstand. Tevens werd beweging van de abdominale endoprothese ten gevolge van de ademhaling gemeten.

Drie-dimensionale endoprothesebeweging kon worden gemeten zonder problemen. Aan het begin van de systole (het samen knijpen van het hart) toonde de thoracale endoprothese een diameter toename en een beweging richting het hart. Dit werd gevolgd door een beweging in tegengestelde richting voorbij het startpunt, gevolgd door een langzame afname van de diameter en een terugkeer naar de uitgangspositie. Als deze beweging met een cine-CT of –MRI wordt gevolgd dan is het segment van aorta met endoprothese alleen tijdens het begin, het passeren van het startpunt en bij het weer eindigen op het startpunt kortdurend in beeld. De rest van de metingen worden steeds verricht aan een ander segment. Om die reden is FRSA een veel krachtiger instrument dan cine-CT en –MRI voor het nauwkeurig meten van

3D-bewegingen van endoprotheses. Daarnaast zijn de verkregen FRSA beelden "real-time", zonder reconstructies aan de hand van het ECG (hartfilmpje) van de patiënt zoals bij CT en MRI.

Als gevolg van de ademhaling werd een beweging van de endoprothese ten opzichte van de wervelkolom gemeten van bijna 6 mm. Als X-BOZ wordt gebruikt voor het vaststellen van endoprothese migratie, zoals in deel 1 werd besproken, dan kan deze beweging van 6 mm t.o.v. de wervelkolom betrekkelijk eenvoudig resulteren in een vals-positieve of vals-negatieve uitslag aangezien de wervelkolom het referentie punt voor deze meting is.

Deze studies tonen duidelijk aan dat FRSA een klinisch toepasbare, niet-invasieve methode is om 3-dimensionale positie veranderingen "real-time" gedetailleerd te kwantificeren, inclusief rotatie bewegingen.

FRSA in endovasculaire chirurgie: toekomstperspectief

Op dit moment is de enige beperking van de techniek dat specifieke markers nodig zijn om beweging te meten en dat het beeldveld beperkt is door de detectorgrootte van het fluoroscopieapparaat. Grotere detectoren zijn verkrijgbaar. Als alternatief voor markerdetectie kan geautomatiseerde patroonherkenning (van het beeldpatroon van de endoprothese) worden gebruikt om de metingen te verrichten.

Meer, gedetailleerde gegevens over endoprothesebeweging tijdens hart- en adem-cyclus zijn nodig om het gedrag van endoprotheses in-vivo beter te begrijpen. Met deze kennis wordt het mogelijk om virtuele modellen te maken en materiaalfalen, zoals metaalmoeheid, te bestuderen. Op basis van de gemeten bewegingen kunnen de krachten die op een endoprothese worden uitgeoefend beter worden berekend. Gecontroleerd kan worden of de preklinische testopstellingen adequaat zijn gebouwd en zonodig kunnen deze worden verbeterd. Nieuwe endoprotheses zouden na beperkte klinische introductie mogelijk moeten worden beoordeeld met FRSA om onverwachte bewegingen op te sporen en om te beoordelen of de preklinische testen adequaat zijn verricht en mogelijk materiaalfalen te voorspellen door modellering op basis van klinische data. Ernstige complicaties en terugnemen van de endoprothese van de markt ten gevolge van materiaalfalen na wijdverbreide introductie zou voorkomen kunnen worden door betere testopstellingen en vroege detectie van onverwachte endoprothese bewegingen.

De medisch ethische toetsingscommissie van het LUMC heeft toestemming gegeven om verder onderzoek te verrichten naar de beweging van verschillende endoprotheses.

Addendum
Risico van stralen belasting tgv beeldvorming rond EVAR

Beeldvormende technieken met röntgenstralen worden gebruikt tijdens de EVAR procedure, de preoperatieve planning en postoperatieve controles. De totale stralenbelasting is relatief hoog en er bestaan zorgen over door stralen veroorzaakte kwaadaardige tumoren. In Hoofdstuk 10 wordt de patiëntdosis en het extra risico op sterfte aan kanker berekend voor een patiënt van 55, 65, 75 en 80 jaar aan de hand van rekenmodellen.

De aanzienlijke cumulatieve stralendosis die werd opgebouwd leidde tot een gering risico voor de patiënten na EVAR, vooral wanneer dit risico werd vergeleken met de sterfterisico's door vaatziekten in deze populatie.

Conclusies

- Röntgen stereofotogrammetrische analyse is een haalbare en nauwkeurige methode om endoprothesemigratie op te sporen in-vivo.
- Eén aorta referentiemarker is voldoende om endoprothesemigratie nauwkeurig op te sporen en moet zo dicht mogelijk bij de endoprothese worden geplaatst voor maximale nauwkeurigheid.

- Standaard buikoverzichtsfoto's zijn onvoldoende nauwkeurig en precies om endoprothesemigratie op te sporen. Dit is met name riskant bij patiënten met een korte aneurysmahals (korter dan 2 - 3 cm).
- Plaatsing van een endovasculaire aorta referentiemarker zal nauwkeuriger detectie van endoprothesemigratie mogelijk maken met CT, zonder gebruik van intraveneus contrastmiddel.

- FRSA heeft een bewezen hoge nauwkeurigheid en temporele resolutie voor het real-time meten van drie-dimensionale endoprothese-dynamica in een pulserende omgeving. Het is mogelijk geworden om 3D metingen te verrichten bij patiënten na EVAR.

- Stralen belasting bij patiënten na EVAR neemt snel toe. Echter, de hieraan verbonden risico's zijn bescheiden en klein vergeleken bij AAA gerelateerde risico's.

13

Dankwoord

Dit proefschrift is het resultaat van een intensieve samenwerking met velen uit verschillende vakgebieden. Het is daardoor, geheel eigentijds, een multidisciplinair product geworden. Vanaf het begin bleek het een mooie uitdaging en soms ook een milde last, maar steeds weer een leerzame en vruchtbare ervaring. Ik heb hier veel plezier aan beleefd. Dank aan allen die hierin een rol hebben gespeeld.

Prof. Dr. J.H. van Bockel, beste Hajo, veel dank voor de begeleiding, geboden kansen en het in mij gestelde vertrouwen in de afgelopen 18 jaar waarvan dit proefschrift de wetenschappelijke kroon van de laatste jaren is.

Dr. E.R. Valstar, beste Edward, dank voor de samenwerking. Het is goed dat er een nieuw veld is ontstaan voor de toepassing van "jouw" RSA.

Hoog geachte leden van de promotie commissie, Prof. Dr. M. Malina, Prof. Dr. J.F. Hamming, Prof. Dr. J.H.C. Reiber, Prof. Dr. H.J.M. Verhagen, dank voor jullie bereidheid zitting te nemen in de commissie en voor de opbouwende kritiek.

Dr. E.H. Garling, beste Eric, veel dank voor je inspanningen bij het werk van deel 1 van dit proefschrift. Het was motiverend om met je van gedachten te wisselen en de haken en ogen te bespreken aan deze nieuwe toepassing van RSA. Dank ook dat je op de meest onmogelijke uren, als ik weer tijd had om me op de materie te storten, hebt meegedacht en geanalyseerd.

Dr. B.L. Kaptein, beste Bart, zonder jouw hulp en expertise was deel 2 niet van de grond gekomen. Na de plaatsing van het bi-plane apparaat bij de interventie cardiologie werd de ontwikkeling en klinische introductie mogelijk van wat we FRSA zijn gaan noemen. Hoe jij onze gesprekken en brainstormsessies over kalibratie en meting (met vragen als: "maar het moet toch niet moeilijk zijn om…..?") hebt vertaald naar programmatuur is mij een raadsel, maar de resultaten liegen er niet om! Ik hoop dat we met deze techniek veel nieuwe aspecten van endoprothese dynamica zullen ontdekken.

Dr. J.W. Hinnen, beste Jan-Willem, wetenschappelijk vliegwiel, het werk aan jouw en mijn proefschrift was een ware kruisbestuiving. Onder het genot van vele koppen koffie hebben we

de verschillende aspecten van beide onderzoeksgebieden doorgeakkerd. Vooral je hulp bij de opzet en uitvoering van de experimenten was waardevol. Hoewel je -midden in de nacht- het migratiemodel kapot knipte tijdens obductie van het eerste varken, waardoor de rest van de nacht besteed moest worden aan de reparatie voor het experiment op de volgende dag, ben ik er van overtuigd dat je een goed en gedreven (vaat?)chirurg zult worden.

Onmisbare hulp kreeg ik van Olivier Oudegeest, werktuigbouwkundige, Martijn Holleman, biomedische wetenschapper en Rozemarijn van der Vijver, toekomstig chirurg. Jullie hebben fraai werk verricht met de analyse van diverse onderdelen. Alle drie komen jullie uit compleet verschillende vakgebieden en dat maakte jullie bijdrage een extra verrijking. Veel succes met jullie carrières.

Michael Boonekamp Jr. en collega's, jullie afdeling Fijne Mechanica van het LUMC is een ware schatkamer. Het was steeds weer een feest om bij jullie te komen rondkijken en samen na te denken hoe de modellen er uit moesten zien. "Ongeveer is ook goed" komt niet in het vocabulaire voor en daardoor zijn alle modellen ware huzarenstukjes geworden. Dank voor steeds weer korte levertijd als het gisteren af moest zijn.

Zoals gezegd is dit een multidisciplinaire inzet geweest. De afdeling Radiologie was hierbij een belangrijke partner. Dr. L.J.M. Kroft, beste Lucia, dank voor je radiologische insteek in dit onderzoek. Het was een hele toer om de dierenexperimenten uit te voeren op de CT en vervolgens de analyse rond te krijgen. Ook veel dank aan Edwin van der Linden, Stephan Frerichs en François Willemssen, voor jullie bijdrage aan de CT-data analyse. Raoul Joemai, jouw kennis van de techniek achter CT heeft grote indruk op me gemaakt. Dank voor je hulp bij de dataverwerking en de colleges "image reconstruction". Afdeling klinische fysica, Dr. J. Geleijns, beste Koos, jouw kennis van de stralenbelasting is een waardevolle aanvulling voor dit proefschrift. Het heeft ondermeer geresulteerd in een mooi artikel dat naar ik hoop een belangrijk spookbeeld uit zal wissen. Dr. P.W. de Bruijn, beste Paul, eerst kwamen we elkaar tegen bij de afdeling Orthopedie, waar we hebben geëxperimenteerd met CT projecties, en jij veel te stellen hebt gehad met mijn "witjassen logica". Later troffen wij elkaar weer in jouw rol als klinisch fysicus in opleiding waarbij je maat en getal wist te geven aan de stralenbelasting van FRSA en zo klinische introductie mede mogelijk maakte. Dank hiervoor.

Het FRSA onderdeel van dit proefschrift was er niet gekomen zonder de medewerking van de afdeling Interventie Cardiologie. Prof. Dr. M.J. Schalij, beste Martin, dank voor het direct

ter beschikking stellen van jullie bi-plane apparaat, terwijl het nauwelijks 24 uur in het LUMC stond. Ook recent hebben we nog patiënten onderzoek gedaan en is de samenwerking erg plezierig en ongecompliceerd. Mede verantwoordelijk hiervoor is ook Els Nachtegaal en haar team van interventie medewerkers, die ons steeds met raad en daad hebben bij gestaan.

N.V. Dias, MD, PhD, dear Nuno, thank you for organizing the „Malmo-end" of the experiments. The data have proven to be interesting and valuable. I hope to continue the fun and exciting collaboration in the future.

Mijn paranimfen, Rombout Kruse en Wim Nuboer, dank voor jullie steun en vriendschap. Gelukkig hebben jullie alles goed gelezen en kan ik zorgeloos elke vraag doorspelen.

Lieve Marjan, dank voor je gastvrijheid, je interesse en je kwaliteits-oog.

Titia, lieve zus, de eerste 20 jaar waren wij redelijk onafscheidelijk. Ondanks het feit dat geografie en drukte belemmerend werken blijft er altijd een bijzondere band.

Lieve Wally† en Willem, vanaf mijn eerste entree in jullie gezin heb ik mij welkom gevoeld en dat is altijd zo gebleven. Jullie boden mij een tweede ouderlijk thuis waarvan ik nog steeds geniet, ook tijdens de vrije dagen waarin ik mij heb gemeld om ongestoord te kunnen schrijven.

Lieve ouders, jullie zijn letterlijk de scheppende voorwaarde voor dit proefschrift geweest. Een meer geborgen omgeving voor mijn jeugd was niet voor te stellen. Lieve Mam, dank voor je liefde, toewijding en steun van af het eerste begin, zij vormden de basis voor dit alles! Veel dank ook voor je geduld en trouw aan je vaak te bezige zoon. Lieve Pap, ondanks je steeds uitgesproken advies niet in dit vak te gaan waren de dagen op de OK tijdens mijn middelbare school TE motiverend. Er is dan ook niets tegen bestand gebleken en het is mooi hetzelfde vak te delen.

Liefste Wally, Charlotte en Juriaan, jullie zijn de diamanten in mijn koningskroon! Wat hebben we toch een geluk dat juist wíj de drie leukste kinderen van de wereld hebben.
En in antwoord op jullie vraag of ik schrijver word: sorry, maar dit is echt het laatste boek…..

Lieve Wally, Grote Liefde, captain en coach van de hele thuisploeg, dank voor alles, dankzij jou was het een makkie!

C H A P T E R

13


List of publications

Publications by the author

1995 Koning OHJ, van Bockel JH, van der Woude FJ, Persijn GG, Hermans J, Ploeg RJ. Risk factors for delayed graft function in University of Wisconsin solution preserved kidneys from multiorgan donors. European Multicenter Study Group on Organ Preservation. Transplantation Proceedings Feb 1995, 27(1) p752-3.

1997 Koning OHJ, Ploeg RJ, van Bockel JH, Groenewegen M, van der Woude FJ, Persijn GG, Hermans J. Risk factors for delayed graft function in cadaveric kidney transplantation. A prospective study on renal function and graft survival after preservation with University of Wisconsin solution in multi-organ donors. Transplantation Jun 1997, 63(11) p1620-8

2005 Koning OHJ, van der Linden E, van Bockel JH. Fatal endovascular device failure in ruptured aneurysm. Eur J Vasc Endovasc Surg. 2005 Jul;30(1):108.

2005 Hinnen JW, Koning OHJ, Visser MJT, van Bockel JH. Effect of intraluminal thrombus on pressure transmission in the abdominal aortic aneurysm. J Vasc Surg. 2005 Dec;42(6):1176-82.

2006 Koning OHJ, Hinnen JW, van Baalen JM. Technique for safe removal of an aortic endograft with suprarenal fixation. J Vasc Surg. 2006 Apr;43(4):855-7.

2006 Hinnen JW, Koning OHJ, Vlaanderen E, van Bockel JH, Hamming JF. Aneurysm sac pressure monitoring: effect of pulsatile motion of the pressure sensor on the interpretation of measurements. J Endovasc Ther. 2006 Apr;13(2):145-51.

2006 Koning OHJ, Oudegeest OR, Valstar ER, Garling EH, Van der Linden E, Hinnen JW, Hamming JF, Vossepoel AM, Van Bockel JH. Roentgen stereophotogrammetric analysis: an accurate tool to assess stent-graft migration. J Endovasc Ther. 2006 Aug;13(4):468-75.

2006 Duijff JW, Koning OHJ, van Baalen JM. Pseudoaneurysma van de arteria dorsalis pedis veroorzaakt door een exostose op de talus bij een hemofilie A patient. Case report en review van de literatuur. Ned Tijdschrift voor Heelkunde. 2006 Dec;15(8): 235-237.

2007 Hinnen JW, Rixen DJ, Koning OHJ, van Bockel JH, Hamming JF. Development of fibrinous thrombus analogue for in-vitro abdominal aortic aneurysm studies. J Biomech. 2007;40(2):289-95.

2007 Koning OHJ, Garling EH, Hinnen JW, Kroft LJM, Van der Linden E, Hamming JF, Valstar ER, Van Bockel JH. Accurate detection of stent-graft migration in a pulsatile aortic model using Roentgen stereophotogrammetric analysis. J Endovasc Ther. 2007 Feb;14(1):30-8.

2007 Hinnen JW, Rixen DJ, Koning OHJ, van Bockel JH, Hamming JF. Aneurysm sac pressure monitoring: Does the direction of pressure measurement matter in fibrinous thrombus? J Vasc Surg. 2007 Apr;45(4):812-6.

2007 Hinnen JW, Koning OH, Van Bockel HJ, Hamming JF. Regarding "Initial results of wireless pressure sensing for endovascular aneurysm repair: The APEX trial--Acute Pressure Measurement to Confirm Aneurysm Sac EXclusion". J Vasc Surg. 2007 Aug;46(2):403;

2007 Hinnen JW, Koning OH, van Bockel JH, Hamming JF. Aneurysm Sac Pressure after EVAR: The Role of Endoleak. Eur J Vasc Endovasc Surg. 2007 Oct;34(4):432-41.

2007 Koning OH, Kaptein BL, Garling EH, Hinnen JW, Hamming JF, Valstar ER, Bockel JH. Assessment of three-dimensional stent-graft dynamics by using fluoroscopic roentgenographic stereophotogrammetric analysis. J Vasc Surg. 2007 Oct;46(4):773-779.

2008 Mieog JS, Stoot JH, Bosch JJ, Koning OH, Hamming JF. Inflammatory aneurysm of the common iliac artery mimicking appendicitis. Vascular. 2008 Mar-Apr;16(2):116-9.

2008 Lips DJ, Koning OHJ. Het koraalrifsyndroom: een thoracale aortastenose als verklaring voor een verzameling van symptomen. Ned Tijdschr Geneeskd.. 2008;152:B32.

2009 Koning OH, Kaptein BL, van der Vijver R, Dias, NV, Malina, M, Schalij, MJ, Valstar, ER, van Bockel, JH. Fluoroscopic roentgen stereophotogrammetric analysis (FRSA) to study 3-D stent-graft dynamics in patients: a pilot study. J Vasc Surg, in press.

Curriculum Vitae

Curriculum Vitae
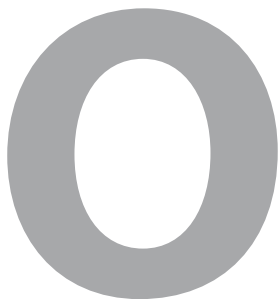
Olivier Henk Jan Koning was born on April 14th 1970 in Amsterdam under the sound of roaring lions at night time. He graduated from the "Huygens Lyceum", Voorburg in 1988 and started medical school at the Rijksuniversiteit Leiden. During his studies he worked as a coordinator of transplantations at Eurotransplant Foundation and spent 9 months in the Medstar trauma unit of Washington Hospital Center, Washington, DC as a medical student. He received his medical degree in 1996 and started his surgical training in 1997 at the Westeinde Hospital (Head: Dr B.C. de Vries and Dr J.C.A de Mol van Otterloo) and the Leiden University Medical Center (Head: Prof. Dr O.T.Terpstra). During his training he was co-founder of "De Jonge Orde", the national union of medical specialists in training and president of the VAGH, the association of surgical residents in the Netherlands. From 2003 to 2004 he received advanced surgical training in vascular surgery (CHIVO) at the LUMC (Head: Prof.Dr J.H. van Bockel) after which he joined the surgical staff at the same institution. Since 2006 he has been practicing surgery at the Jeroen Bosch Ziekenhuis in 's-Hertogenbosch. The author is married to Wally van der Eerden and has three great children: daughters Wally and Charlotte and son Juriaan.